ENVIRONMENTAL MONITORING OF DREDGING AND PROCESSES IN THE UPPER LAGUNA MADRE, TEXAS

Final Report, Year 1

by

Adele Militello, Nicholas C. Kraus, and Robert D Kite II

with contributions by

James E Kaldy and Kenneth H Dunton

Prepared for

U S Army Corps of Engineers, Galveston District
2000 Fort Point Road
Galveston, Texas 77553

July 23, 1997

Conrad Blucher Institute for Surveying and Science
Division of Coastal and Estuarine Processes
Texas A&M University-Corpus Christi
6300 Ocean Drive, Corpus Christi, Texas 78412-5503

Texas A&M Research Foundation

EXECUTIVE SUMMARY

This one-year study was conducted for the U S. Army Corps of Engineers, Galveston District, to investigate physical processes and sediment transport in the vicinity of dredged material placement sites bordering the Gulf Intracoastal Waterway (GIWW) The study was conducted by staff of Texas A&M University-Corpus Christi (TAMU-CC) and the University of Texas Marine Science Institute with the lead responsibility at the Conrad Blucher Institute for Surveying and Science, TAMU-CC. The study site extends from the southern end of Corpus Christi Bay to the southern end of the Upper Laguna Madre (ULM), Texas. Sections of the GIWW in the southern portion of Corpus Christi Bay and in the ULM from the mouth of Baffin Bay and south have historically been locations of high shoaling rates and frequent dredging Typically, these regions must be dredged every 2 to 3 years The goals of this study are to determine the processes responsible for sediment deposition in the high-shoaling reach areas and to propose effective means of reducing the deposition rate. Reduction of shoaling within the channel will improve the economic efficiency of the GIWW through reduction in the frequency of dredging and may also reduce the environmental impacts of dredging The main issues of concern in the monitoring project are: 1) Encroachment of sediment on seagrass beds and reduction of light within the water column; 2) Transport of dredged material back into the GIWW and loss of material from placement sites; and 3) Understanding cause-and-effect relations between hydrodynamic forcing and sediment movement This report presents the findings of the study and recommendations for improving dredging efficiency through reduction of deposition of sediment in the GIWW

Components of the study were performed through a multidisciplinary monitoring effort consisting of three components 1) Sustained monitoring at three fixed platforms, 2) Hydrographic surveys, and 3) Seagrass distribution The study was conducted by intensive sustained monitoring at three fixed platforms for a period of 1 year. Two platforms were located in the direct vicinity of dredged material placement sites, and one platform was located in the mouth of Baffin Bay, 0.8 km west of the GIWW Data collected in this study were supplemented by wind and water-level measurements collected at three sites within the study area as part of the Texas Coastal Ocean Observation Network

The monitoring platforms were located in southern Corpus Christi Bay, the mouth of Baffin Bay, and in the ULM near the northern end of the Land Cut The platforms were serviced at approximately weekly intervals, a procedure involving substantial physical effort in reaching these remote locations. The data, some of which were acquired by line-of-sight radio, are archived in the Blucher Institute Environmental Database and are available for analysis. This study focuses on selected data from the large data set obtained

The major results and conclusions of the study are

1 The regions of highest shoaling occur in the northern 10,000 ft of the study site and in the reach extending from the mouth of Baffin Bay to the northern end of the Land Cut.

2 The main cause of sediment resuspension is wind-induced waves, especially in the vicinity of south Corpus Christi Bay and the mouth of Baffin Bay The sediment resuspended by waves can then be transported by wind-induced currents and the tidal current.

3 Based on seven months of data, in the southern end of Corpus Christi Bay, the current flows across the GIWW such that suspended sediments may be deposited into the GIWW.

4. It is hypothesized that the high shoaling rate in the southern end of the ULM may be caused by water-borne transport of fine-grained material from the mud flats south of the ULM, as well as by wind-borne transport

5 Deposition of material into the GIWW at the mouth of Baffin Bay may be due to two causes, 1) Material suspended by wind-induced waves that is carried into the GIWW, and 2) Material migrating northward that has been deposited south of the mouth of Baffin Bay

6 Significant differences in underwater light in association with dredging were not found Presence of the brown tide may have dominated light attenuation such that the degree of reduced light from dredging could not be detected.

Recommendations resulting from this study to reduce the environmental impacts and cost and frequency of dredging are

1 Location of dredged material placement sites on the west side of the GIWW in south Corpus Christi Bay may reduce deposition in that region, but further analysis should be undertaken before implementation

2 Emplacement of sand fencing on Padre Island and other countermeasures to wind-blown sand intrusion in the southern reaches of the ULM will reduce the volume of wind-transported material into the GIWW

3. Diking of the GIWW within the Land Cut will reduce the volume of water-borne sediment transported off of the shallow mud flats.

4 Overdredging of the GIWW in the southern portion of the ULM will reduce the frequency of dredging by creating a deeper channel in which sediment will be deposited

5 Measurement of wind waves for a period of at least 1 year is recommended so that the influence of waves on sediment resuspension in the study area can be quantified

TABLE OF CONTENTS

LIST OF FIGURES

LIST OF TABLES

PREFACE

The one-year environmental monitoring study of dredging and physical processes in the upper Laguna Madre described herein was conducted for the U S Army Corps of Engineers, Galveston District, under the recommendation of the Laguna Madre Interagency Coordinating Team sponsored by the Galveston District. This study was authorized on October 7, 1994, through a Memorandum of Agreement between the U.S Army Corps of Engineers, Galveston District, and the Texas A&M Research Foundation. Data collection began on November 1, 1994

This study was conducted by a multidisciplinary team comprised of staff from the Conrad Blucher Institute for Surveying and Science, Texas A&M University-Corpus Christi (TAMU-CC), University of Texas at Austin Marine Science Institute (UTMSI), Center for Coastal Studies (CCS) at TAMU-CC; College of Science and Technology, TAMU-CC The study was originally planned and undertaken by Co-Principal Investigators Dr Nicholas C Kraus and Dr C. Faucette of the Blucher Institute In July, 1995, Ms Adele Militello replaced Dr Faucette as Co-Principal Investigator. Mr Robert D. Kite II of the Blucher Institute joined the Blucher Institute team in May, 1996, and contributed to preparation of this report as well as data reduction Dr. Kenneth H Dunton and Mr. James E Kaldy, UTMSI, conducted the light irradiance analysis and many of the light irradiance measurements. Mr Charles Medina and Mr Larry Hyde, TAMU-CC graduate students, under the direction of Dr J. Wesley Tunnell, Jr , CCS, conducted the seagrass distribution component of this study to be submitted as a separate contribution Ms Rachael Brooks, TAMU-CC graduate student under the direction of Dr. Roy Lehman, conducted the sampling and nutrient analysis for the water quality and brown tide aspect of the study, whose report contribution will be prepared separate from this volume. Blucher Institute staff designed, installed, and maintained the data-collection equipment, imported and archived the data; conducted hydrographic surveys and associated data reduction; analyzed the data; and reported on the progress and status of the study

Assistance in this study was provided by numerous Blucher Institute staff members Messers Daniel Prouty, Donald Waechter, Greg Hauger, and John Adams performed the hydrographic surveying component of the study Radio communications expertise was provided by Mr Mark Earle Computer and database support was provided by Messers. Scott Duff, Gerardo Garza, and Ms Rocky Freund Location maps were generated by Ms Deidre Williams

and Mr. Daniel Prouty Instrumentation and datalogger expertise was provided by Messers. Daryl Slocum and Mike Grady The fixed stations were maintained by several Blucher Institute personnel including John Adams, Mark Earle, Scott Fagan, James Rizzo, and Daryl Slocum Analysis of water samples and associated data entry were performed by TAMU-CC students Layla Elder and Scott Gisler. Assistance in data preparation was provided by TAMU-CC students Kristie Degelo and Julie Celum

Recent dredging data were furnished by Mr Noe Cadena of the Corpus Christi field office of the U.S Army Corps of Engineers, Galveston District Historical dredging data were provided by Mr Neil T. McLellan of the Galveston District. The encouragement and assistance of Mr McLellan and Ms June Keller of the Galveston District are greatly appreciated

1. INTRODUCTION[1]

The U.S. Army Corps of Engineers is responsible for maintenance dredging of the Gulf Intracoastal Waterway (GIWW), which includes placement and management of the dredged material During dredging and material placement, sediments can be resuspended into the water column, transported, and deposited in environmentally sensitive areas such as seagrass beds. Issues of concern to the Corps are the environmental consequences of dredging and material placement, as well as reduction of cost and frequency of maintenance dredging This study was initiated to reduce the frequency and cost of dredging, and to determine the impact, if any, of dredging on the health of seagrass beds through monitoring of physical, biological, and water quality parameters associated with seagrasses

1.1 Study Background

Environmental concerns regarding sediment resuspension and deposition are the reduction of light available through the water column and sediment coatings on seagrasses The light reduction and sediment coatings reduce the capability of seagrasses to perform photosynthesis and can degrade the health of the seagrass beds An assessment of increased turbidity and suspended material into the water column in relation to dredging will provide information that can be applied to maintenance dredging operations and material placement locations and methods

The predominant forcings responsible for the resuspension and transport of sediments are the wind-induced current, waves, tidal current, and vessel-induced motions Resuspension and scouring of the bottom by trawling is another means of redistributing sediment but is not investigated in this study. Other factors that control sediment transport are water depth, fetch, bottom morphology, sediment type (mineralogy, organic material), grain-size distribution, and bottom coverage of aquatic plants. Many of these factors are examined in this report. During periods of strong winds, wave action and strong currents apply stress to the bottom, which, in turn, resuspends sediments into the water column Once suspended, the sediment particles are transported by the currents to another location where they are deposited. The areas of deposition are lower energy regions of the flow.

[1] Adele Militello and Nicholas C Kraus, Conrad Blucher Institute for Surveying and Science, Texas A&M University-Corpus Christi

A distinction of sediment transport induced by dredging and by naturally occurring processes must be made to determine the material transport related to each cause. Long-term monitoring of physical processes can provide the data necessary to distinguish the dredging and ambient or background-level sediment transport characteristics. Separation of dredging-induced sediment transport from the ambient sediment transport must be inferred through comparison of physical processes data during weak and strong wind conditions and during periods when dredging occurs and when no dredging occurs

Light attenuation in the water column is related to suspension of several types of materials comprised of dissolved substances, phytoplankton, and other substances (Onuf 1994) including sediments. In the Upper Laguna Madre (ULM), defined as the region extending from the northern end of the Land Cut to Corpus Christi Bay, an added factor confounding the light reduction problem is the presence of the brown tide, an algal bloom that has persisted since 1990 and has been associated with reduction in growth rates and below-ground biomass in seagrasses (Dunton 1994) At present, the brown tide exists throughout most of the ULM The brown tide is believed to originate in the region of Baffin Bay and is pumped into and out of the bay by diurnal land seabreeze and frontal passages from the north The GIWW promotes water exchange, allowing brown tide to move through the lagoon on the one hand, while bringing bay and Gulf water to the lagoon on the other hand.

This study was undertaken to monitor processes related to light attenuation and sediment transport in the ULM with the objective of identifying possible modifications of the dredging practice such that 1) environmental impacts are reduced, and 2) the cost and frequency of dredging are minimized Within the framework of the objective, the main issues of concern in the monitoring are:

1. Encroachment of sediment on seagrass beds and reduction of light within the water column (dredging-activity induced concentrations above normal background level sediment concentrations)
2. Transport of dredged material back into the GIWW and loss of material from placement sites
3. Understanding cause-and-effect relations between hydrodynamic forcing and sediment movement.

1.2 Site Description

The study site consists of the southern portion of Corpus Christi Bay and ULM as shown in Figure 1 1 These bay and lagoon systems are located on the south Texas coast where the climate is classified as semi-arid, having a mean annual precipitation of 70 cm and a mean annual evaporation of 134 cm (Friedman and Sanders 1978). Corpus Christi Bay and the ULM are shallow systems with mean depths of 3 45 m (Smith 1989) and 1 m (Behrens 1966), respectively. The Corpus Christi Bay-ULM system extends from Aransas Pass at the northern end to the Land Cut, approximately 74 km to the south of the intersection of Corpus Christi Bay and the ULM The ULM is the northern section of the entire Laguna Madre which consists of the ULM and the Lower Laguna Madre (LLM) as shown in Figure 1 2 The southerly extent of the LLM is at Port Isabel, Texas, about 10 km north of the mouth of the Rio Grande near the border with Mexico The two sections of the Laguna Madre are separated by an expanse of wind-tidal flats that are approximately 20 km long and 10 km wide (Miller 1975) but are hydraulically linked by the Land Cut, a section of the GIWW that was dredged through the wind-tidal flats connecting the two basins Mansfield Pass is the northernmost inlet in the LLM and is 32 km south of the southern extent of the Land Cut. Tides at Port Mansfield, located on the western side of the LLM across from Mansfield Pass, are small with diurnal amplitudes of approximately 0.6 cm for both the O_1 and K_1 diurnal tidal constituents and 0 1 cm for the M_2 semi-diurnal constituent (Zetler 1980) Because of the weak tidal signal and presence of the Land Cut, the possible influence of Mansfield Pass does not enter the study

Corpus Christi Bay has a direct opening to the Gulf of Mexico through Aransas Pass, which is located on the northeastern end of the bay, 24 km to the north of the intersection of the ULM and Corpus Christi Bay Aransas Pass is the only direct connection to the Gulf of Mexico within the Corpus Christi Bay-ULM system. Tidal forcing of the system is limited to tidal energy that propagates into the system from Aransas Pass The Nueces River is the primary tributary to Corpus Christi Bay, having a 29-year mean discharge of 23 4 m^3/s (Diener 1975) Corpus Christi Bay is connected to the ULM at its southeast corner and shallow shoals at the northernmost end of the ULM limit the exchange of water between the ULM and Corpus Christi Bay

The ULM is a narrow, shallow, bar-built lagoon separated from the Gulf of Mexico by Padre Island. The ULM is micro-tidal at its northern end and non-tidal at its southern end Tidal energy is damped toward the south because of frictional effects and shallow depths (Smith 1988).

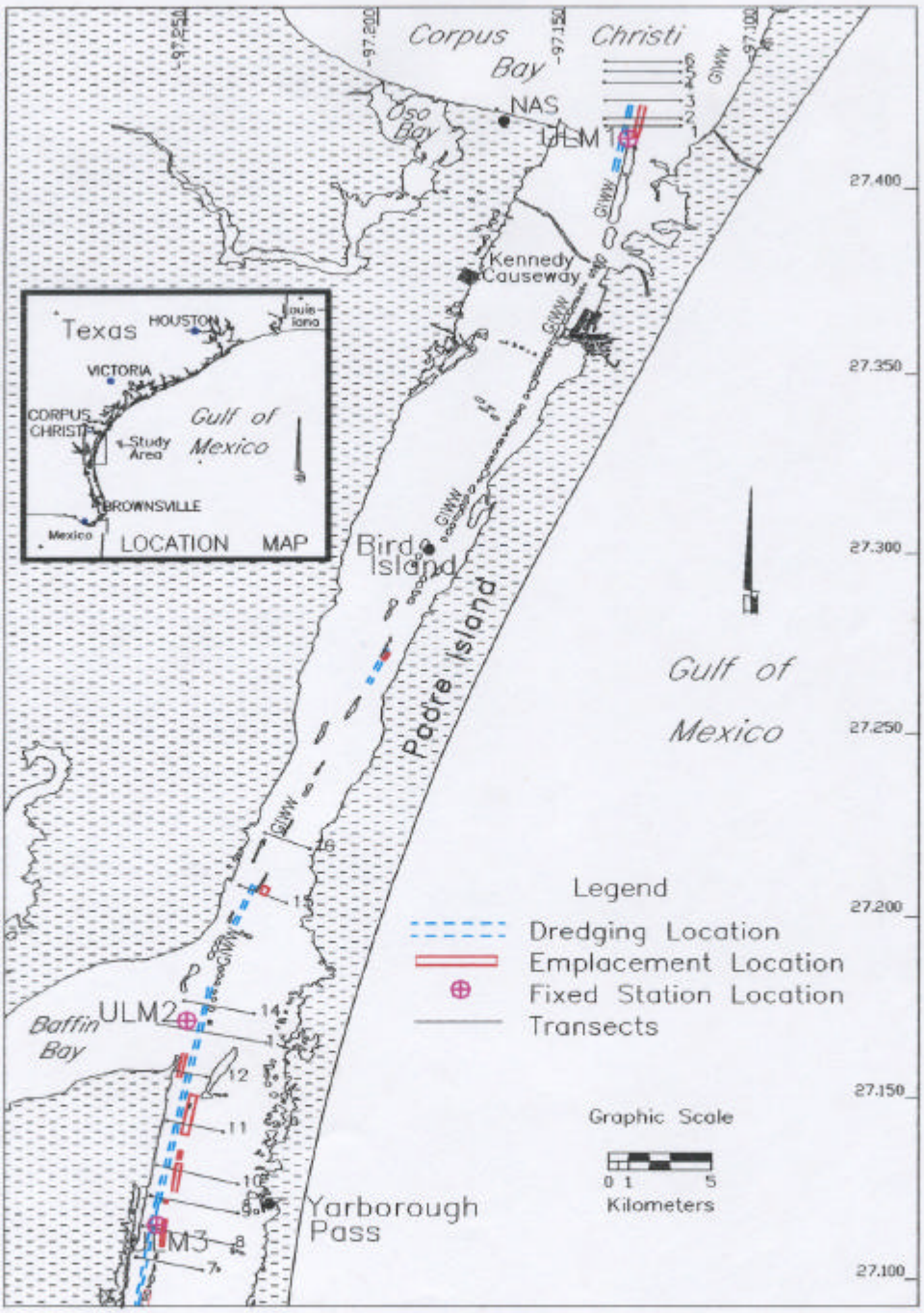

Figure 1.1. Site map of study area.

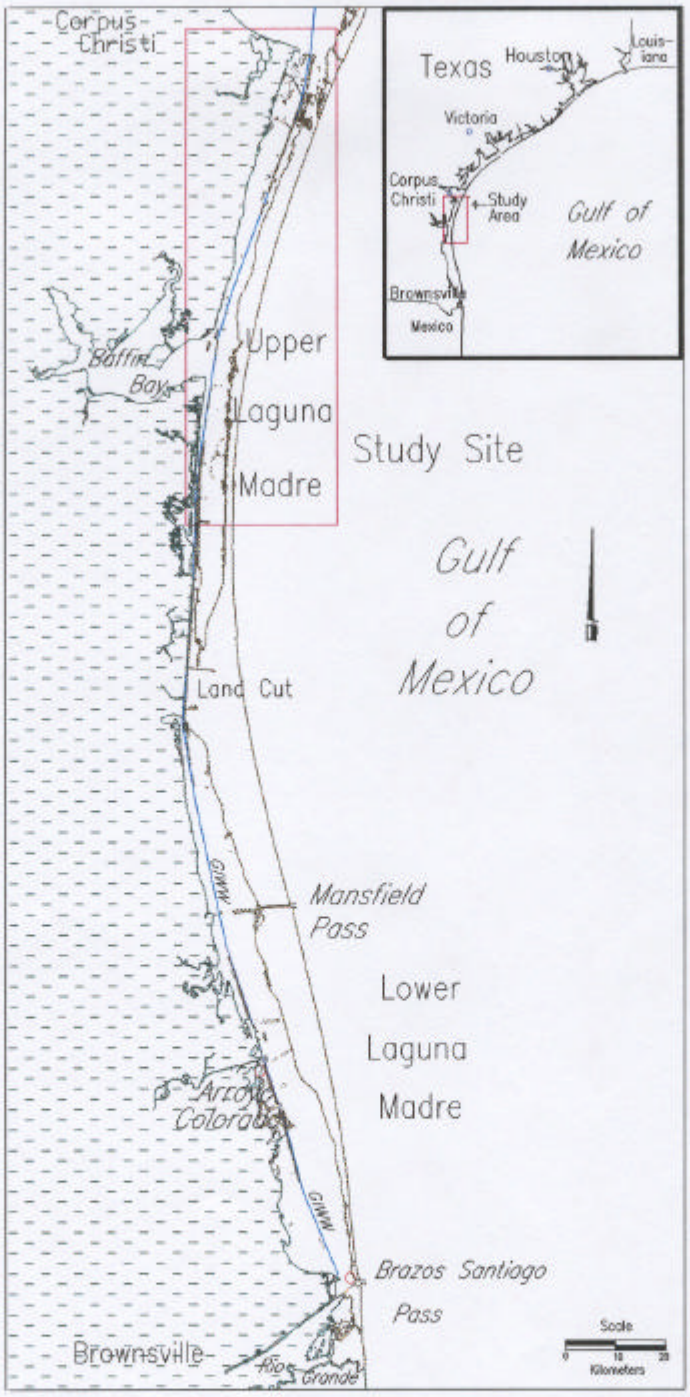

Figure 1.2. Laguna Madre Location map.

The ULM has no major stream tributaries The lack of point-source fresh water input coupled with the semi-arid climate (evaporation exceeds precipitation) has caused hypersaline conditions prior to the opening of the GIWW with salinity values reaching 100 ppt (Collier and Hedgpeth 1950). Since opening of the GIWW through the ULM in 1949, salinity levels have been reduced and rarely reach the extremes observed prior to the opening of the Land Cut. Salinity in the Upper Laguna Madre south of Baffin Bay did not rise above 60 ppt from 1967 to 1989 (Quammann and Onuff 1994)

Baffin Bay is located on the western side of the ULM approximately 9 km south of the northern end of the ULM and was formed by submergence of a stream valley (Friedman and Sanders 1978) Baffin Bay receives limited freshwater input via a few minor intermittent stream tributaries The mean depth of Baffin Bay is 1.5 m (Behrens 1966), but 3-m depths are commonly found along the main axis of the embayment. The longitudinal axis of Baffin Bay is oriented approximately perpendicular to the main axis of the ULM Serpulid reefs are present at the mouth of Baffin Bay, and it has been reported that these reefs have limited the exchange between Baffin Bay and the ULM (Shepard and Rusnak 1957)

Winds play a major role in driving circulation in the ULM, especially in the southern regions where the astronomical tides are non-existent. Because the ULM is long, narrow, and is oriented with its major axis aligned approximately north-south, the system is fetch limited in the west-east direction, with the exception of the mouth of Baffin Bay.

In addition to the natural features of the study area, anthropogenic modifications include dredging of the GIWW, placement of dredged material, other dredging of minor channels, and construction of the John F Kennedy (JFK) Causeway, which is a primarily dirt-fill causeway connecting the mainland to Padre Island Initial dredging of the GIWW within the study area was completed in 1949 Design dimensions of the GIWW are 91 m at the top, 38 m at the bottom, and a depth of 3.7 m Dredged material has been placed in subaqueous and subaerial deposits near the GIWW

The monitoring site for ULM1 is approximately 7 2 km north of the JFK causeway in the southern portion of Corpus Christi Bay and resides 0 4 km east of the GIWW. The site is sheltered on the southeast side by Mustang Island Dredged material disposal islands lie to the east and south of the platform. The northern side of the monitoring site is exposed to Corpus Christi Bay The average depth of the site area is approximately 2 1 m. This depth is uniform throughout the monitoring site, excluding the depth for the disposal area to the east and the GIWW to the west.

The ULM2 monitoring site is located at the mouth of Baffin Bay approximately 45 km south of the JFK causeway The platform lies 0 8 km west of the GIWW The average water depth for the monitoring area is approximately 2 m. Serpulid reefs exist in the mouth of Baffin Bay, leaving less than 20% of the flow through the mouth unrestricted The ULM2 platform lies in the southernmost edge of the opening in the reefs. Completely exposed on all sides, this site receives the full impact of all storm and frontal passages.

The monitoring site for ULM3 is located 10 2 km south of ULM2 and is approximately 0 3 km east of the GIWW and 4 8 km north of the Land Cut. The study site is located just inside a dredged material disposal area to the east To the south and east small exposed disposal sites exist The region southeast of the platform is where Padre Island and the expansive mud flats to the south merge. This joining area forms the southern terminal basin of the ULM and has an arc shape The ULM3 platform lies 4 km, at its maximum distance, from the barrier island The leading edge of the western shoreline is approximately 0 8 km from the platform. The average depth at this site is 1 8 m.

1.3 Report Structure

Chapter 1 describes the background and orientation to the study site Chapter 2 describes the data-collection systems and procedures Chapter 3 presents a survey of historical and recent dredging activities in the study area Chapter 4 describes the measured wind, water level and currents of the study area, which are the driving forces for sediment transport. Chapter 5 discusses sediment resuspension and transport Chapter 6 discusses the light attenuation component of this study. Chapter 7 presents conclusions and recommendations Appendix A contains dredging volumes and locations within the study site for the 1994-1995 dredging cycle. Appendix B contains a Julian Day calendar

2. FIELD DATA COLLECTION[2]

The field data collection consisted of sustained long-term in-situ monitoring of physical, chemical, and biological parameters from three fixed platforms, and collection of water samples for laboratory analysis Instrumentation and associated support equipment were installed in November, 1994, and dates of instrumentation installation are given in Table 2.1. This chapter describes the platforms and the instrumentation and equipment installed on them, together with the general data-collection process.

2.1 Monitoring Platforms and Instrumentation

Locations of the three monitoring platforms are shown in Figure 1 1, and coordinates, dates of installation, and local water depths for each platform are provided in Table 2.1. The northern-most platform, designated as ULM1, is located in Corpus Christi Bay near the northern terminus of the ULM approximately 0.4 km east of the GIWW. This platform provided data in the vicinity of dredging sites on the southern side of Corpus Christi Bay. The central platform, ULM2, lies at the mouth of Baffin Bay, approximately 0.8 km west of the GIWW The southernmost platform, ULM3, is located approximately 10 2 km south of ULM2, and 0.3 km east of the GIWW The southernmost stations provided information in the vicinity of dredging sites along the GIWW in the vicinity of the mouth of Baffin Bay In addition, consideration was given to emplacement location for providing of physical processes and water quality data for Baffin Bay, a relatively unstudied site

Table 2.1. Installation dates, locations, and representative water depths at ULM platforms.

Station	Installation Date	Latitude, N	Longitude, W	Depth, m
ULM1	11/01/95	27 41 4576	97 13 2960	2 1
ULM2	11/16/95	27 17 1360	97 24 9480	2
ULM3	11/04/95	27 11 5450	97 25 7040	1 8

[2] Robert D Kite II and Adele Militello, Conrad Blucher Institute for Surveying and Science, Texas A&M University-Corpus Christi

2 1 1 Description of Monitoring Platforms

The monitoring platforms are fully-instrumented data-collection stations constructed of marine-treated wood ULM1 and ULM2 are quad-leg platforms 6-ft by 6-ft on each side, each with a deck and railing The two platforms are supported by four 6-in by 6-in beams with cross-bracing on each side ULM3, a Corps of Engineers platform refurbished for this study, is a tri-leg wood structure 10-ft on the hypotenuse and 8-ft on both the adjacent sides, with a deck and railing. Support for this platform consists of three 6-in by 6-in beams with cross-bracing on each side

Platforms are equipped with data-collection instrumentation and equipment that log, store, and transmit the data. Each station is instrumented with sensors to measure physical and water-quality parameters listed in Table 2.2. Two photosynthetically active radiation (PAR) sensors are located at each platform, one above the water surface and one approximately 1 m below mean sea level. In addition to *in situ* measurement sensors, the platforms are equipped with ISCO automatic water samplers. These samplers collect water at specified times (here, twice daily as described below) and store the water sample until they are retrieved and taken to the Blucher Institute for analysis of total suspended solids (TSS) and particle size distribution

Table 2.2. Measured parameters and instrumentation at ULM platforms.

Parameter	Instrument
Current speed and direction	Sontek Acoustic Doppler Velocimeter (ADV)
Water temperature, conductivity, salinity, dissolved oxygen pH, turbidity	Hydrolab H20 unit
Chlorophyll-a	Chelsea Instruments flourometer
Total suspended solids	ISCO 2700
Photosynthetically active radiation (PAR)	Licor LI-193SA spherical (4π) quantum-sensor (underwater), LI-190SA cosine-corrected (2π) quantum sensor (surface)

The three monitoring platforms for ULM are each equipped with one environmental enclosure to ensure minimal exposure of electronics to the external environment. Each environmental enclosure houses the data collectors, signal processing units, radio communications controller, and batteries The instruments and data loggers are powered by two 4-amp/hr gel cell batteries that are charged by two 30-watt solar panels. A low-power consumption microcomputer of 6-amp/hr/day yields an on-site data storage capacity of approximately 13 days Each station employs a packet controller, consisting of a radio and modem, which allows remote communication with the data-collection system from the Blucher Institute ULM1 has a UHF omni-directional antenna which allows direct connection with the Blucher Institute ULM2 and

ULM3 each have a UHF whip-antenna affixed to the platform Presently, data generated at platforms are relayed from a radio tower located in Riviera, Texas, to the Blucher Institute Once at the Institute, the data are decoded and imported into the Blucher Institute Environmental Database where 6-min averages of all parameters are stored.

2 1 2 Platform Maintenance

Platform maintenance is performed weekly unless weather or other circumstances prevent scheduled servicing Regular maintenance consisted of cleaning the ADV and flourometer, exchange of Hydrolab units with laboratory-calibrated units, retrieval of water samples, and replacement of a polyethylene bag that protected the subsea PAR sensor In addition, electronically acquired data were downloaded and taken back to the Blucher Institute to be uploaded into the database. On February 8, 1995, no radio contact was possible with ULM1. It is believed that a vessel had tied up to the platform during a storm the previous day and had uprooted the station. Repairs were made, and the station was back on line by February 15, 1995 An ADV was lost in this event

2 1 3 Instrumentation

Acoustic-Doppler Velocimeter (ADV)

Three components of water velocity (north-south u, east-west v, and vertical w) were measured continuously by ADVs (SonTek, San Diego, California, USA), which is a new type of current meter that is highly accurate (even at weak water velocities) and robust against drift due to aging and biofouling. The ADV acoustically measures the three components of flow velocity at a point based on the Doppler-shift principle The ADV has a centrally-located transmitting transducer surrounded by three receiving transducers mounted on arms orientated at 120-deg angles The transmitting transducer emits periodic short acoustic pulses which are scattered by material in the water column, such as bubbles and suspended material which are assumed to move at the speed of the water flow These acoustic echoes are detected by the receivers. By knowledge of the orientation of the acoustic beams and the principle that the frequency of the echo is Doppler shifted according to the relative motion of the scattering material, the orthogonal components of current velocity are computed. The ADV has a resolution of 0 1 mm/s over the range of 0 to 2.5 m/s and an accuracy of ±0.25% or ±0 25 cm/s, whichever is greater (Kraus, *et al* 1994). In this study, the sampling rate of the ADV was 1 Hz with 6-min averages of each component of the water velocity, signal-to-noise ratio, and correlation coefficients stored in the

on-site datalogger The signal-to-noise ratio and correlation coefficients were used to determine the quality of the velocity data and to identify problems associated with the hardware, such as misaligned receivers or biofouling of the transmitters or receivers The position and distance for the transmitter and each of receivers are correlated against preset factory values of their positions The ADVs were mounted at mid-depth with the probe oriented in such a manner that positive flow components (u, v, w) are directed toward the north, west, and upward, respectively

During the first 6 months of data collection, the range setting for the ADVs was set incorrectly The ADV range settings were corrected in May, 1995 This incorrect setting caused parts of the ADV data to be invalid and unrecoverable. Because of this problem, ADV data in this report are shown and analyzed from June, 1995, through December, 1995

Photosynthetically Active Radiation (PAR) Sensors

Measurements of PAR (400 to 700 nm wavelength) were collected continuously using a LI-193SA spherical (4π) quantum-sensor (underwater) and a LI-190SA cosine-corrected (2π) quantum sensor (surface) The underwater sensor was mounted on a 3-cm diameter PVC slider arm about 25 cm above the seabed to minimize fouling by drift algae and seagrass blades. The terrestrial sensor was mounted above the platform. Sensor locations were selected to avoid shading by the platform structure (southeast corner) Instantaneous PAR was measured at 1-min intervals and integrated hourly Light sensors are calibrated or checked for accuracy annually and are accurate to ±5% (traceable to National Bureau of Standards); stability is ±2% over any 1-year period, and data are recorded with a precision of ± 0.01 µmol photons/m^2 s

Water Quality Multiprobe

Water-quality parameters were monitored using an H20® Water Quality Multiprobe (Hydrolab® Corporation, Austin, Texas, USA), equipped with turbidity, water temperature, conductivity, pH, and dissolved oxygen sensors. The Hydrolab unit sampled every 2 min and data were logged using the Blucher Data Collector The Hydrolab units deployed in the field were calibrated in the laboratory prior to deployment, with approximately weekly change-outs of instruments The specific conductance, pH, and turbidity sensors were calibrated using standard solutions The pH and turbidity sensors were calibrated using a slope-calibration method and the conductivity sensor was calibrated using a one-point calibration with a standard solution having a conductivity similar to that observed in the field. The turbidity sensor is calibrated using 0.2-µm filtered, deionized water and 90 ntu formazin standard. The dissolved oxygen sensor was air-calibrated at atmospheric pressure The temperature sensor was calibrated by the manufacturer during fabrication and is considered stable for 3 years The calibration procedure followed for

the conductivity probe was such that an error of ±3 ppt was typical for the resultant salinity data Improvements to the calibration procedure are being made.

Fluorometer

Chlorophyll-a levels were continuously monitored at mid-depth using an Aquatrack III fluorometer (Chelsea Instruments, Surrey, UK) The fluorometer optically determines the concentration of chlorophyll-a by exciting a specimen within the sampling volume with a beam of pulsed visible and ultra-violet light, and comparing the intensity of the fluorescence excitation to that of a reference beam generated by the same light source Chlorophyll-a is measured over a range of 0 to 100 µg/L with an accuracy of ± 0.02 µg/L plus 5% of value However, because the fluorometer optically determines the concentration of chlorophyll-a, it is susceptible to biofouling when deployed in a biologically-productive environment such as the ULM. The fluorometer measurements were logged using a Blucher Data Collector and sampled at a rate of one reading every 2 min

Water Samples

Mid-depth water samples were collected twice daily at 6 00 AM and 6:00 PM (local time) using a 2700 Portable Sampler (Isco®, Lincoln, Nebraska, USA) During approximately weekly routine servicing, the samples were removed from the water sampler and transported to the Blucher Institute for analysis. The samples were analyzed for total suspended solids and particle-size distribution of the suspended solids. Total suspended solids concentration was determined by filtering a known volume of the sample twice, using two pre-weighed filters, a 1-µm glass fiber filter and a 0.45-µm cellulose filter, which were then dried at 65°C to constant weight The volume of sample filtered was typically 500 mL, however, if the sample contained a relatively large amount of sediment, as determined visually, the volume filtered was reduced to 250 to 300 mL Once the concentration of total suspended solids was determined, the filters were archived in labeled bags. Particle size of the suspended solids was determined, using a laser-particle analyzer (Mastersizer/E, Malvern Instruments, Worcestshire, UK), which determines the particle-size distribution based on laser-diffraction principles for diameters ranging from 0.1 to 600 µm The accuracy of the particle analyzer is ±2% of the median diameter (traceable to National Bureau of Standards), and the instrument is checked annually to confirm accuracy

2.2 Other Available Data

In addition to data collected specifically for this study, water-level, wind, and air temperature data are available from the Texas Coastal Ocean Observation Network (TCOON) These real-time measurements are collected at approximately 40 stations along the Texas coast and stored in a database at the Blucher Institute TCOON stations in the vicinity of the ULM monitoring area and the parameters that are measured at those stations are listed in Table 2 3. The station at Riviera was removed in March, 1995

Water-level data from the Naval Air Station, Bird Island, and Yarborough gauges and wind data from the Naval Air Station and Yarborough gauges are included in this report as supplemental data The wind measurements are of particular significance for understanding the role of the physical driving forces for the resuspension and transport of sediment (discussed in Chapter 5) Water level and wind data are available at 6-min and 1-hr intervals, respectively

Table 2.3. Supplemental TCOON data available in the vicinity of the ULM monitoring area.

Location	Parameters
Naval Air Station	Water level, wind
Packery Channel	Water level, wind, air temperature
Bird Island	Water level, wind, air temperature
Riviera (in the Laguna Salada, western end of Baffin Bay)	Water level, air temperature
Yarborough	Water level, wind , air temperature

3. DREDGING ACTIVITIES AND CHANNEL SHOALING ANALYSIS[3]

Although there are areas that must be dredged at a certain typical frequency, maintenance dredging of the GIWW varies spatially and temporally because of variation in current patterns, wind patterns, sediment type, amount of overdredging, and location and method of dredged material placement An assessment of physical parameters and their role in the resuspension and transport of sediment can provide information applicable to improving dredging efficiency, thereby reducing costs and potential environmental impacts. This chapter reviews the historical and recent dredging activities, and the results of hydrographic surveys performed during this study.

3.1 Historical Dredging Activities

Dredging of the GIWW in the study area was completed in 1949 (USACE dredging records). The channel design shape is trapezoidal with a depth of 14 ft (4 3 m), which includes 1 ft (0 3 m) advance and 1 ft over dredging. The design criteria for the channel width is 300 ft (91 m) across the top and 125 ft (38 m) across the bottom. Maintenance dredging of the GIWW in the study area has been required since the initial dredging of the channel was completed Typically, maintenance dredging within the study area is required every 1 to 2 years, although some intervals between dredging cycles have been 3 years (1974 to 1977, and 1991 to 1994).

The volume of material dredged for maintenance of the GIWW varies spatially along the channel. Figure 3 1 shows the volume of material dredged throughout the study area over 5-yr intervals starting in 1955, and also the average yearly volume over the corresponding 5-yr time period Figure 1.1 shows locations of the stations relative to features in the study region The volumes of dredged material were obtained from dredging records provided by the Galveston District For the present analysis, volumes were linearly distributed over 5,000-ft (1.5 km) intervals, and the distances reported are the center of each interval relative to Station 0+000 (Galveston District notation) Figure 3 1 shows that the areas of most frequent dredging and

[3] Adele Militello and Robert D Kite II, Conrad Blucher Institute for Surveying and Science, Texas A&M University-Corpus Christi

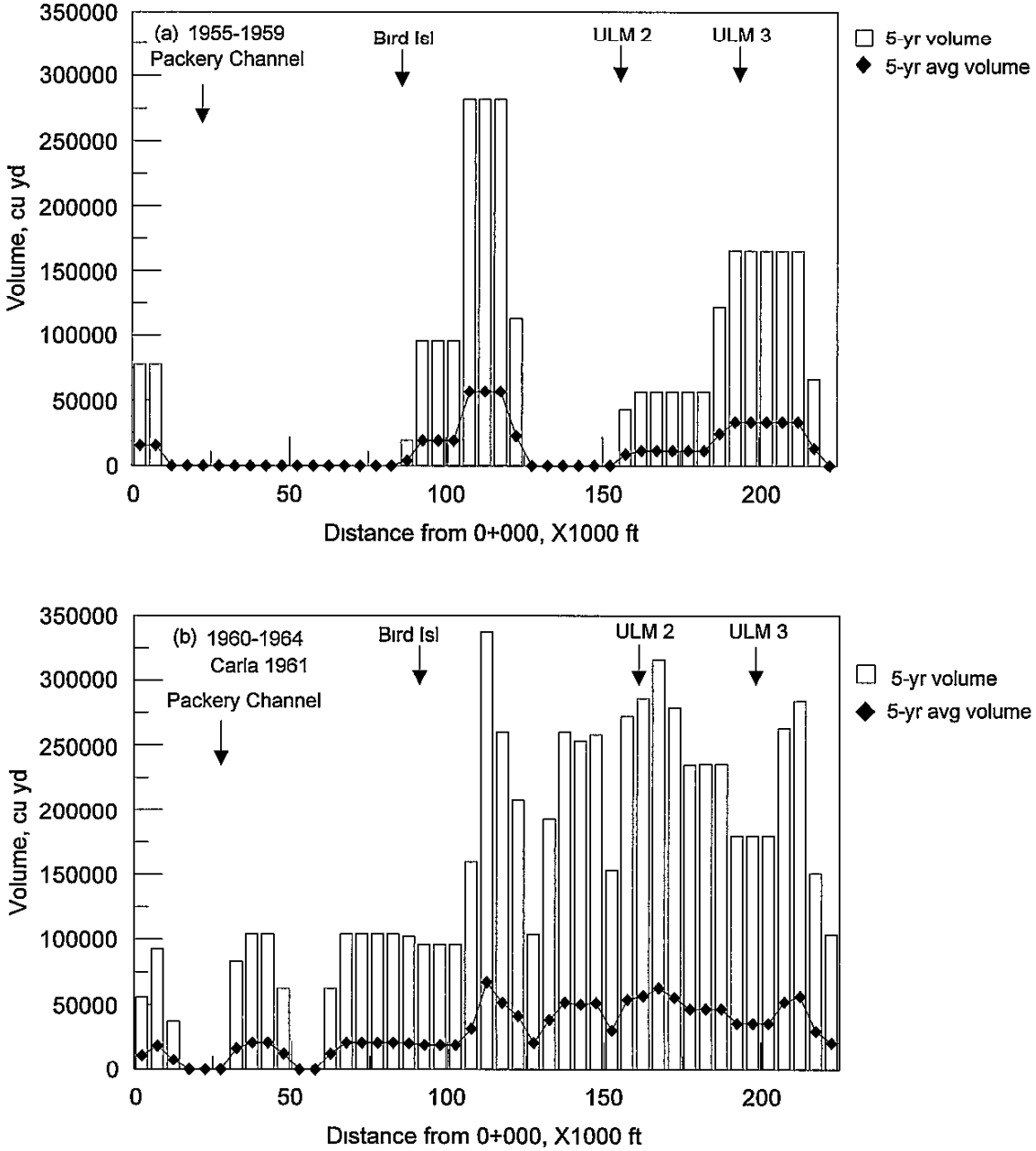

Figure 3 1a-b Volume of material dredged for maintenance over a 5-yr period in the GIWW from Corpus Christi Bay to the Land Cut (a) 1955-1959; (b) 1960-1964

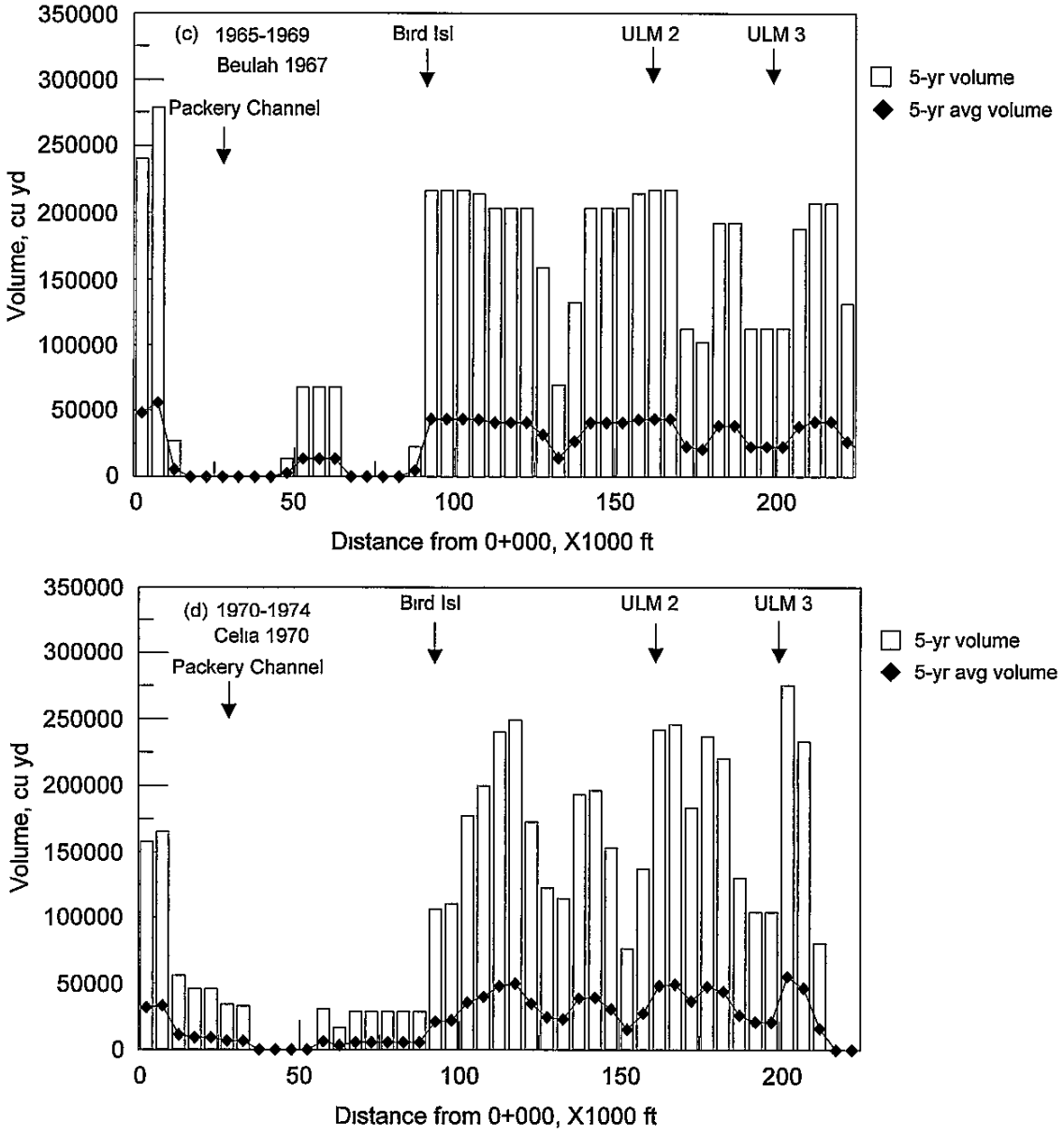

Figure 3 1c-d Volume of material dredged for maintenance over a 5-yr period in the GIWW from Corpus Christi Bay to the Land Cut (c) 1965-1969, (d) 1970-1974

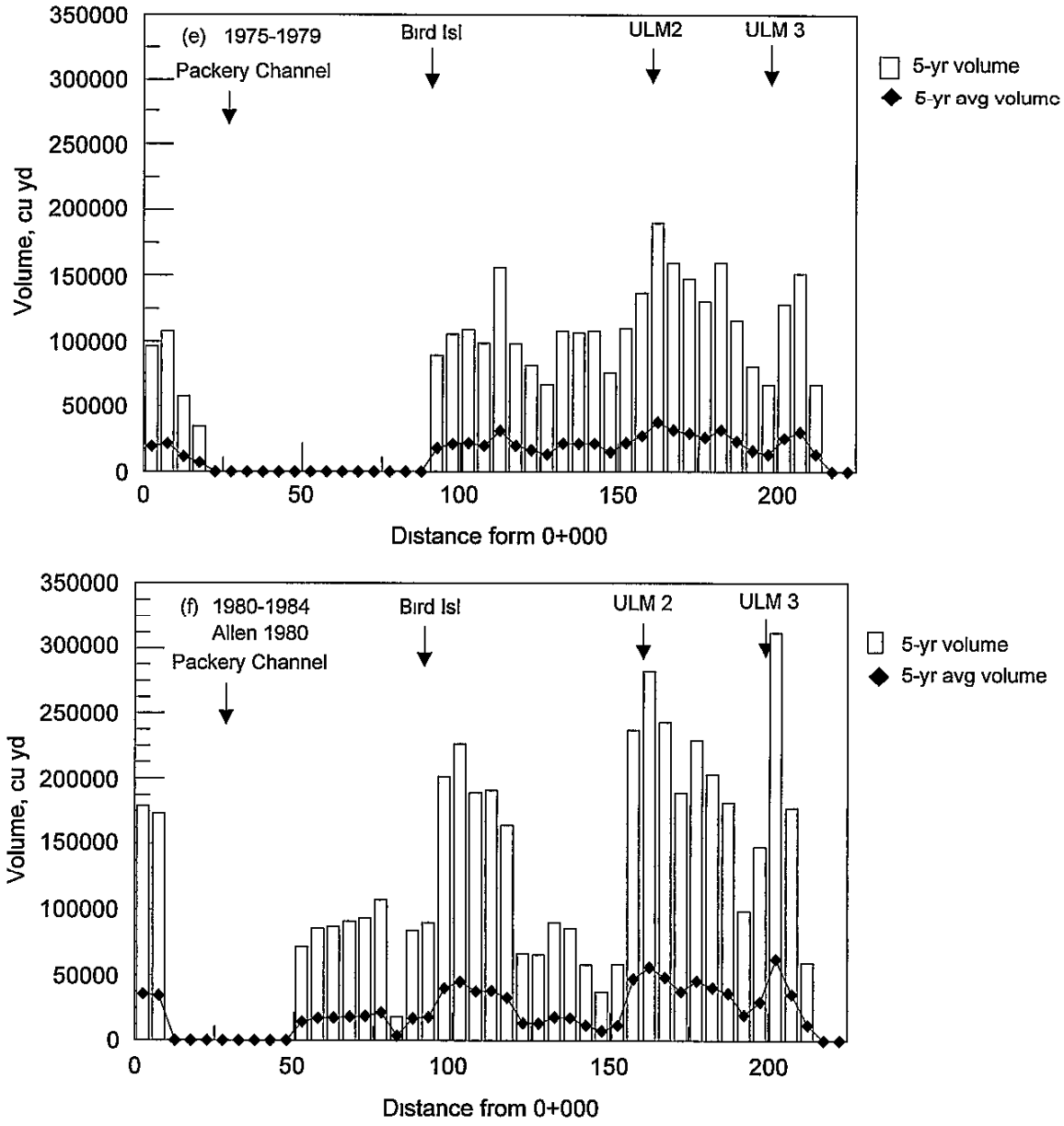

Figure 3.1e-f Volume of material dredged for maintenance over a 5-yr period in the GIWW from Corpus Christi Bay to the Land Cut. (e) 1975-1979, (f) 1980-1984

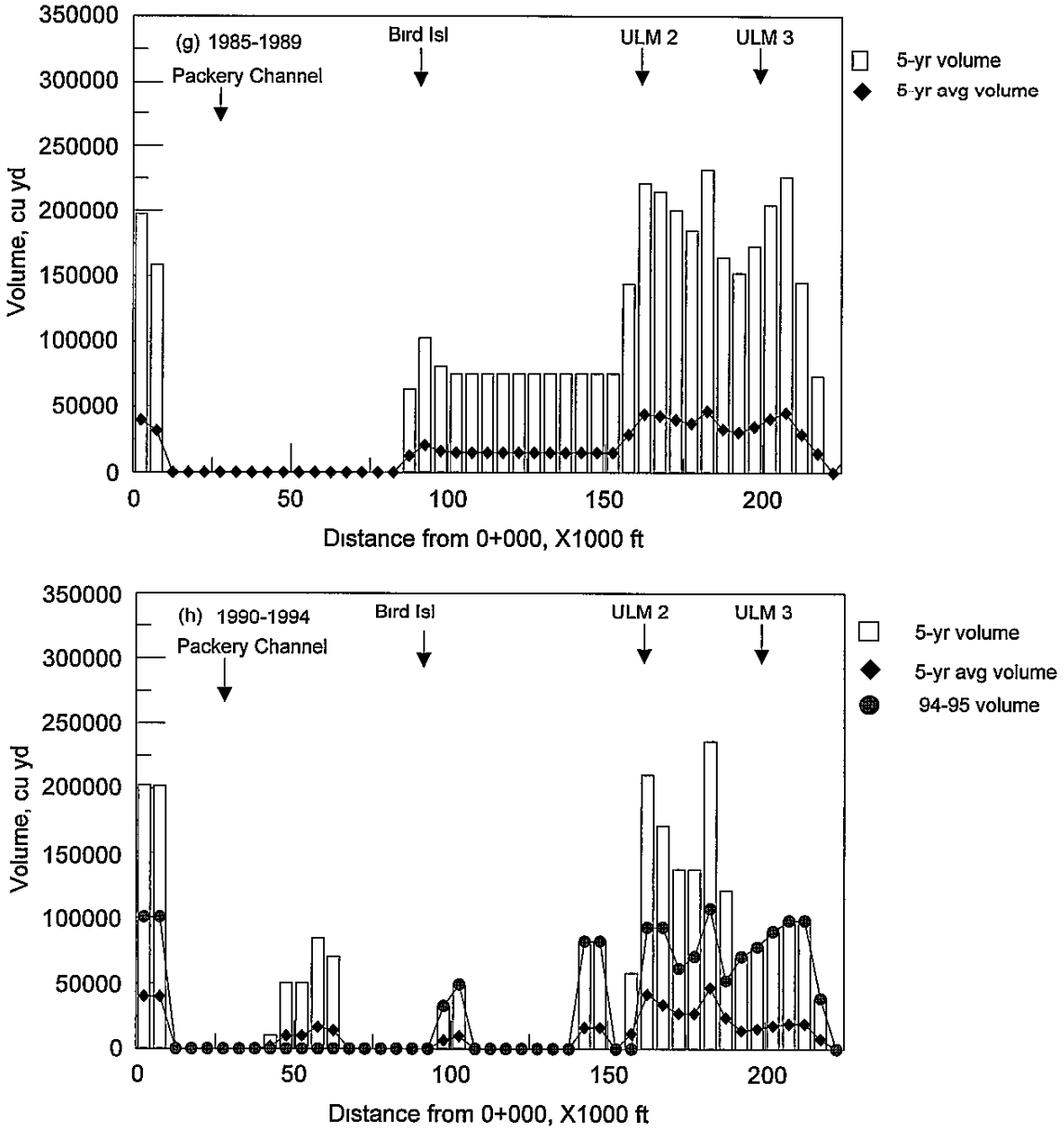

Figure 3 1g-h. Volume of material dredged for maintenance over a 5-yr period in the GIWW from Corpus Christi Bay to the Land Cut (g) 1985-1989, (h) 1990-1994.

greatest material volumes are located at the northern extent of the study area, in the vicinity of ULM1, and from approximately Sta 105+000 to the intersection of the Land Cut and the ULM (the southernmost extent of dredging shown in the figure)

Figure 3.1 indicates within the plots whether or not a major hurricane (catagory 3 or higher) struck the south Texas coast within the 5-yr interval for each plot by listing the hurricane name and year. During intervals when a major hurricane occurred, the amount of material dredged from the GIWW was increased over the 5-yr intervals in comparison to intervals when no major hurricanes occurred. The largest volume of material dredged from any of the 5-yr intervals occurred during the interval when Hurricane Carla (1961) hit the Texas coast (Figure 3.1b). Dredged material volumes were elevated along most of the channel length, particularly south of Packery Channel Storm tides associated with Hurricane Celia were highest at Port Aransas and Aransas Pass reaching a maximum elevation of 11 0 ft (3 4 m) above mean sea level (USACE 1971). Hurricanes Carla and Beulah (1967) caused breaching of Corpus Christi Pass which would account for increased deposition in the northern reaches of the study site The maximum hurricane tide in bays and estuaries associated with Beulah was found to occur in Cayo del Grulla, a branch of Baffin Bay, at a height of 10.9 ft (3 3 m) above mean sea level (USACE 1968). Similarly, high water elevations determined for passage of Hurricane Allen showed that the Cayo del Grulla experienced some of the highest water levels, 8 9 ft (2 7 m) above mean sea level, of the ULM and Baffin Bay region during the passage of the storm (USACE 1981) This elevated water level and associated flooding of the surrounding area would have increased land-derived runoff and sediment deposition into Baffin Bay and the southern portion of the ULM

3.2 Recent Dredging Activities

The GIWW was dredged from Corpus Christi Bay to the southern end of the ULM from November, 1994, through February, 1995, at a time interval for which monitoring was conducted in this study. Records for the 1994-1995 dredging cycle were obtained from the Corpus Christi Field Office of the Corps of Engineers. Dates, locations, and volumes for the period of recent dredging are given in Appendix A.

Dredging in Corpus Christi Bay occurred from November 19, 1994, through December 4, 1994, extending from Station 0+000 to Station 10+000 On November 25, 1994, dredging took place in the GIWW directly adjacent to ULM1 Dredging in the vicinity of ULM2 started on December 20, 1994 Work in the region within 5,000 ft of Station 162+000 continued through December 27, 1994 Dredging of the GIWW near ULM2 occurred on December 22, 1994 Dredging in the

region within 5,000 ft of ULM3 occurred from January 15, 1995, through January 20, 1995, covering the distance from Station 196+500 to Station 202+000 The GIWW was dredged directly adjacent to ULM3 on January 16, 1994

The volume of material dredged per unit length along the GIWW during the 1994-1995 dredging cycle is plotted in Figure 3.1h The greatest volumes of material were taken from the northern terminus of the study area, which is near the intersection of Corpus Christi Bay and the ULM, and in the vicinity of Baffin Bay. Only a relatively small volume of material was dredged from the GIWW between Station 10+000 and Baffin Bay This small volume is most likely the outcome of lack of hurricane passage and the drought that south Texas has been experiencing for the past 4 years

3.3 Hydrographic Surveys

Shoaling rates and transport of material into the GIWW were assessed from hydrographic surveys conducted in regions of the study area near dredged material placement sites that were active during the 1994-1995 dredging cycle. Surveys were performed before, immediately after, and 6 and 10 months after dredging, and the survey dates are given in Table 3 1 The surveys were concentrated in two regions north of ULM1 and in the vicinity of the mouth of Baffin Bay and ULM3. Sixteen cross-channel survey transects were established in the study area and the locations of these transects are shown in Figure 1 1

Table 3.1. Chronology of hydrographic surveys.

Period of Survey	Date of Survey
Pre-dredging	December 1-2, 1994
Post-dredging	January 10-11, 1994
6-months post-dredging	June 20-22, 1995
10-months post-dredging	October 19-20, 1995

Depths along survey lines were determined with a dual-frequency (24 kHz and 200 kHz) Echotrac MKII echosounder having an accuracy of ±0 1 ft (0 03 m) for a solid sand bottom Position during the surveys was determined with a Starlink differential Global Positioning System (GPS) receiver Equipment malfunction caused loss of the pre-dredging survey data for transect survey Lines 7 through 16. Post-processing of the data included an adjacent averaging technique to eliminate noise The number of points over which the measurements were averaged

ranged from 10 to 30 depending on the amount of noise in the signal. Depths given in plots of hydrographic survey lines are not referenced to a datum, but to inferred fixed elevations common to individual plots

Comparison of the amount of material deposited in the GIWW between post-dredging surveys can provide information on seasonal variation in deposition rate. The interval between the initial post-dredging survey and the 6-month post-dredging survey covers predominantly winter conditions and is referred to as the "winter survey interval " The interval between the 6-month post-dredging survey and the 10-month post-dredging survey occurred mostly over the summer and is referred to as the "summer survey interval." Plots of survey Lines 4 and 5, performed in the vicinity of ULM1, are shown in Figures 3 2 and 3 3 Both of these locations experienced sedimentation in the GIWW after the post-dredging survey. For each of the three surveys, the volume of material deposited over the winter survey interval was approximately equal to that over the summer survey interval, with about 1 ft (0.3 m) of material deposited over each interval. The deposition rate at the location of survey Line 4 was slightly higher over the summer survey Because the time elapsed between surveys (6 months for the winter survey interval and 4 months for the summer survey interval) was shorter for the summer survey interval, and the volume of material deposited in the GIWW was approximately equal over the two intervals, the higher deposition rate may have occurred during the summer.

The change in elevation of a dredged material placement area is shown in Figure 3 3 as a mound that exists between distances of approximately 4,500 ft to 5,000 ft The material placed at this disposal site is seen to erode, particularly on the eastern side of the mound, over the period of the winter survey interval There is substantially less material eroded from the placement site during the summer survey interval The reduced volume of erosion is most likely due to lower-energy conditions during the summer, and because the most vulnerable material (at shallower depths) was eroded during the winter survey interval

Figure 3 4 shows survey Line 9 near ULM3 The break in the survey line east of the GIWW occurs over a region where the water was too shallow to cross in a boat Deposition in the GIWW is approximately equally distributed between the two survey intervals

Survey Lines 12 and 13, in the vicinity of the mouth of Baffin Bay, are shown in Figures 3 5 and 3.6. Deposition in the channel occurs mainly during the summer survey interval with approximately 1 ft (0.3 m) of material deposited in the GIWW The two surveys show movement of material on the east side of the GIWW Survey Line 12 shows erosion of material from distance 3,500 ft to 5,000 ft, at positions east of the placement site Survey Line 13 appears

to show westward migration of the top of the placement site, however, the 10-month post-dredging survey line was located approximately 60 m north of the initial post-dredging survey line The spatial variation in bottom topography may account for the apparent movement of the dredged material placement mound

Survey Line 16, north of the mouth of Baffin Bay, is shown in Figure 3.7 No significant change in the profiles occurs along the transect outside of the GIWW. Within the GIWW, approximately 1 ft (0.3 m) of material was deposited in the channel over both survey intervals combined Most of the deposition occurred over the summer survey interval

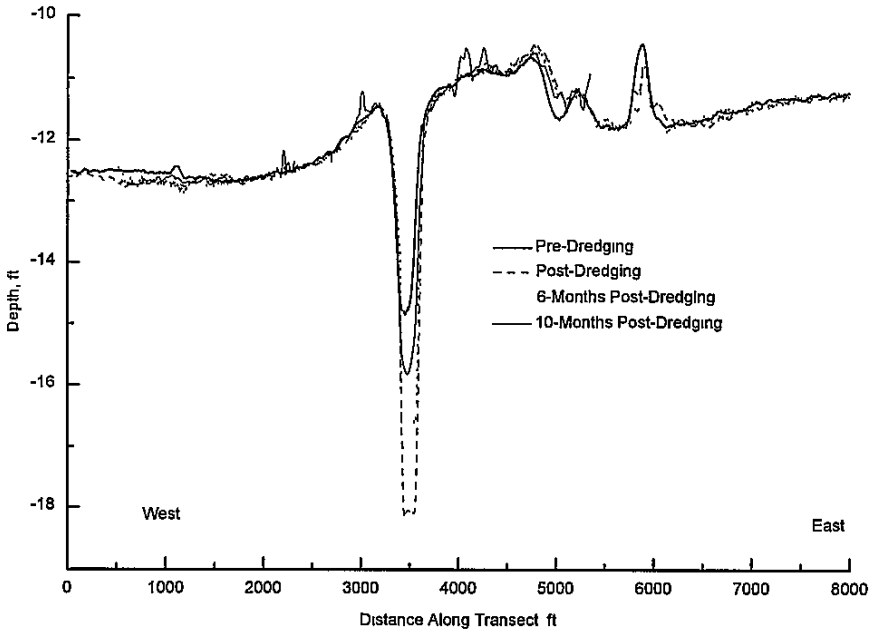

Figure 3 2 Survey Line 4, near ULM1.

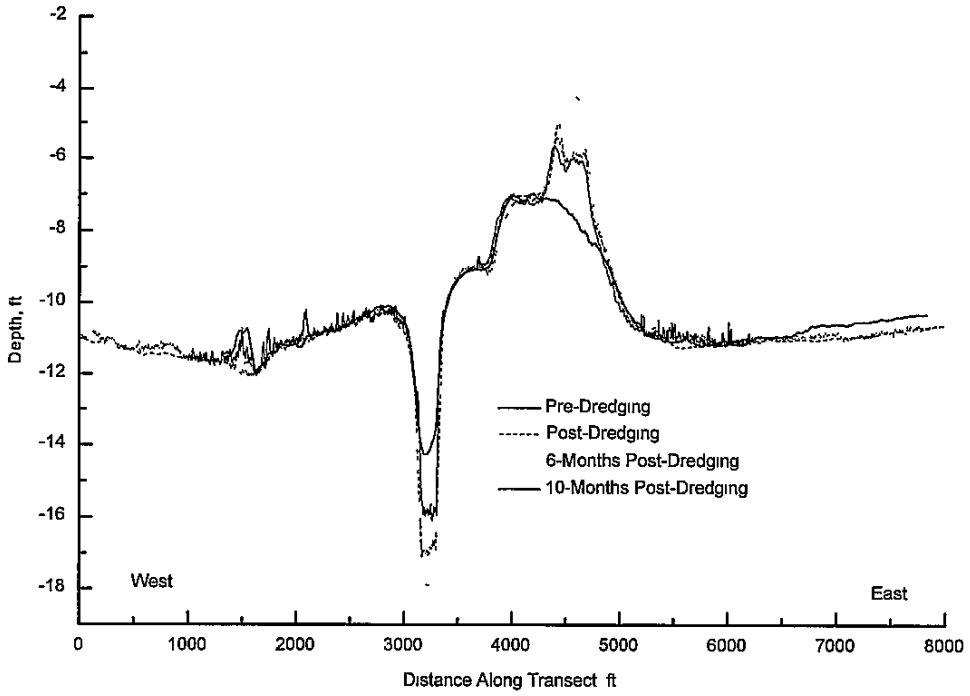

Figure 3.3 Survey Line 5, near ULM1

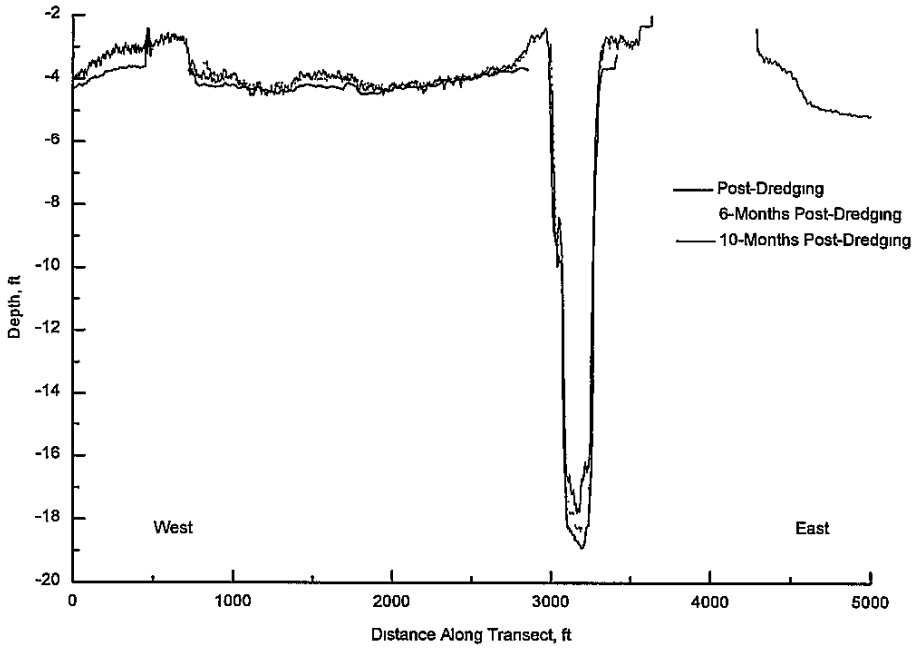

Figure 3.4 Survey Line 9, near ULM3

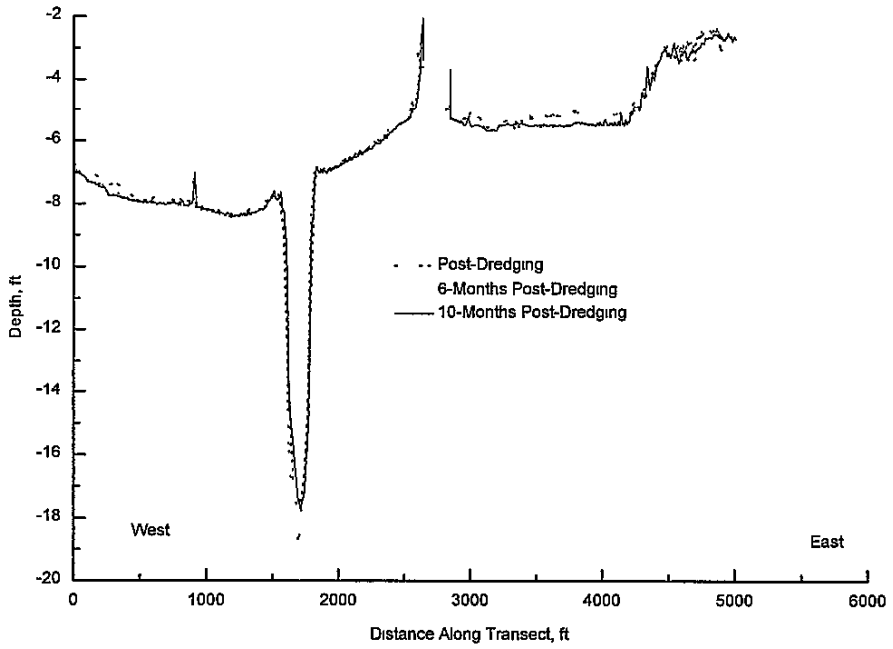

Figure 3.5. Survey Line 12, near southern extent of the mouth of Baffin Bay

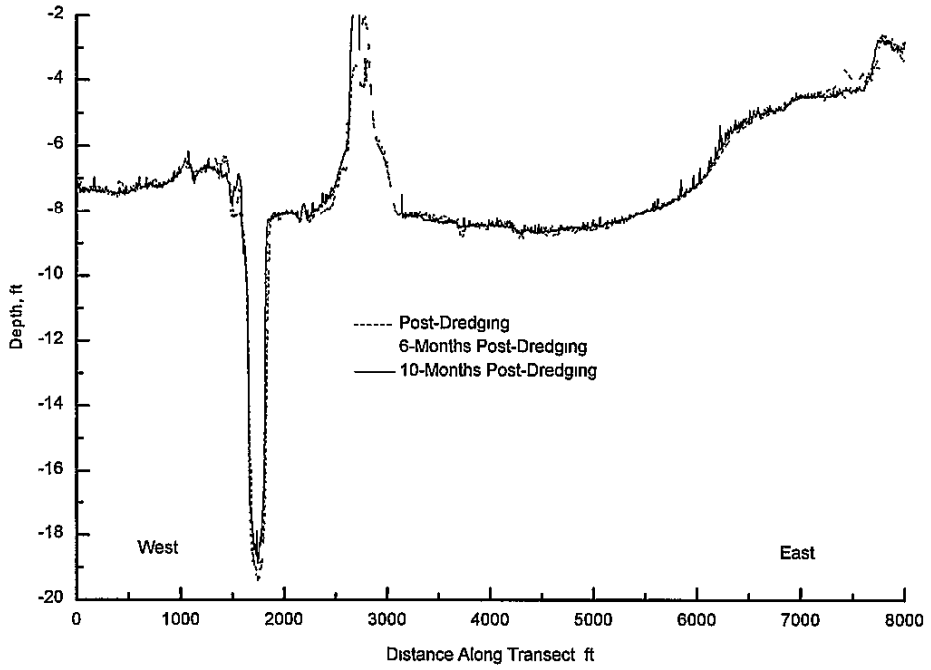

Figure 3 6 Survey Line 13, near ULM2 (mouth of Baffin Bay).

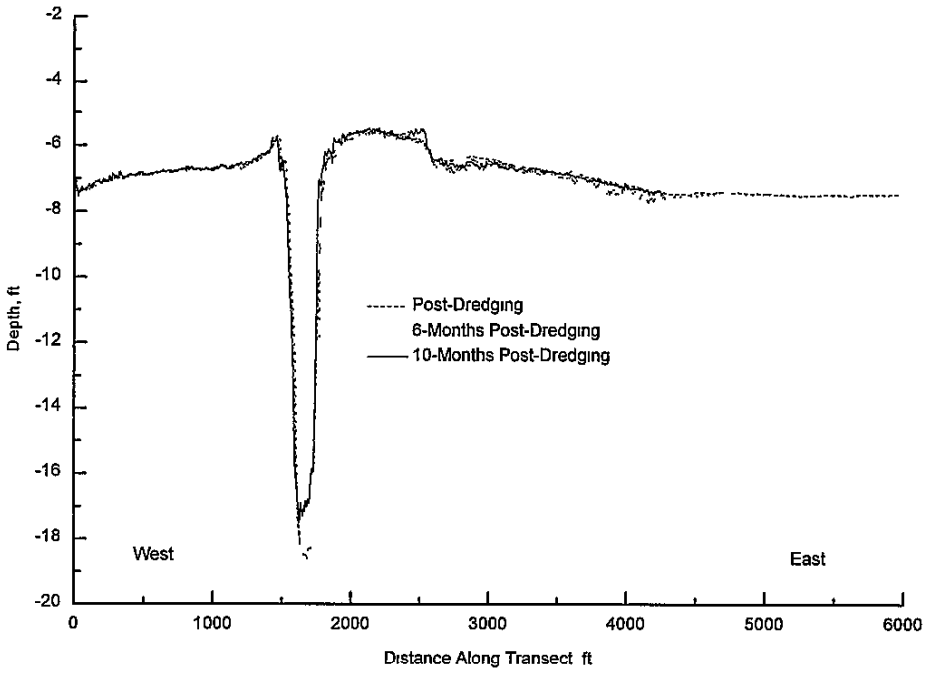

Figure 3.7. Survey Line 16, approximately 2 km north of ULM2.

4. WIND, WATER LEVEL, AND CURRENTS[4]

Wind, water level, and currents vary through a range of time scales from seconds, as associated with wind waves, to years, as associated with the astronomical tide and climatic variability. The interaction of physical processes, both forcing and response, and the resultant motion and water-level changes, control the distribution and transport of sediments An analysis of the characteristics of the wind, water level, and currents is presented in this chapter for monthly and seasonal time periods. This analysis is expected to aid in the understanding of the physical processes of the study site and provide supporting data for correlations with suspended sediment and sediment movement inferred from the monitored flow and the hydrographic surveys.

4.1 Wind

The wind of the region has characteristic seasonal and daily patterns. A persistent southeast wind occurs throughout the year, but is most prominent during the period from approximately April through September From October through March, winds originate from the north as winter fronts that move through the area. Summer winds are characterized by the diurnal land-sea breeze, and this daily wind cycling can be seen in Figure 4 1 as high-frequency fluctuations with a typical range of approximately 6 m/s. Time is given in Julian Day (JD) A Julian Day calendar is provided in Appendix B for reference. Daily fluctuations of the wind speed are produced by a thermal gradient between the land and the Gulf during the day that generates an onshore-directed wind in the afternoon.

Monthly wind roses for the 12-month period January, 1995, to December, 1995, are shown in Figures 4 2 and 4 3 for the Naval Air Station and Yarborough sites, respectively. Both sites show a persistent SE wind throughout the year The winter months experience wind from the north over a significant portion of the time The frequency of occurrence of the north winds is controlled by the number and frequency of winter fronts that move through the study area From April through September, the winds are almost exclusively from the southeast. Wind from the west is rare.

[4] Adele Militello and Nicholas C Kraus, Conrad Blucher Institute for Surveying and Science, Texas A&M University-Corpus Christi

Tables 4.1 and 4 2 give the percent frequency of occurrence for monthly wind speed ranges, mean, standard deviation, and maximum wind speed for measurements taken at Naval Air Station and Yarborough TCOON stations, respectively The spatial difference between Naval Air Station referenced from ULM1 is 3 miles to the west and the Yarbrough station referenced from ULM3 is 1 ½ miles to the south The maximum wind speed is the greatest hourly value that was measured during the month The calmest month is September (see Figure 4 1) which had peak frequencies of occurrence in the 3 to 6 m/s bin for both sites and the lowest mean monthly wind speed The peak mean wind speed occurred in May at both sites, and May had the highest wind speeds of any month of 1995 The maximum recorded wind speed occurred during March at both sites. Because the wind data are collected on a time span of 6 min during each hour, the actual maximum wind speed that occurred during the year may not have been captured although it would not be expected to differ greatly from the measurements.

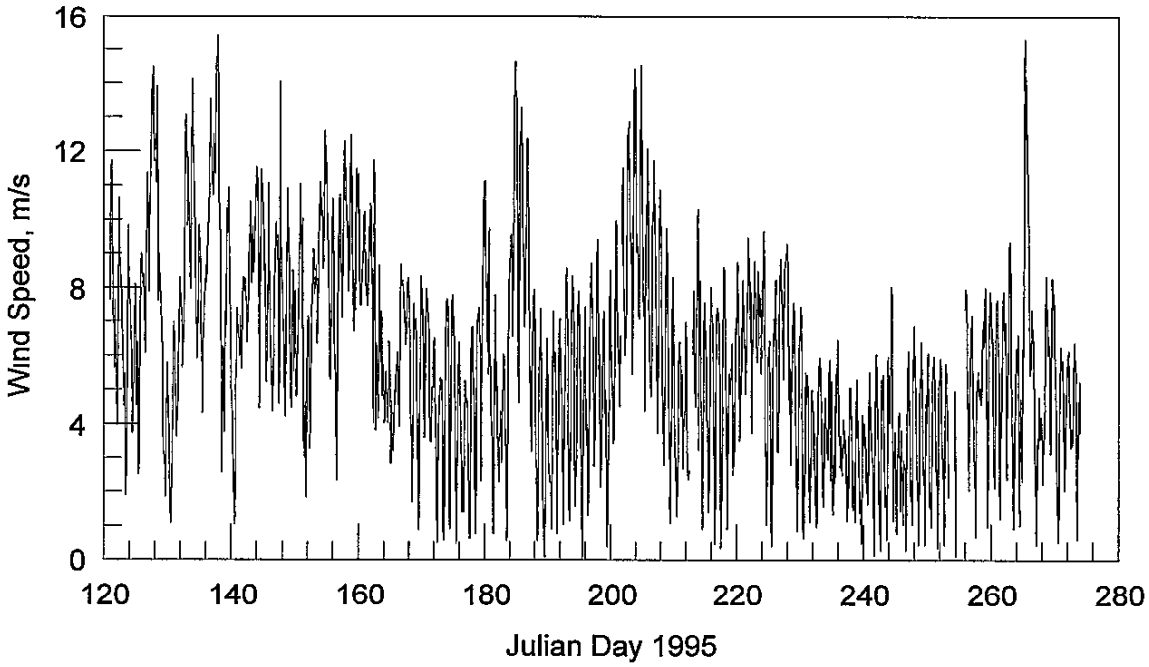

Figure 4 1 Wind speed at Yarborough during May, 1995, through September, 1995.

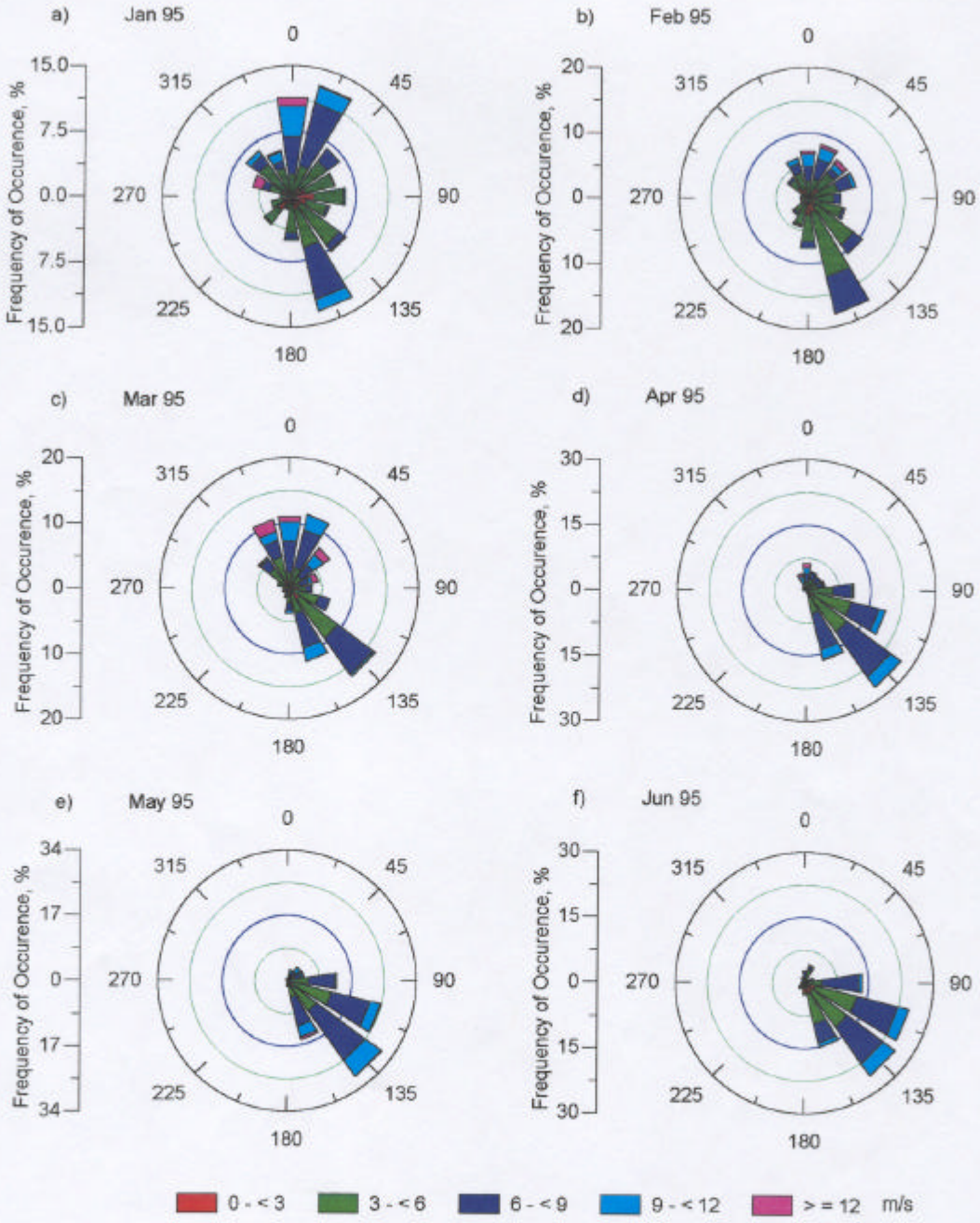

Figure 4.2a-f. Monthly wind roses for Naval Air Station, January, 1995 through June, 1995.

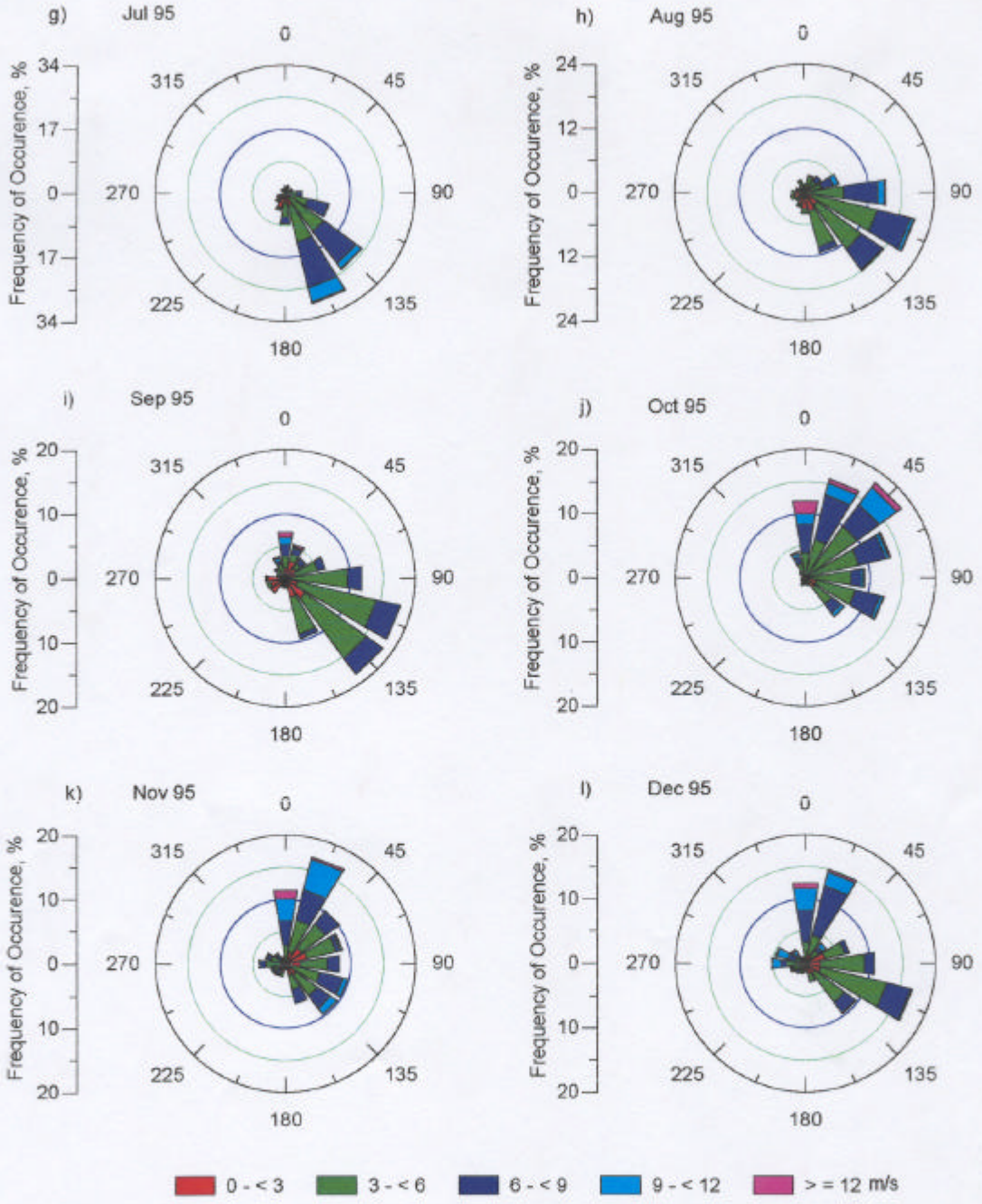

Figure 4 2g-l Monthly wind roses for Naval Air Station, July, 1995 through December, 1995

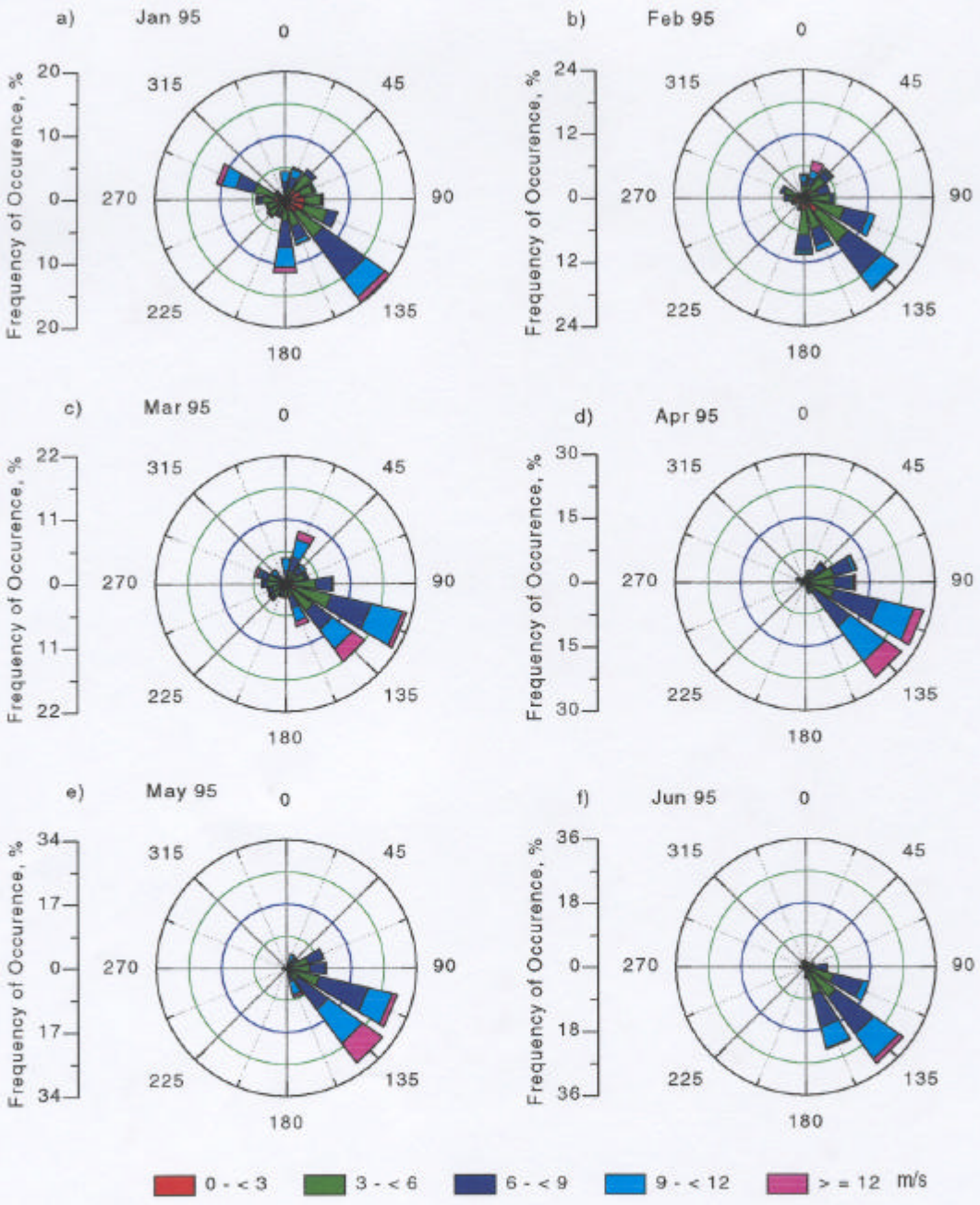

Figure 4.3a-f. Monthly wind roses for Yarborough, January, 1995 through June, 1995.

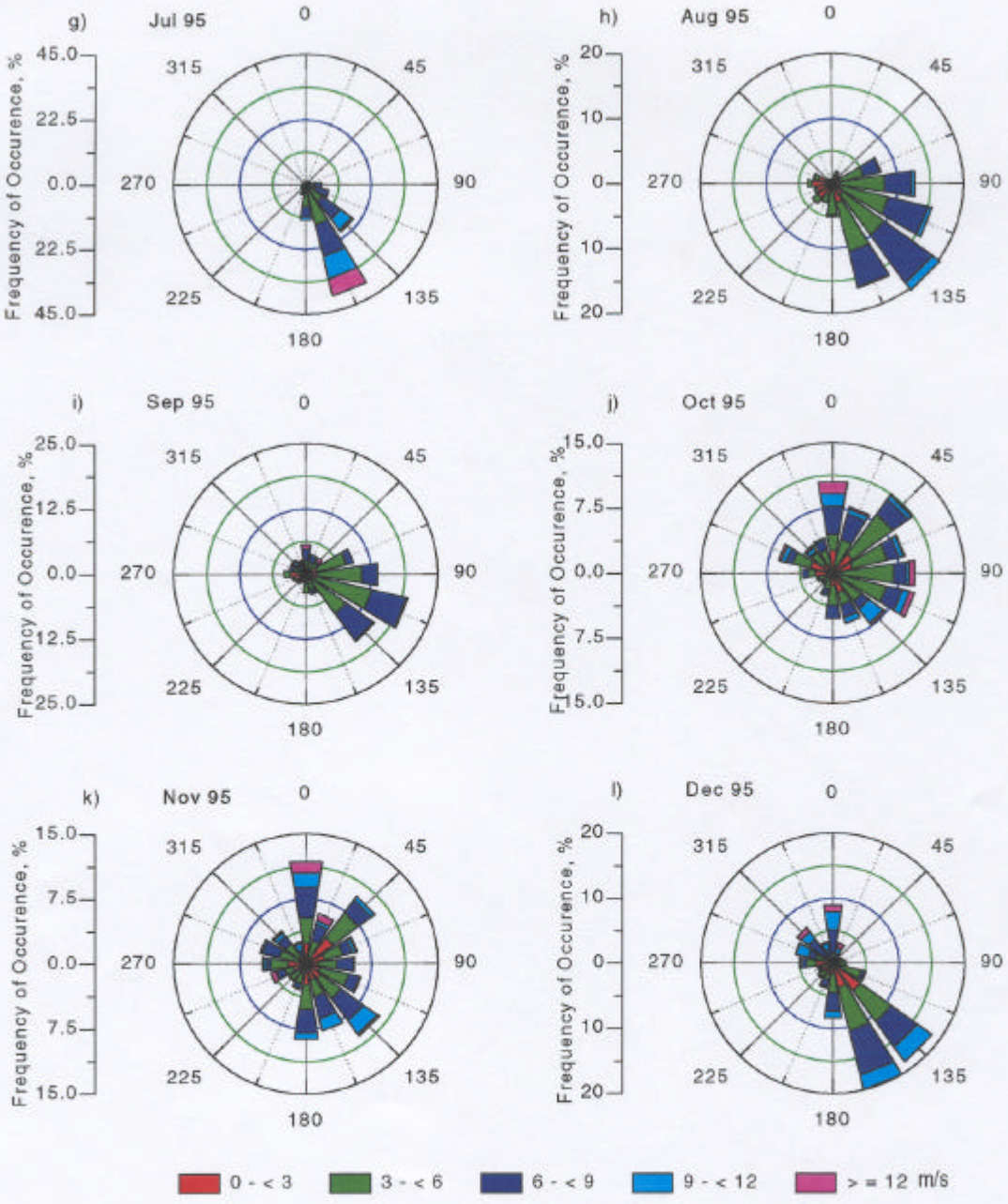

Figure 4.3g-l. Monthly wind roses for Yarborough, July, 1995 through December, 1995.

Table 4.1. Percent frequency of occurrence, mean, standard deviation, and maximum monthly wind speeds at Naval Air Station for the period Dec., 1994, through Dec., 1995.

Month	Frequency of Occurrence, %					Mean m/s	Standard Deviation m/s	Maximum m/s
	0 - < 3 m/s	3 - < 6 m/s	6 - < 9 m/s	9 - < 12 m/s	≥ 12 m/s			
11/94	10	39	40	10	1	6 0	2 5	14 7
12/94	21	47	26	5	2	4 8	2 2	15 4
01/95	18	46	25	9	2	5 2	3 0	15 4
02/95	21	50	22	6	2	4 9	2 8	16 1
03/95	16	31	35	13	5	6 1	3 4	16 9
04/95	9	38	40	11	2	6 2	2 7	15 4
05/95	7	30	46	16	1	6 6	2 6	13 6
06/95	16	38	37	9	0	5 4	2 8	13 2
07/95	19	40	34	7	1	5 1	2 8	13 3
08/95	28	46	22	4	0	4 2	2 8	14 9
09/95	30	51	16	2	1	4 0	2 8	15 7
10/95	13	44	28	10	4	5 7	3 1	16 4
11/95	21	38	26	13	2	5 3	3 2	15 4
12/95	21	40	26	11	2	5 3	3 2	13 5

Table 4.2. Percent frequency of occurrence, mean, standard deviation, and maximum monthly wind speeds at Yarborough for the period Dec., 1994, through Dec., 1995.

Month	Frequency of Occurrence, %					Mean m/s	Standard Deviation m/s	Maximum m/s
	0 - < 3 m/s	3 - < 6 m/s	6 - < 9 m/s	9 - < 12 m/s	≥ 12 m/s			
12/94	26	41	24	9	1	4 9	2 8	13 0
01/95	25	33	26	13	3	5 5	3 4	16 5
02/95	22	39	26	10	3	5 4	3 1	16 2
03/95	14	31	27	20	7	6 7	3 6	21 4
04/95	8	25	35	23	8	7 4	3 2	15 6
05/95	6	23	38	24	9	7 8	3 0	17 8
06/95	11	32	38	17	2	6 5	2 8	14 8
07/95	18	32	30	14	7	6 2	3 3	15 1
08/95	25	44	28	3	0	4 7	2 4	11 0
09/95	24	48	24	2	1	4 6	2 5	16 4
10/95	24	42	21	9	4	5 2	3 2	14 8
11/95	21	38	26	12	2	5 3	3 2	15 4
12/95	23	30	29	15	3	5 8	3 4	17 7

Winds from the Naval Air Station and Yarborough gauges were decomposed into their N-S and E-W components, and monthly spectra were computed from the components Prior to the spectral analysis, motions with periods longer than 30 days were removed from the monthly data by application of a high-pass filter. Figures 4 4 and 4 5 show the monthly spectra for the Naval Air Station and Yarborough gauges, respectively. Frequencies are given in units of cycles/day (cpd) where a value of 1 cpd indicates one completed cyclical motion (assumed to be sinusoidal) over a 24-hr period Note that the vertical axis limits are not the same for all plots of wind spectra.

Seasonal variation in the wind speed spectra can be seen from the existence long-period (low-frequency) wind speeds during the winter months and shorter-period (diurnal) motions in the summer months Winter fronts from the north are readily evident from the low-frequency high-energy peaks seen during December, 1994, through April, 1995, which begin to decline in amplitude in May, 1995 The diurnal winds are evident in the spectra from February through November, but peak in energy in September The onshore direction of the sea breeze is denoted by the diurnal peak occurring in the E-W wind speed curve.

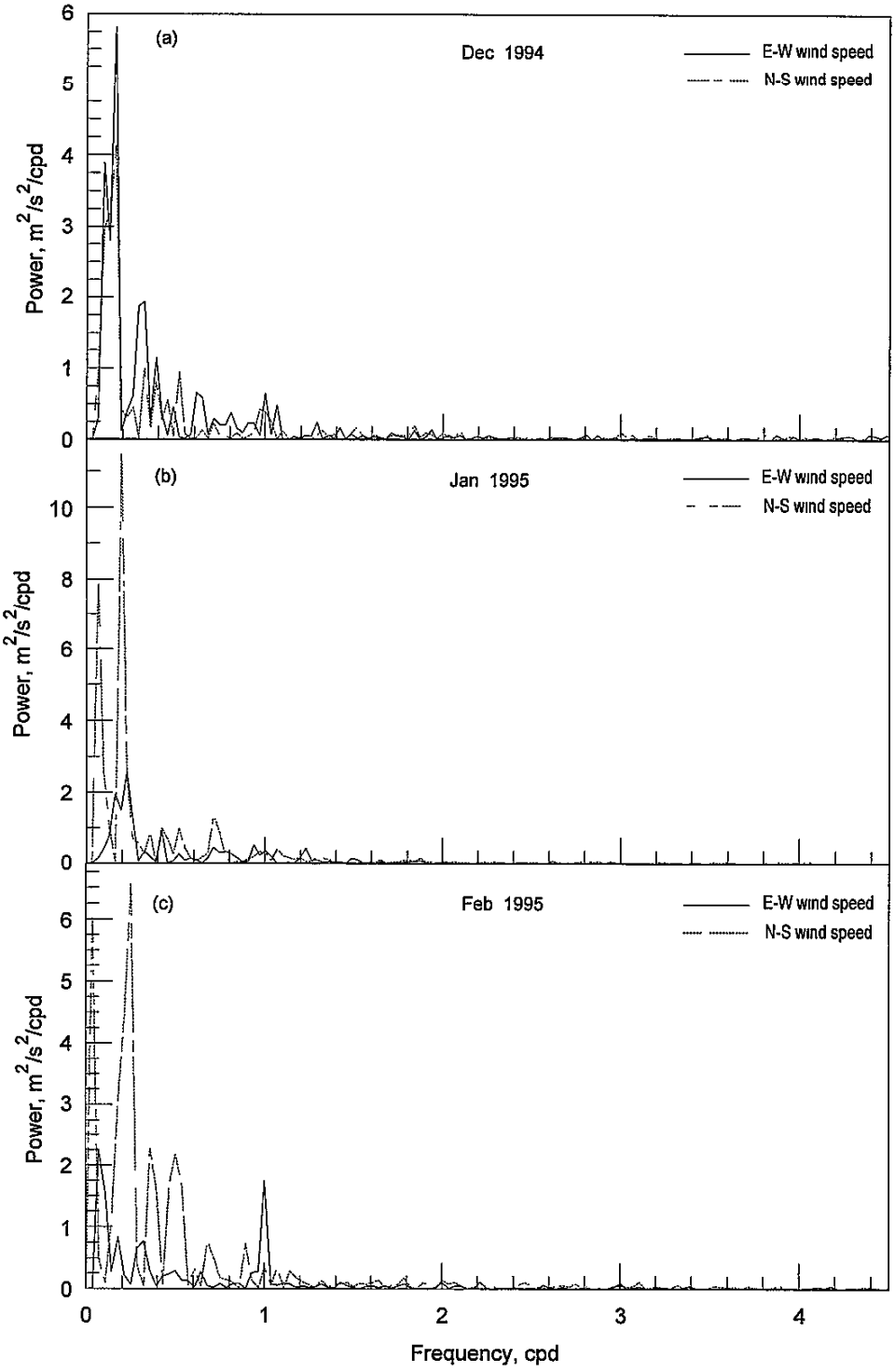

Figure 4 4a-c Monthly N-S and E-W wind speed spectra for December, 1994, through February, 1995, at Naval Air Station

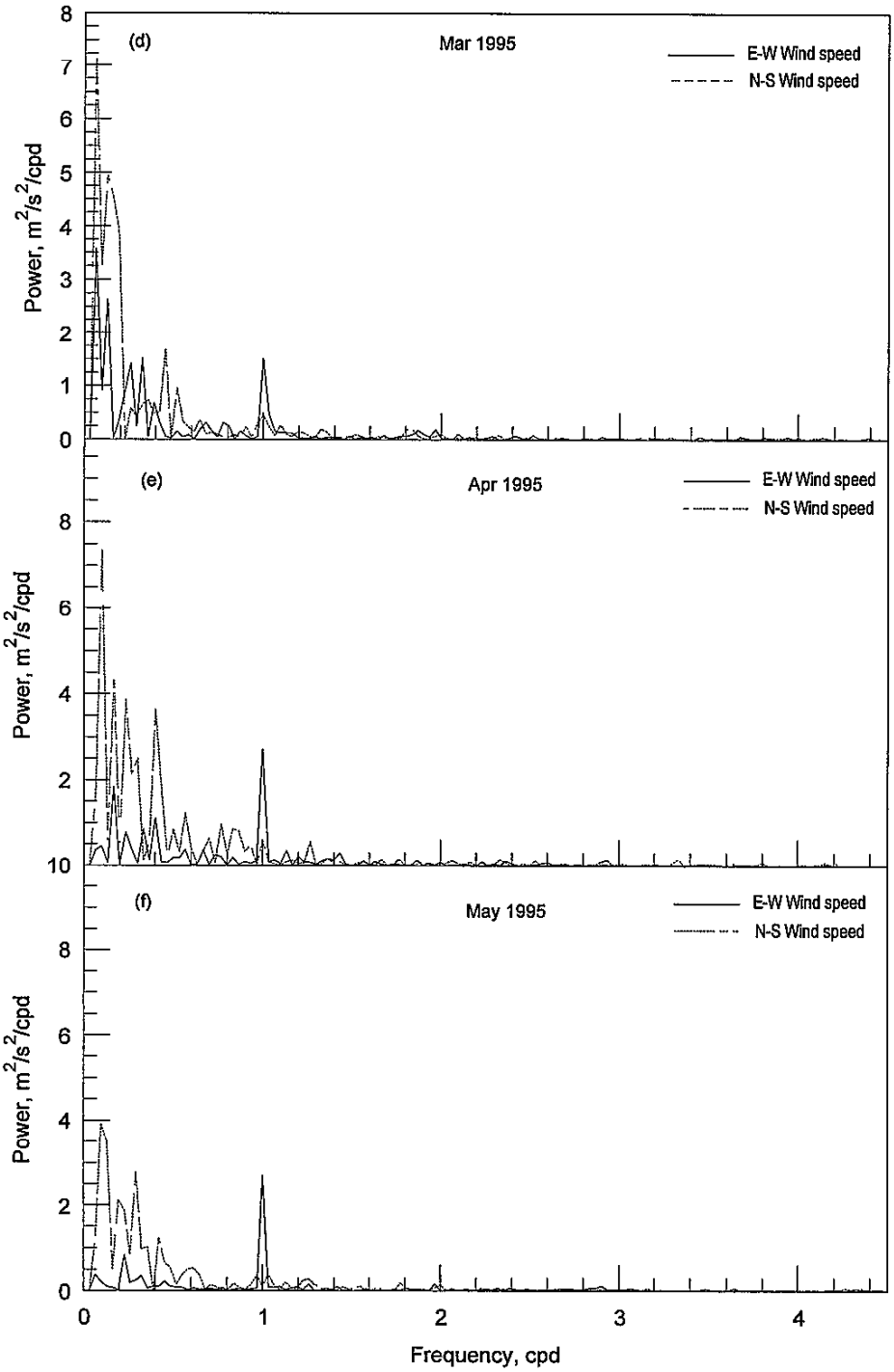

Figure 4 4d-f Monthly N-S and E-W wind speed spectra for March, 1995, through May, 1995, at Naval Air Station.

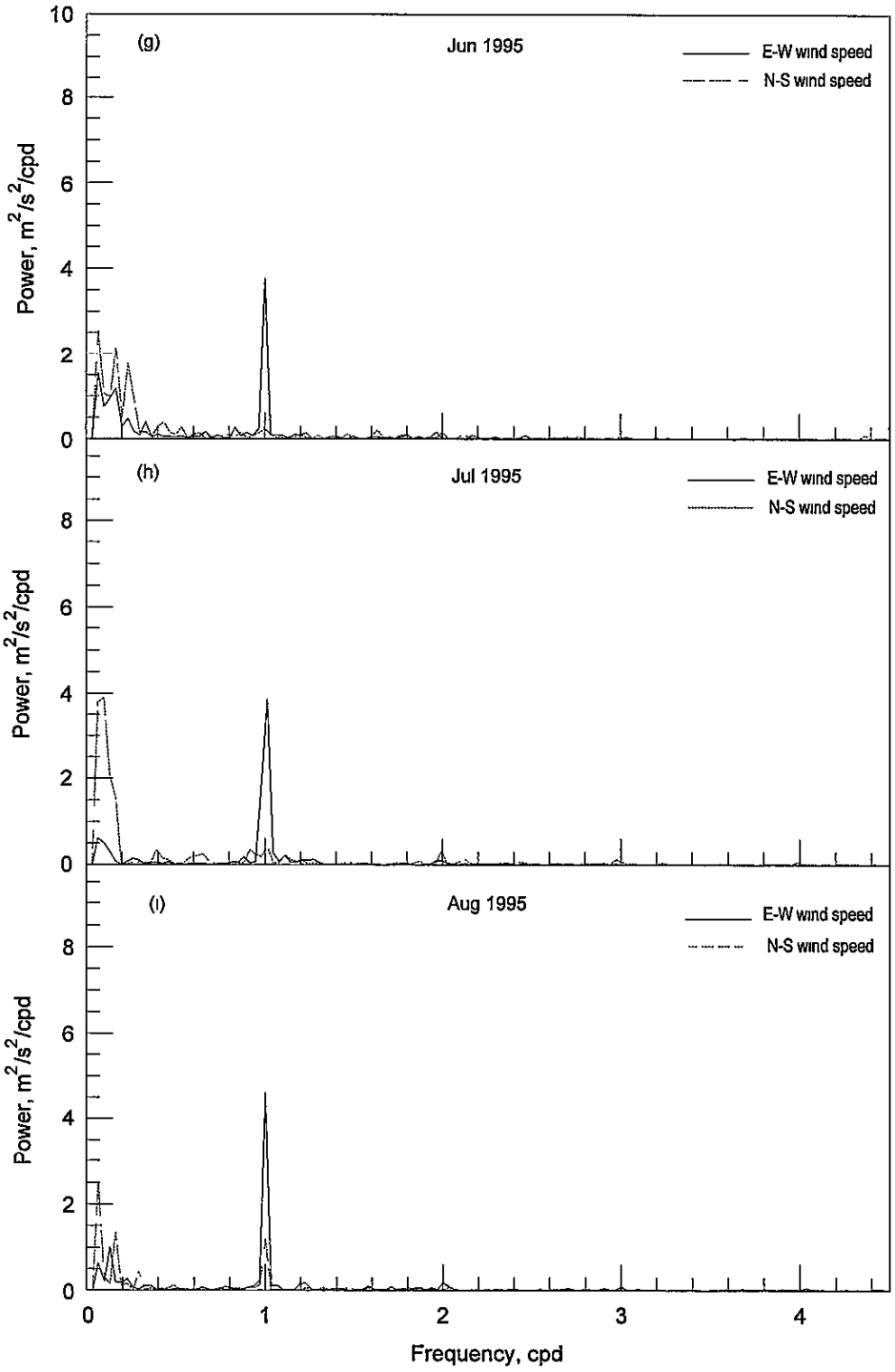

Figure 4 4g-i. Monthly N-S and E-W wind speed spectra for June, 1995, through August, 1995, at Naval Air Station

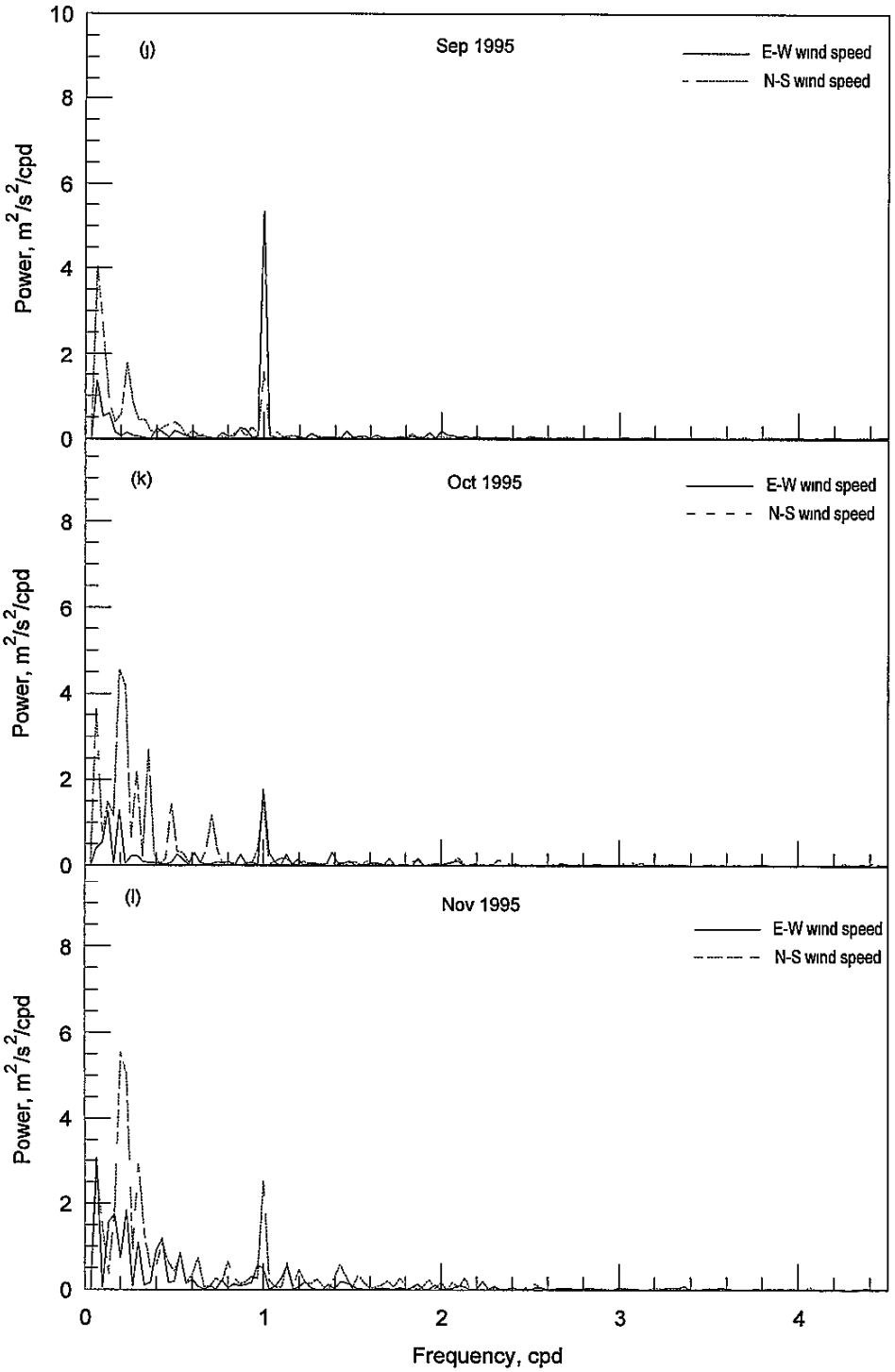

Figure 4.4j-l. Monthly N-S and E-W wind speed spectra for September, 1995, through November, 1995, at Naval Air Station

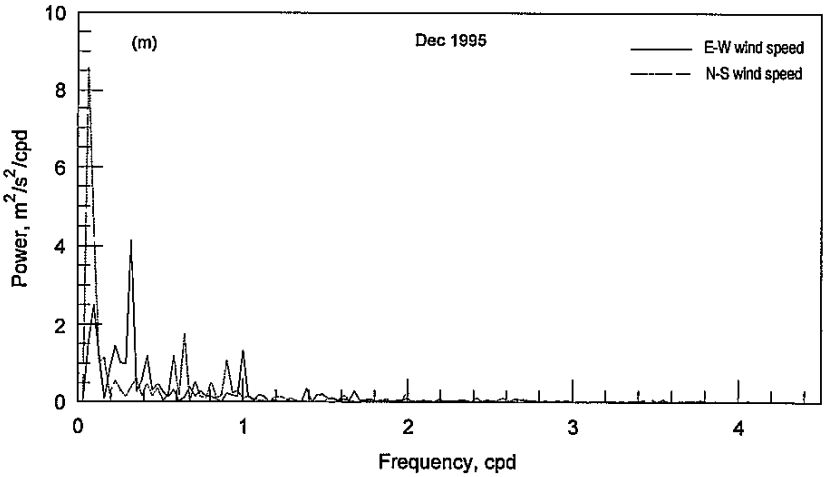

Figure 4 4m Monthly N-S and E-W wind speed spectra for December, 1995, at Naval Air Station

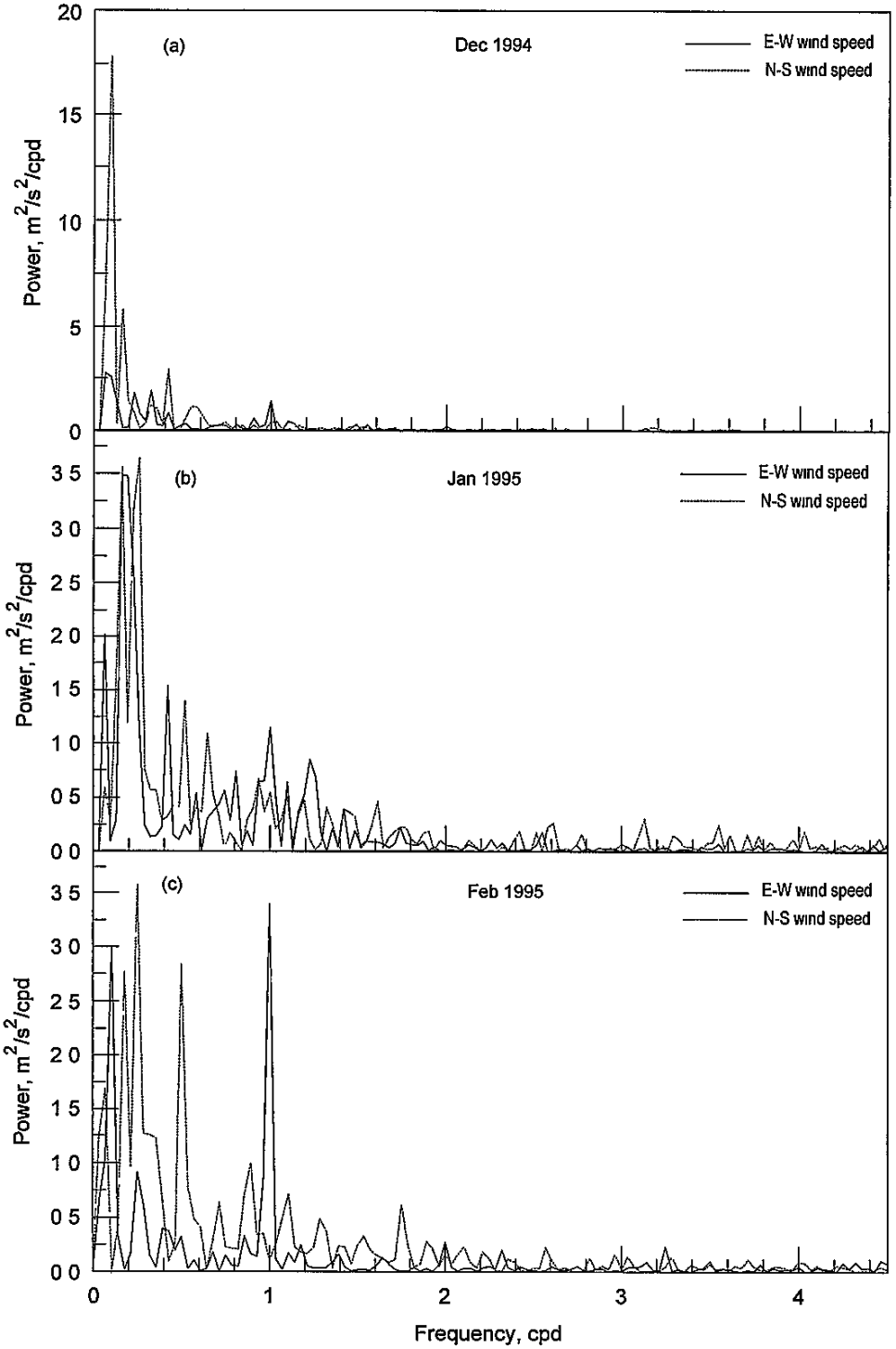

Figure 4 5a-c Monthly N-S and E-W wind speed spectra for December, 1994, through February, 1995, at Yarborough

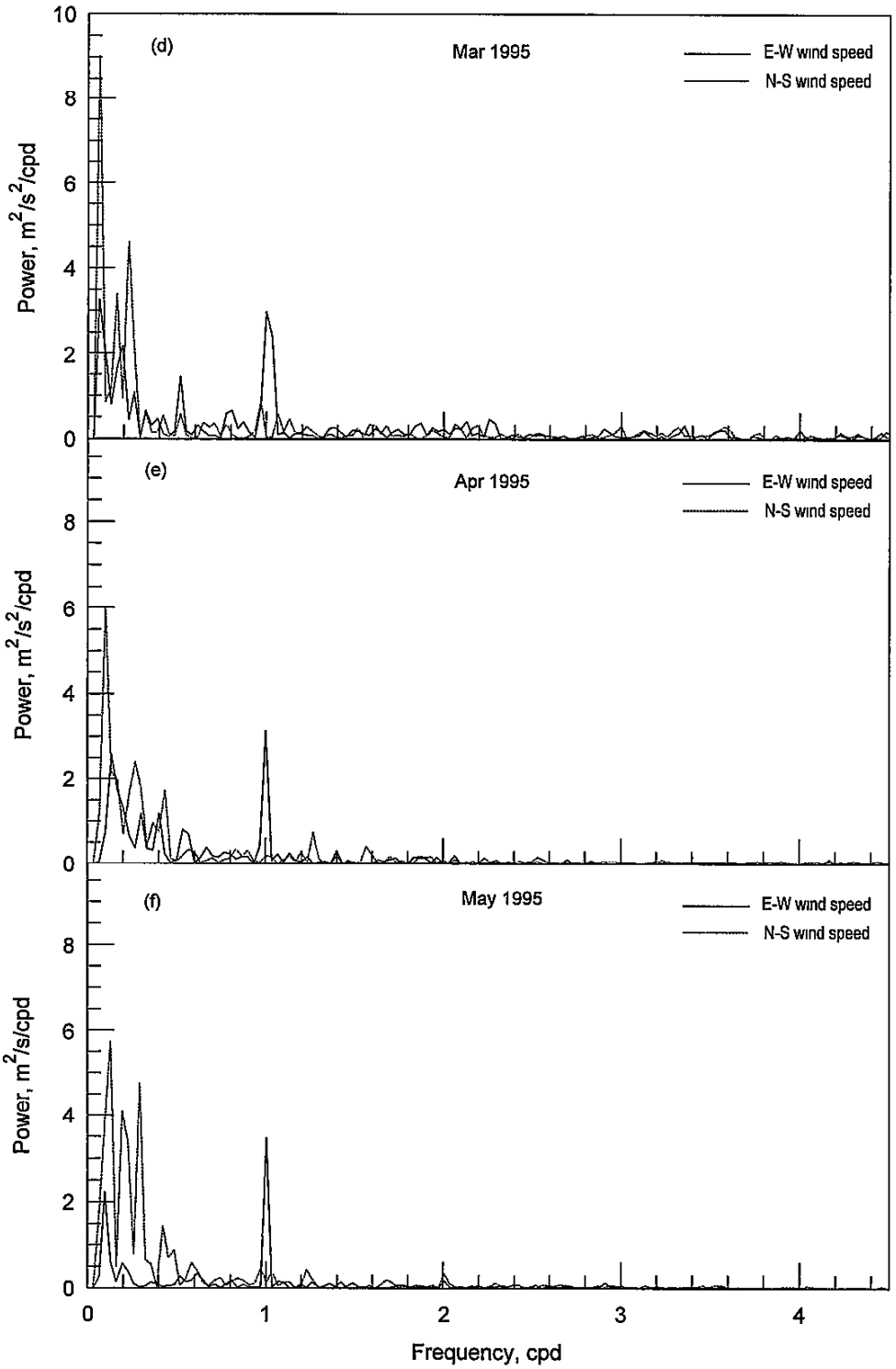

Figure 4 5d-f Monthly N-S and E-W wind speed spectra for March, 1995, through May, 1995, at Yarborough

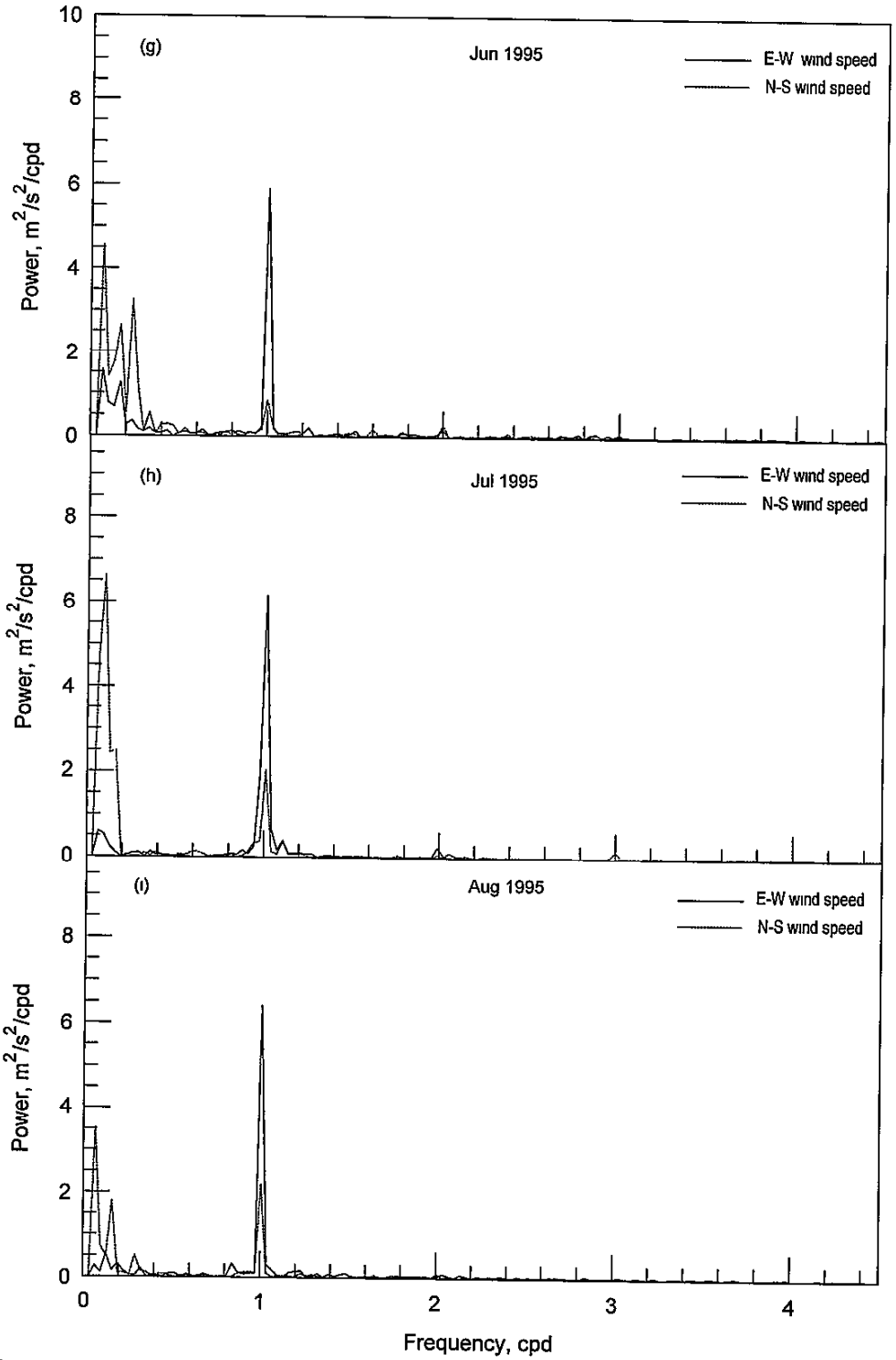

Figure 4.5g-1 Monthly N-S and E-W wind speed spectra for June, 1995, through August, 1995, at Yarborough.

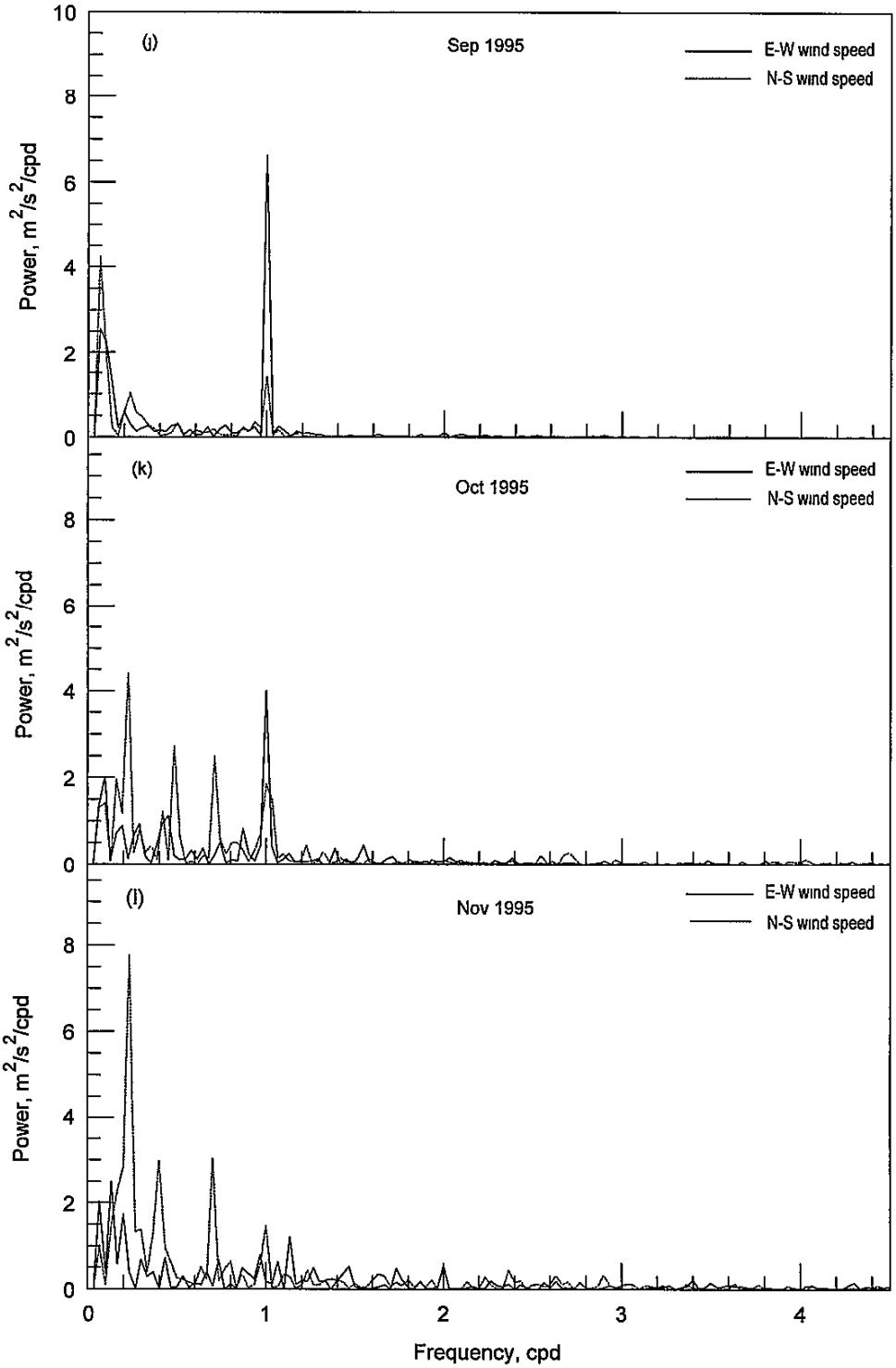

Figure 4 5j-l Monthly N-S and E-W wind speed spectra for September, 1995, through November, 1995, at Yarborough

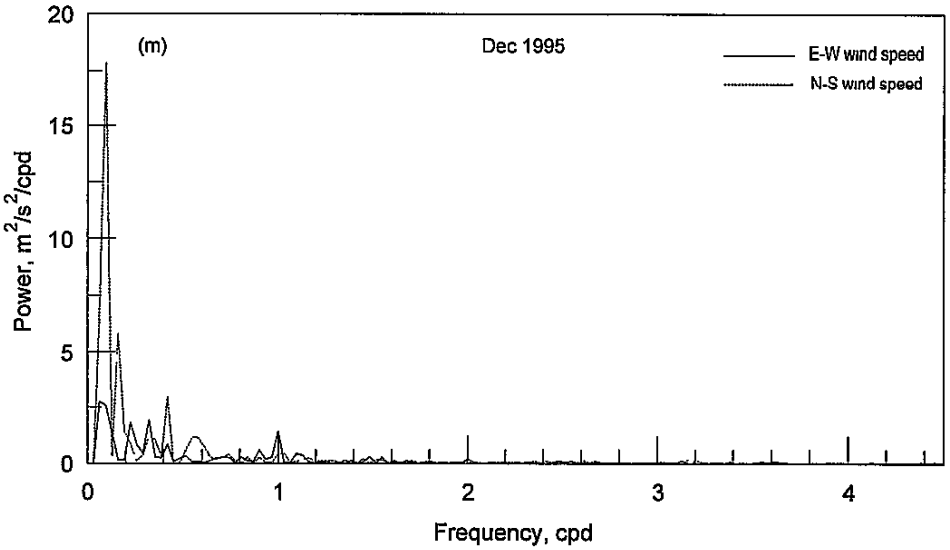

Figure 4 5m. Monthly N-S and E-W wind speed spectra for December, 1995, at Yarborough.

4.2 Water Level

The daily tides along the south Texas coast have both diurnal and semidiurnal components, but are primarily diurnal. The daily tidal ranges in the Gulf of Mexico are relatively small, with the diurnal tide being approximately 0.5 m at the Bob Hall Pier, fronting the Gulf across from Corpus Christi Bay, and the semi-diurnal tide range being approximately 0.1 m Propagation of the diurnal and semi-diurnal tides into bays and estuaries of the Texas coast produces water-level fluctuations that are relatively small compared to the Atlantic and Pacific Coasts of the United States because of the limited tidal range in the Gulf

Fluctuations in the water level over the study site vary spatially due to differences in forcing and depth In the northern reach of the study site the tidal range is larger than in the southern reach because of the proximity of Aransas Pass and attenuation of the tidal signal with distance from the tidal forcing location From Corpus Christi Bay to the ULM, the tidal signal is exponentially attenuated as it propagates through Aransas Pass (Smith 1977), narrow channels, and shallow regions (Smith 1988) Because of the shallow water of the ULM, the tidal signal attenuates steeply, leaving little to no daily tidal signal at the Yarborough gauge. The mouth of Baffin Bay has been documented to contain no astronomical tidal signal (Smith 1988). Thus,

water level fluctuations at ULM2 and ULM3 are produced by 1) low-frequency motions of the Gulf modulating the water level in the ULM, and 2) wind forcing providing direct stress on the water surface. The low-frequency Gulf motions arise through a number of influences including coastal wind-induced setup, seasonal fluctuations, and atmospheric pressure variations

Demeaned water level at the Naval Air Station, Bird Island, and Yarborough stations during September, 1995, are shown in Figure 4 6. Diurnal fluctuations can be seen at each of the stations The tidal signal decreases from Naval Air Station toward the south Tidal peaks at Bird Island follow those at Naval Air Station and occur consistently approximately 5 hr later. A cross-correlation analysis between band-pass filtered (cutoff periods of 10 hr and 38 hr) water levels at Naval Air Station and Bird Island for September, 1995, revealed a lag of 4.9 hr ($r = 0.8199$) between diurnal peaks

The diurnal water level fluctuation at Yarborough is predominantly wind-driven, even during September, which is the calmest month of the year. Evidence for this source of motion is that the peaks of the diurnal water level fluctuations at Yarborough do not consistently follow those at Naval Air Station and Bird Island This inconsistency is revealed by the slight period difference between the diurnal tidal forcing (25 82 hr) and the wind forcing (24 hr) In addition, the peak in water elevation on JD 265 (Sep 22) was due to the passage of a front that had a peak wind speed of 16 4 m/s. For comparison, typical diurnal wind speeds at the Yarborough gauge during September ranged from approximately 6 m/s to 9 m/s.

The dominant water-level fluctuations in the study area occur on the seasonal time scale Figure 4 7 shows low-pass filtered (cutoff frequency of 0 333 cpd) and demeaned water level at Yarborough for 1995. Peaks associated with particular tidal constituents and the diurnal wind are denoted with T indicating the period of motion Seasonal lows occur in the January-February time frame and seasonal high water occurs in the September-October time frame Superimposed on the seasonal signal are fluctuations in water level on many other scales Figure 4 8 shows the demeaned water level spectrum for 1995 at Naval Air Station The dominant peak occurs at a period of 181 days corresponding to the solar semi-annual tidal period (S_{sa}). The dominance of motion on the semi-annual time scale determined here agrees with the findings of Smith (1978) Diurnal motions contain a much smaller amount of energy as compared to the semi-annual motion, however, they are readily visible in the spectrum shown in Figure 4.8. The two diurnal peaks shown in Figure 4 8 correspond to the principal lunar diurnal (O_1) tide at a period of 1.07 day and a peak at 1 day that contains both the luni-solar diurnal (K_1) tide at a period of 0 997 day and the motion induced by the diurnal wind.

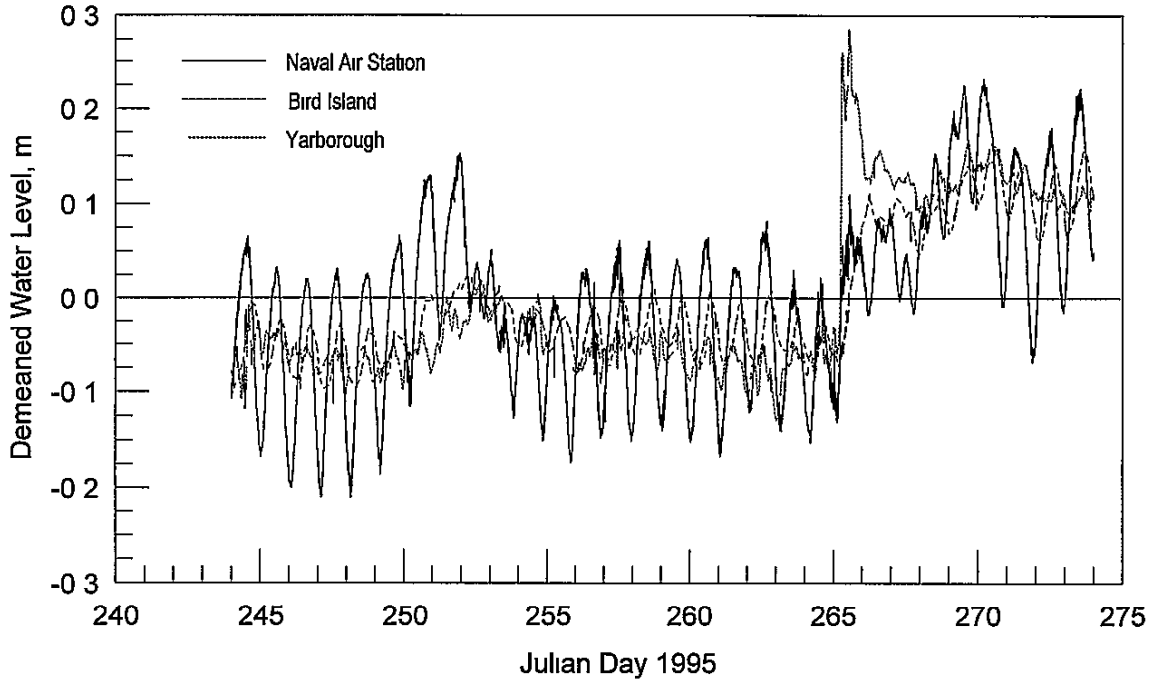

Figure 4.6. Demeaned water level at Naval Air Station, Bird Island, and Yarborough during September, 1995.

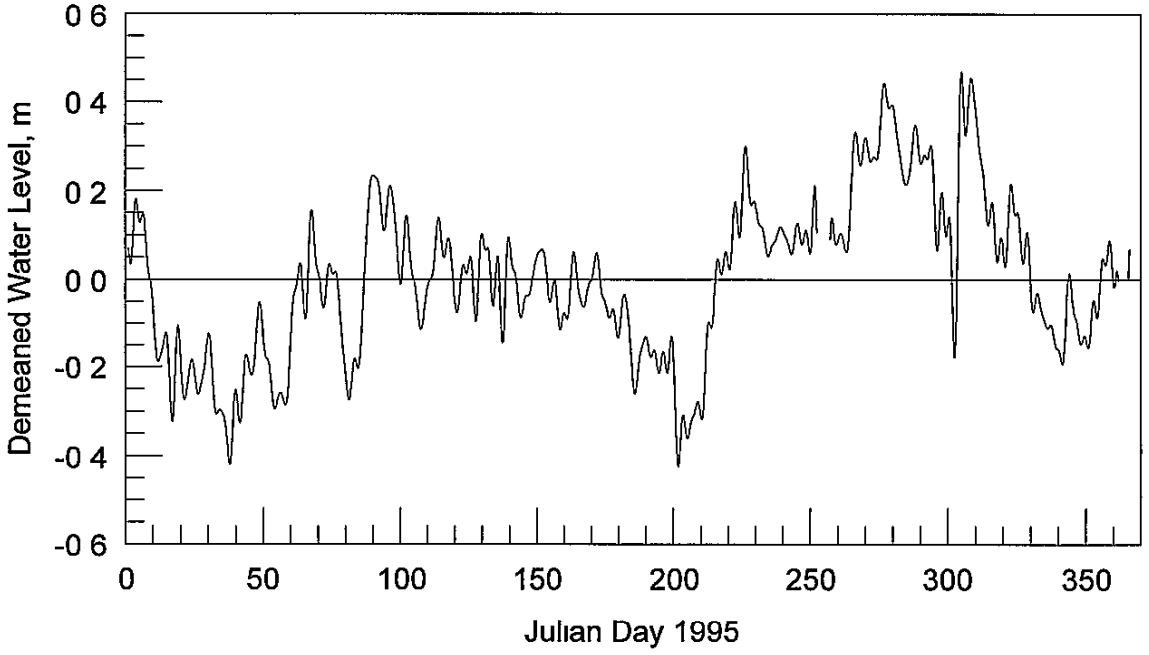

Figure 4.7. Demeaned water level at Yarborough for 1995.

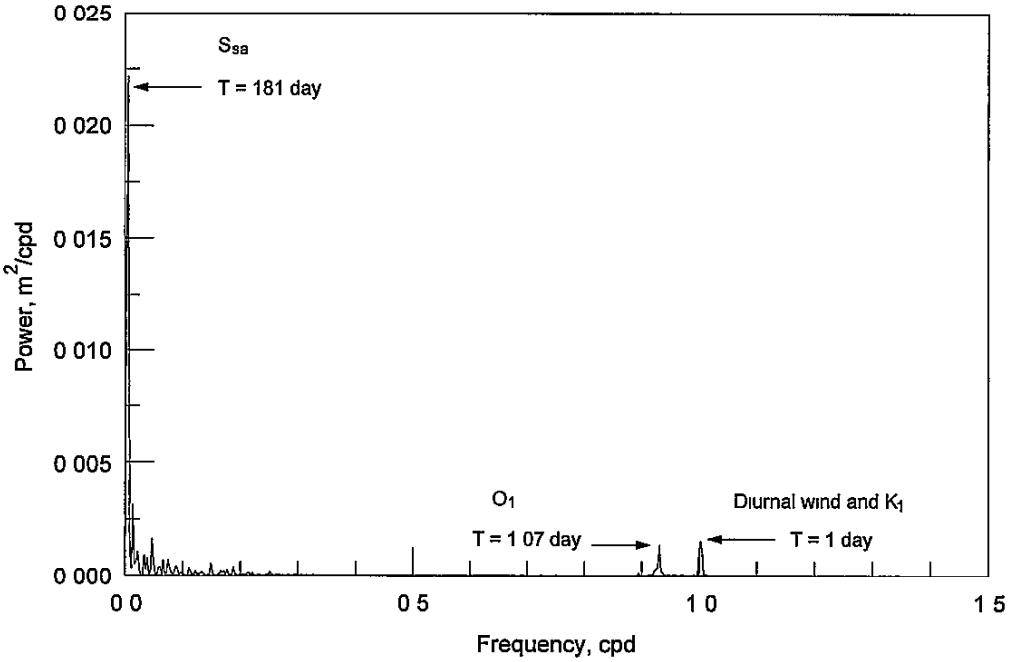

Figure 4 8 Spectrum of 1995 demeaned water level at Naval Air Station

The spectrum for 1995 water level at Yarborough is shown in Figure 4.9. Similar to the spectrum for the Naval Air Station, the dominant motion is on the seasonal time scale and corresponds to the solar semi-annual tidal period. Other low-frequency motions exist and are associated with meteorological phenomena occurring on a range of long-period time scales as well as long-period tidal fluctuations Almost no energy occurs on the diurnal time scale, indicating the attenuation of the Gulf diurnal tide as it propagates south along the Laguna Madre Water-level fluctuations due to the land-sea breeze at the location of the Yarborough gauge are also small due to the limited cross-channel fetch (the land-sea breeze moves predominantly on-offshore corresponding to the across-channel direction)

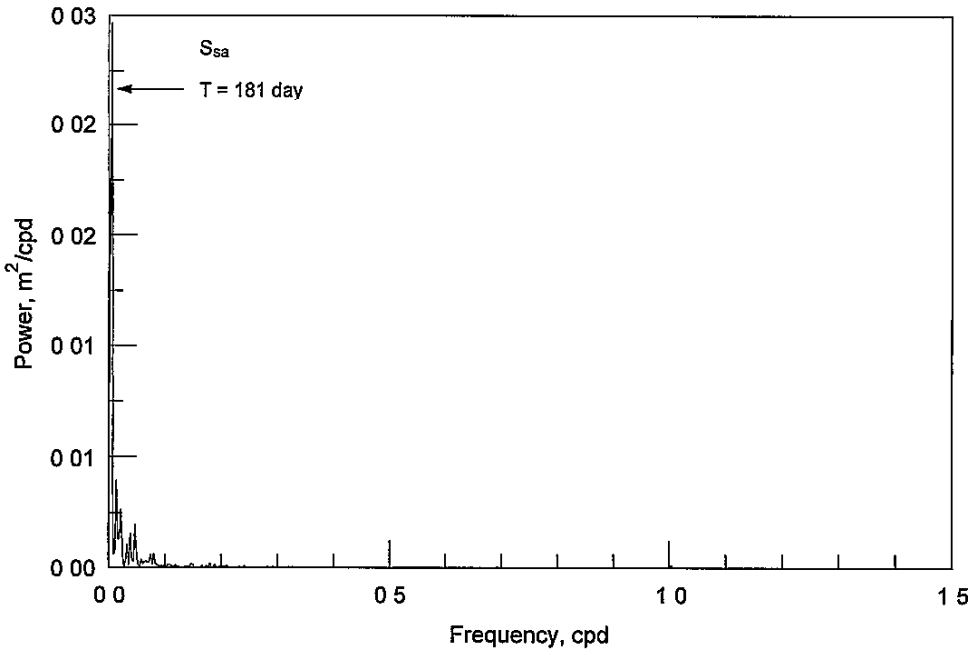

Figure 4.9 Spectrum of 1995 demeaned water level at Yarborough.

4.3 Currents

Currents in Corpus Christi Bay and the ULM are strongly wind driven, but do contain tidal components in the northern areas Monthly spectra for ULM1, ULM2, and ULM3 are shown in Figures 4.10 through 4.12 for the period June, 1995, through December, 1995. Spectra were not computed for months when more than 10% of the data were missing or bad. The scale of the vertical axis is not constant for the spectra plots owing to the variability of peak energy throughout the year Additionally, directional preference in the currents is referred to as occurring on the NS or EW axis This reference merely indicates the relative strength of motion on one axis or the other and does not indicate that currents are confined to only those axes

The current spectra at ULM1 closely follows the pattern of the wind spectra at Naval Air Station shown in Figure 4 4 Relative changes in the low-frequency and diurnal wind spectra occur in the current spectra The current spectra show two energy peaks near 1 cpd for some months The peaks correspond to forcing by the diurnal wind and diurnal tide The semi-diurnal tide is not distinctly revealed in the spectra indicating that its influence on the current is insignificant

During the months of July and August, the low-frequency motions at ULM1 are generally dominated by flow roughly aligned with the EW axis In June, there is a significant low-frequency flow along the NS and EW axes indicating that the long-period trend in the summer current is for the current to flow across the GIWW in the vicinity of ULM1

The southeast winds of summer generate cross-channel flow on the diurnal time scale, with approximately equal energies associated with the NS and EW current components. This energy distribution indicates that the flow has a cross-channel component in the diurnal time scale.

The December current spectra at ULM1 shows the dominant energy at low-frequencies of 0.76 cpd (13 days) and 0.15 cpd (6 6 days), with the NS current having the most energy The EW current, however, has a significant amount of energy as well, such that some cross-channel flow will exist Energy on the 6 6-day period may be a response to the frontal energy at a frequency of 0 24 cpd (4 2 day) in the NS wind (see Figure 4.4m) The current motion on the 13-day period corresponds to the peak in wind energy at 0 065 cpd (16 day) Because the current and wind data are collected at 6-min and 1-hr time intervals, respectively, comparison of the computed frequencies for the current and wind will show differences, with the most difference occurring in the lower frequencies. Thus, low-frequency peaks that occur on periods differing by a few days can actually be at the same frequency

Current spectra for measurements taken at ULM2 are shown in Figure 4 11. Similar to the currents at ULM1, the spectral distribution for currents at ULM2 closely follows that of the wind. Summer currents are characterized by the highest energy peaks occurring on the diurnal time scale associated with the diurnal wind. In general, the easterly component of the wind induces current along the longitudinal axis of Baffin Bay However, because Baffin Bay is not oriented directly along the EW axis and the mouth region is open, currents are not completely restricted to EW flow under the southeast winds. The diurnal current in July has dominant energy along the NS axis, whereas in August and September, the dominant energy is along the EW axis. This rotation of maximum energy direction is associated with the fluctuations in wind direction shown in Figure 4.3g-1 The small energy peaks at a frequency of 2 cpd during July and August are the result of nonlinear interactions of the current through bottom friction.

Low-frequency motion during the summer at ULM2 has less energy than the diurnal motion indicating that the dominant variance in current is on the diurnal time scale In August, there is more energy at low frequencies than during July and September. This low-frequency energy has a peak at 0 07 cpd (15 days) and corresponds to a peak in the NS spectra of the wind found at Yarborough during the same time period.

The spectra at ULM3, given in Figure 4 12, shows that almost all of the energy in the currents is contained in the NS current component The EW current component contains an insignificant amount of energy for the six months shown As with the ULM1 and ULM2 measurements, the current spectra at ULM3 closely follow those of the wind The main difference between ULM3 and the other two stations is that the current is almost completely restricted to flow along the axis of the laguna, which is oriented approximately NS. During October, the currents at ULM3 contain energy at frequencies other than those seen in the wind at Yarborough, and these motions range from the low-frequency end of the spectrum to almost 2 cpd Because the winds of October contain a wide variety of directions and frequencies, being the transition period from summer to winter, water motion in the southern portion of the ULM may experience nonlinear and residual motions on various frequencies associated with the variety of wind motion

In addition to monthly changes in the spectra of the current, monthly variations in current direction also occur and are induced mainly by changes in the wind field Figure 4 13 shows scatter plots of the N-S and E-W components of the current at ULM1 for the period June, 1995 through December, 1995. The summer months are characterized by grouping of the currents predominantly in the NE, NW, and SW quadrants The tendency for westward flow is a response to the SE winds prevalent in the summer, and the peak flows generally occur in the SW direction As the fall months approach, the distribution of the currents changes to predominantly NE and SW flows, and the magnitude of the peak currents is greater than during the summer months

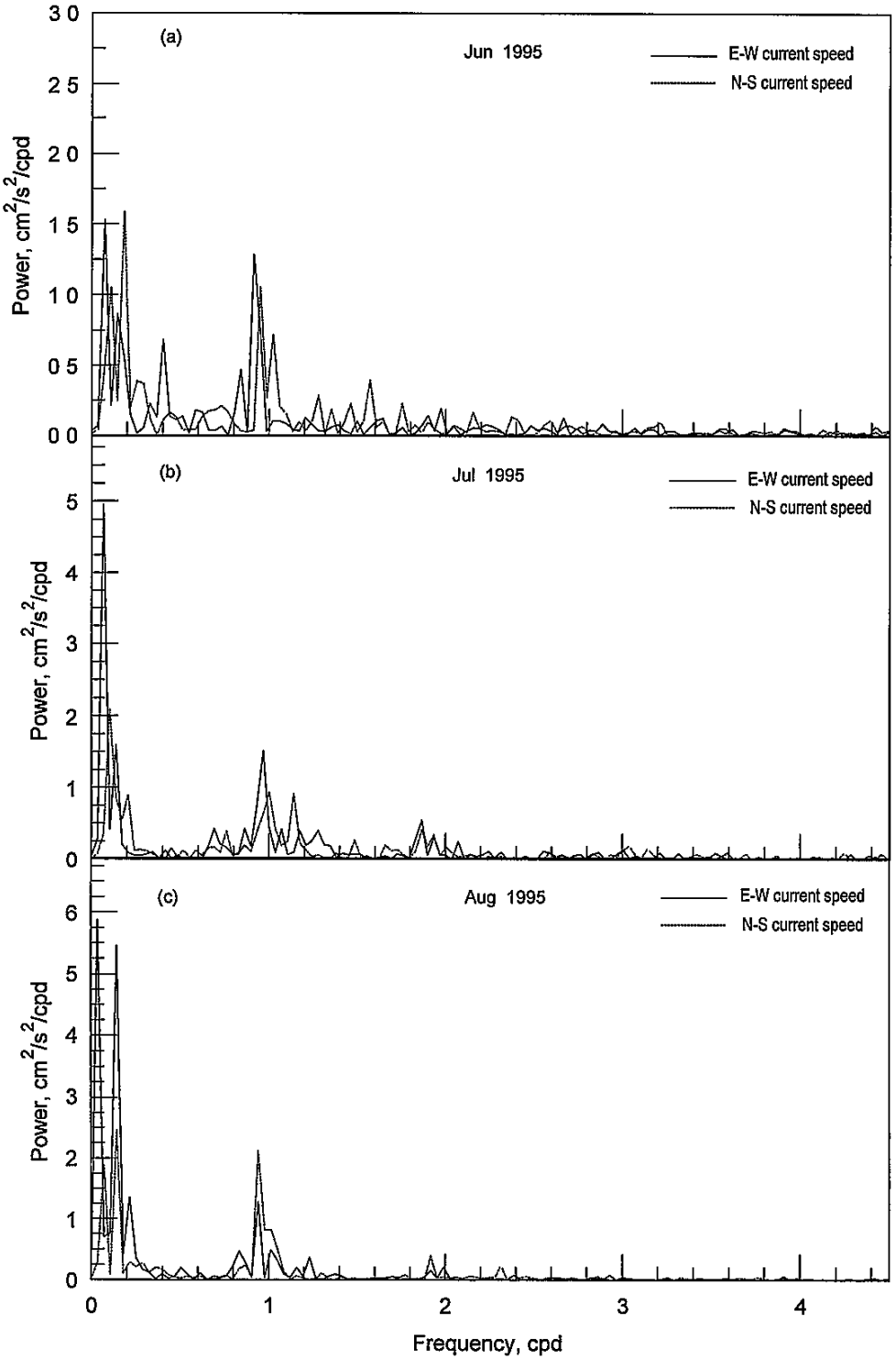

Figure 4.10a-c Monthly N-S and E-W current speed spectra for June, 1995, through August, 1995, at ULM1.

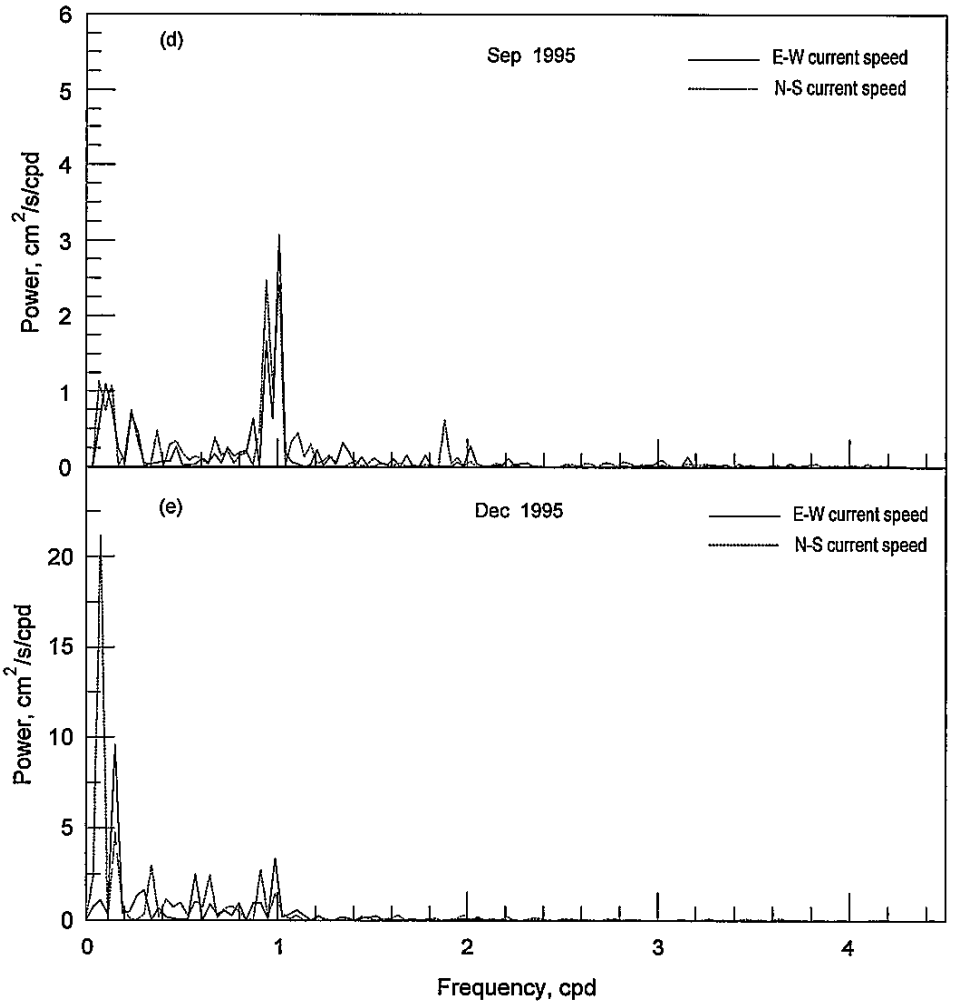

Figure 4 10d-e. Monthly N-S and E-W current speed spectra for September, 1995, and December, 1995, at ULM1.

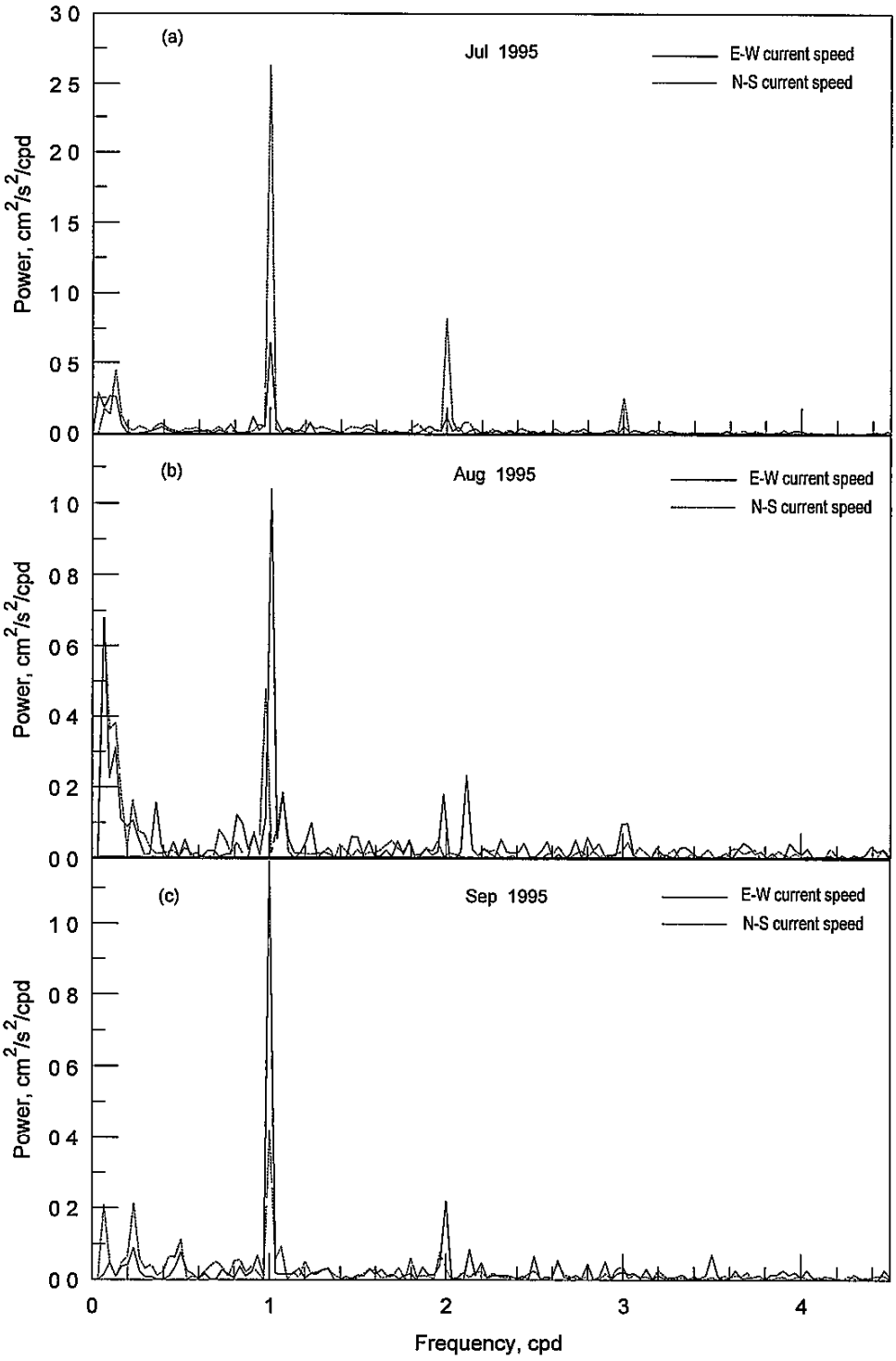

Figure 4.11a-c Monthly N-S and E-W current speed spectra for July, 1995, through September, 1995, at ULM2

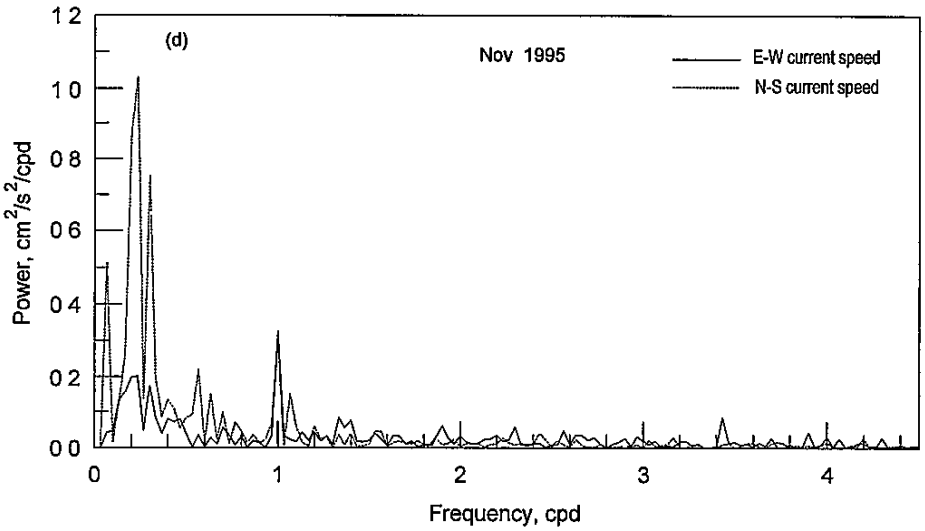

Figure 4 11d Monthly N-S and E-W current speed spectra for November, 1995, at ULM2.

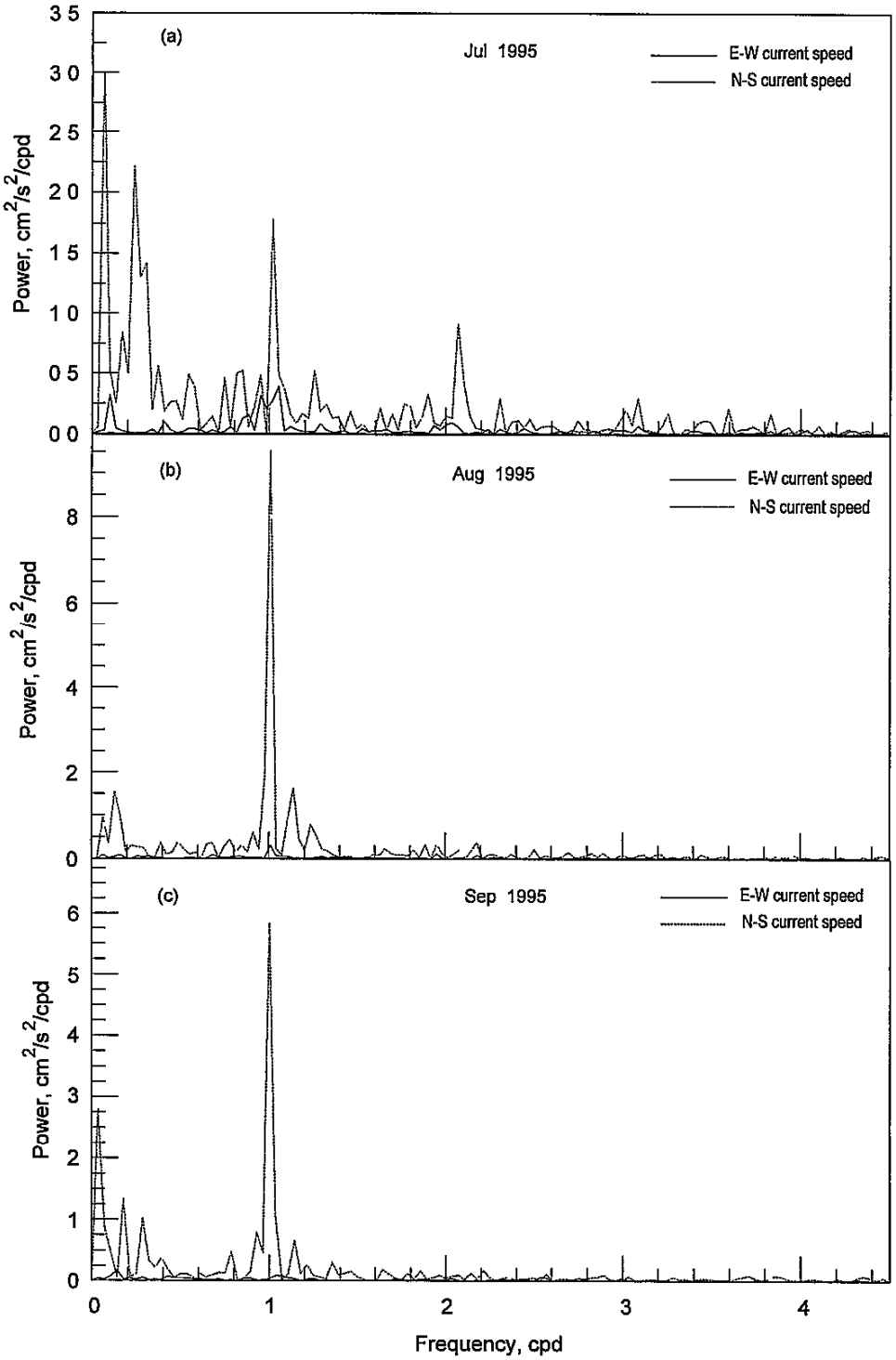

Figure 4 12a-c. Monthly N-S and E-W current speed spectra for July, 1995 through September, 1995, at ULM3

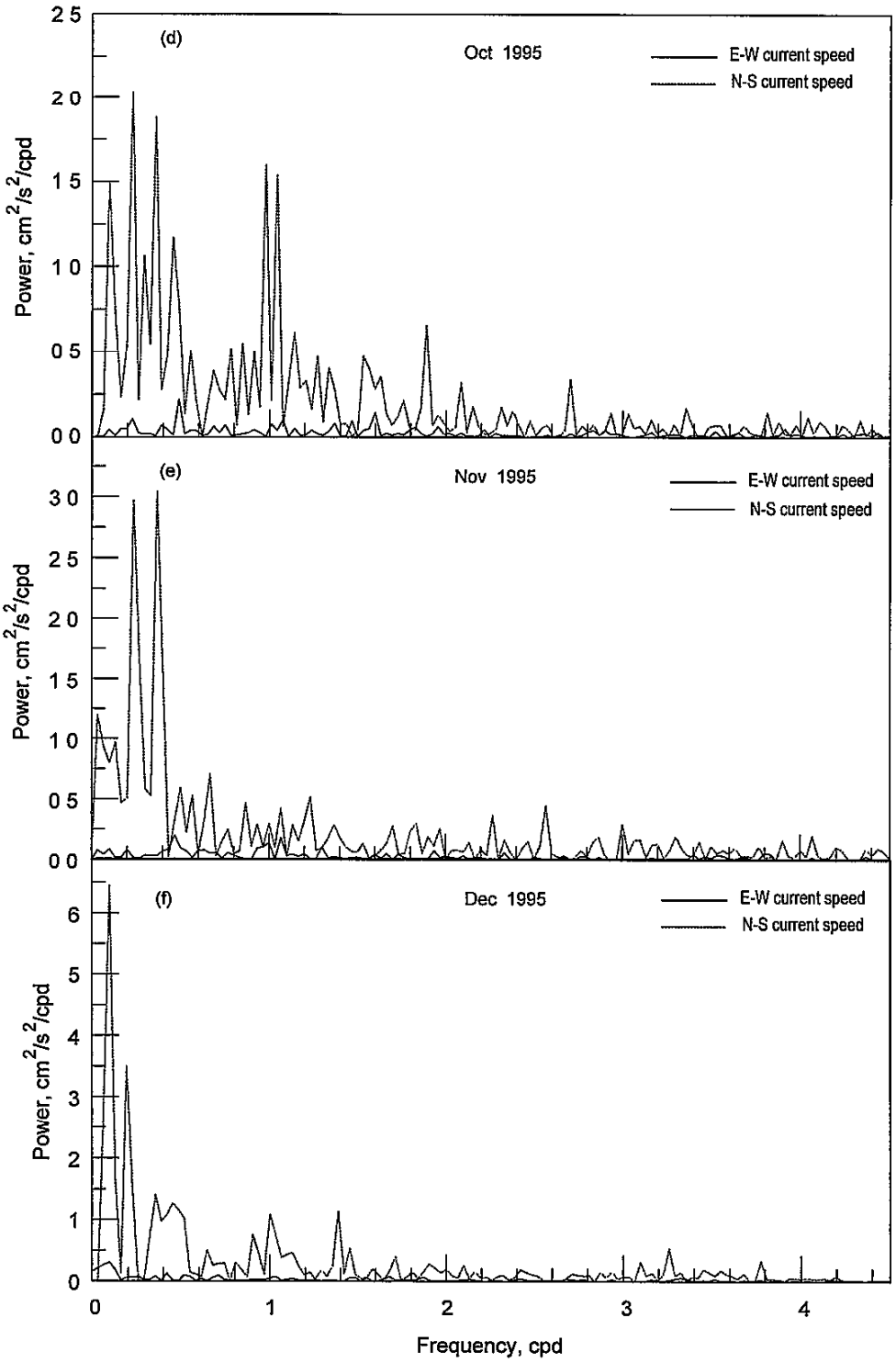

Figure 4.12d-f. Monthly N-S and E-W current speed spectra for October, 1995 through December, 1995, at ULM3

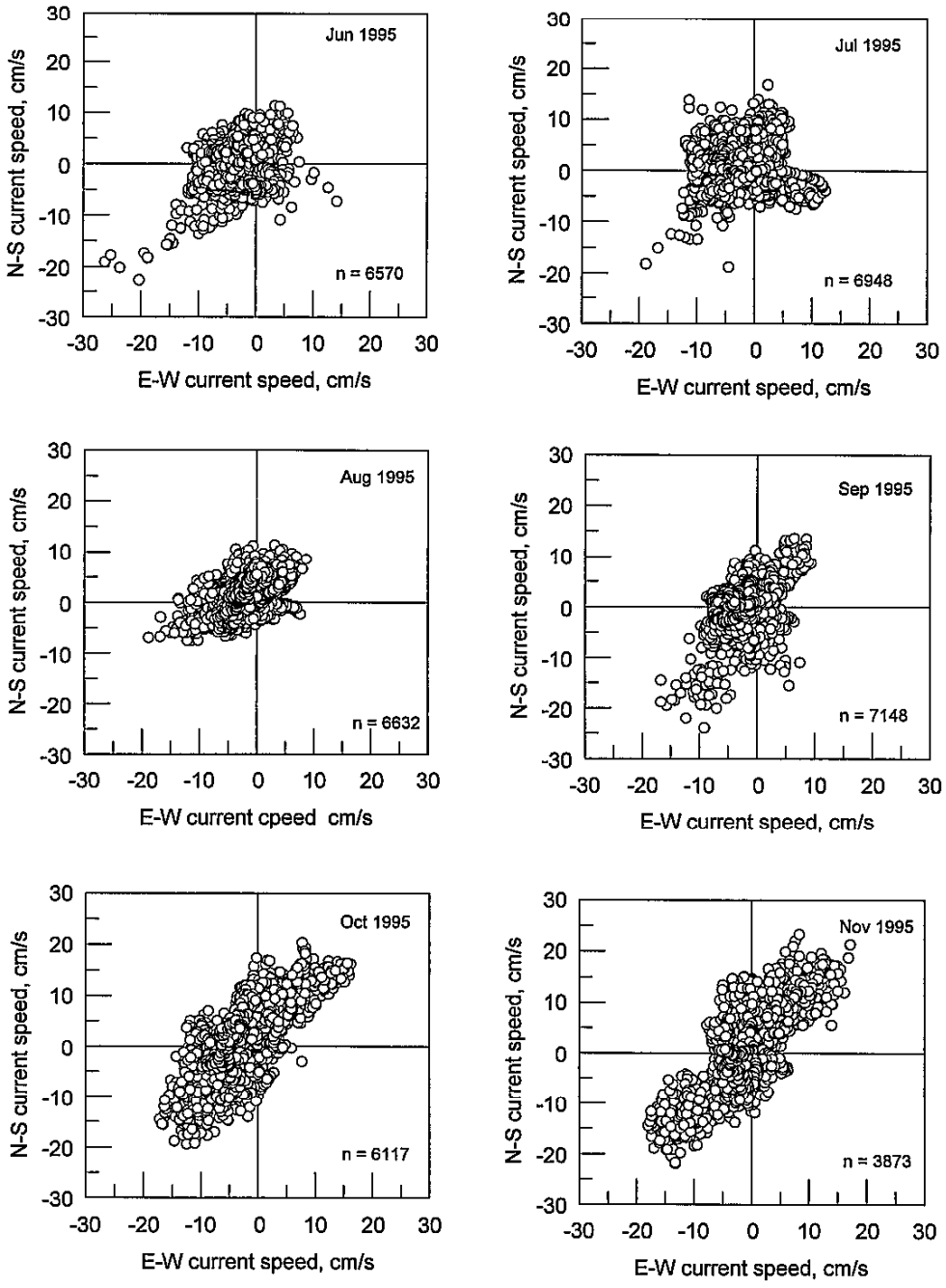

Figure 4.13a Scatter plots of current speed at ULM1, June, 1995, through November, 1995

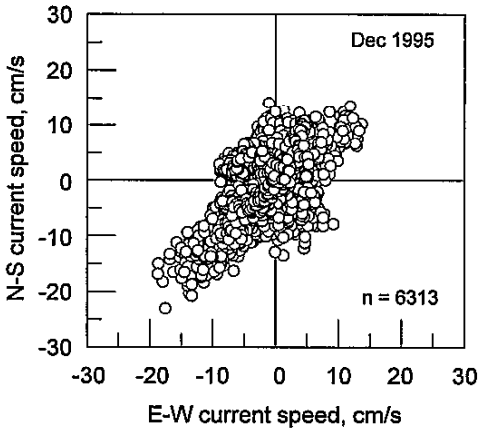

Figure 4.13b Scatter plot of current speeds at ULM1, December, 1995

Scatter plots of the NS and EW components of the current at ULM2 for the period June, 1995, through December, 1995, are shown in Figure 4 14. Seasonal changes in the current distribution are not great at ULM2. The currents, in general, are roughly equally distributed in each of the directional quadrants over the 7-month period of available data The maximum current speeds tend to occur in the NE and SW directions

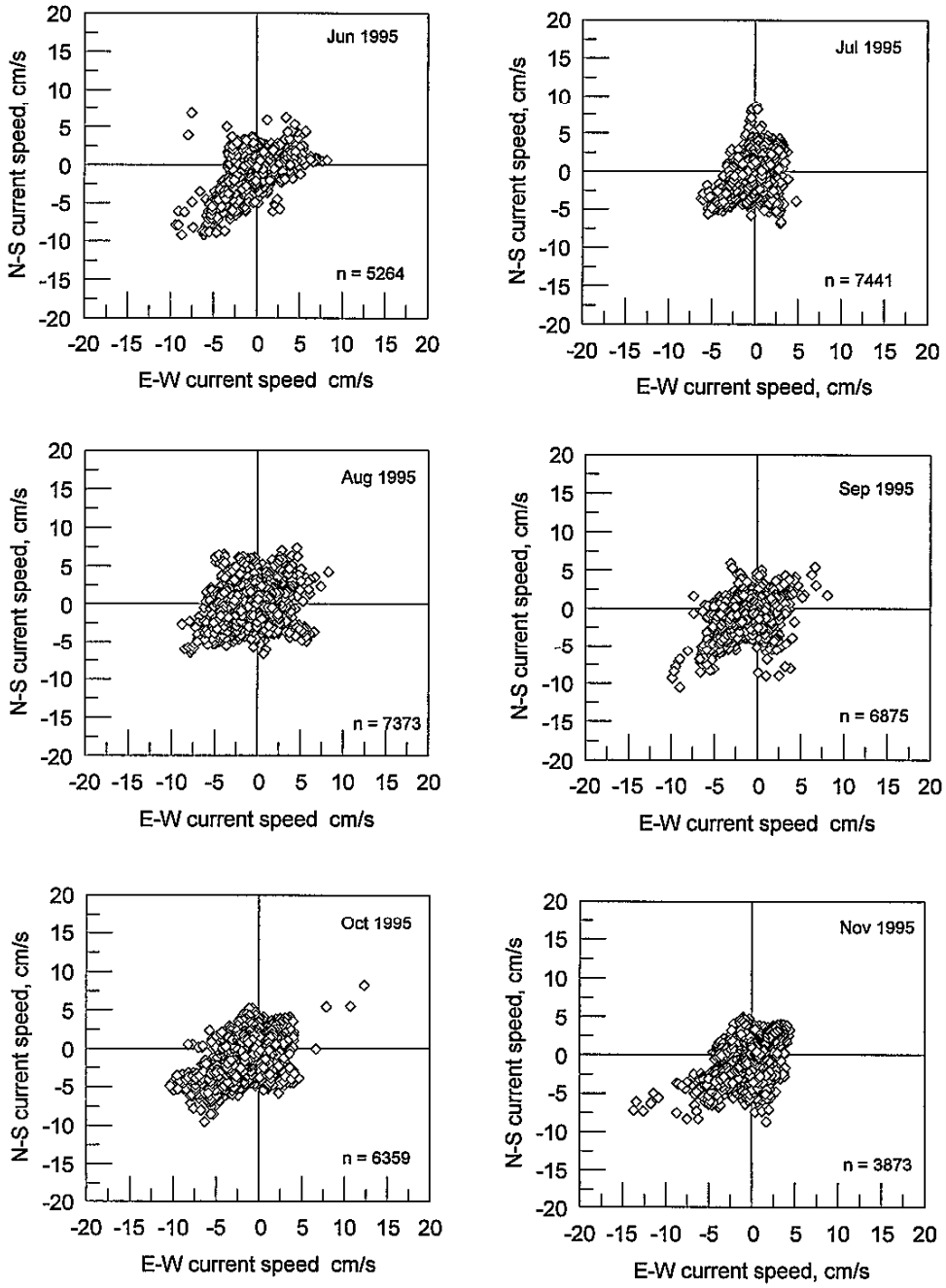

Figure 4 14a. Scatter plots of current speed at ULM2, June, 1995, through November, 1995

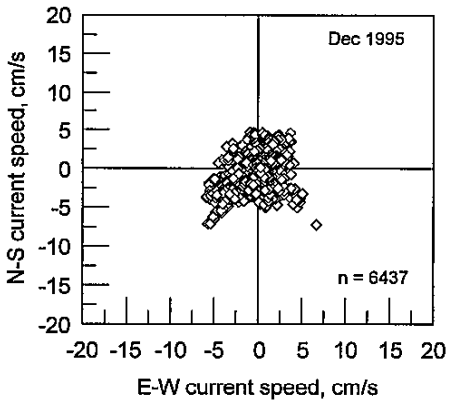

Figure 4 14b Scatter plot of current speeds at ULM2, December, 1995

Scatter plots of the currents at ULM3 for the period June, 1995, through December, 1995, are shown in Figure 4 15 The currents tend to flow along the NS axis with very little EW movement during any of the seven months shown The restricted EW currents are a result of the limited cross-channel fetch at the site of the ULM3 platform During July, 1995, and August, 1995, the current speeds are increased over other months possibly due to an increased circulation induced by the summer wind. August, 1995, shows a predominance of northward flowing current which is a response to relatively strong southerly winds that occurred during that time period

4.4 Physical Processes Interactions

A description of the general motions of water at each of the three ULM platforms in response to wind is presented here This discussion is included to provide a qualitative understanding and background of the circulation patterns of the study site. The relationship between currents, winds, and sediment transport is discussed in Chapter 5.

The NS and EW components of the wind are expected to move water in their corresponding directions. The NS and EW wind and current components were compared for each of the three stations Processing of the orthogonal wind and current components was performed by first calculating a 4-hr average of the measurements and then applying a low-pass filter (0 9 cpd cutoff frequency) to remove diurnal variations The strength of the diurnal wind was sufficient to obscure the longer-period wind fluctuations, and the low-pass filter was applied to remove variations on the diurnal time scale. In all figures showing wind and current components,

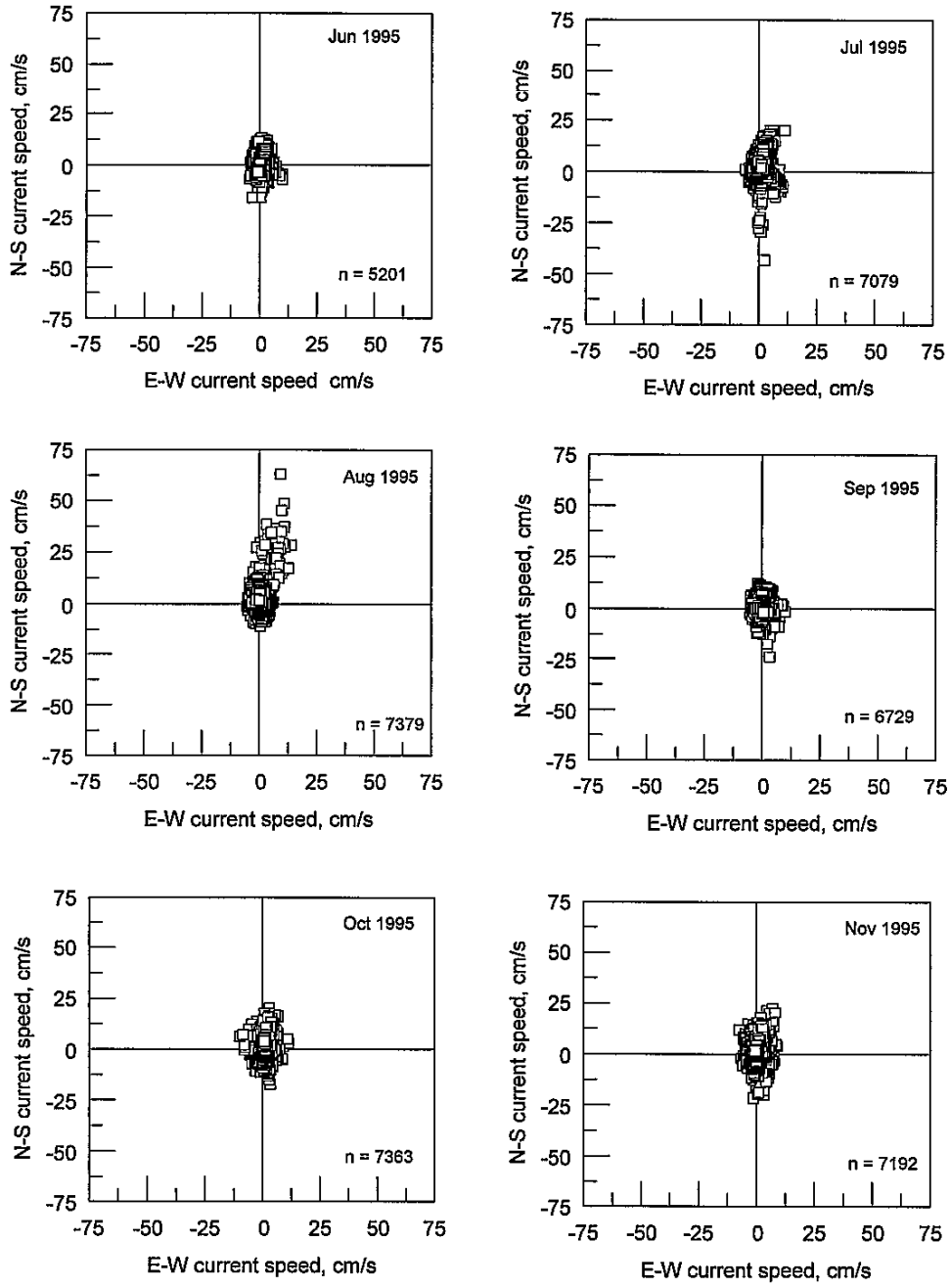

Figure 4.15a. Scatter plots of current speed at ULM3, June, 1995, through November, 1995.

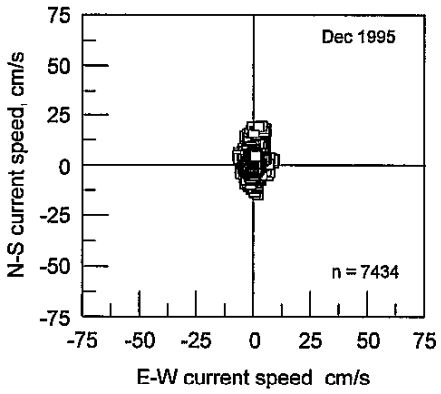

Figure 4 15b Scatter plot of current speeds at ULM3, December, 1995.

positive values indicate North or East and negative values indicate South or West. The wind curves have the convention of "direction that the wind is originating from" and the current curves have the convention of "direction that water is moving toward."

The processed NS and EW wind and current components for ULM1 over the period June, 1995, through December, 1995, are shown in Figure 4 16 The currents respond to both the N-S and E-W wind components, and this response appears as a near mirror image of the wind curves, i.e., the wind induces a current in the direction that it is traveling At the ULM1 station location, the SE winds of summer cause a persistent NW flowing current. The current at this location may be indicative of a clockwise gyre that could form under persistent SE wind conditions. The existence of a gyre cannot be confirmed with flow measurements at only one point, but a consistent flow at one point in space strongly suggests the existence of a wide-scale gyre.

Scatter plots of the wind components vs the current components are shown in Figure 4 17 for the Naval Air Station and ULM1, respectively. The N-S components of the wind and current are linearly related, although some scatter in the data exists. Scatter is expected as wind is not the only driving force for the current, and other factors, such as sheltering in some directions and changes in bottom topography, can alter the current speed and direction Changes in bottom topography and interference with the wind (sheltering and modification of the air-sea boundary layer) cause a non-isotropic response of the current to direct wind forcing. The N-S component

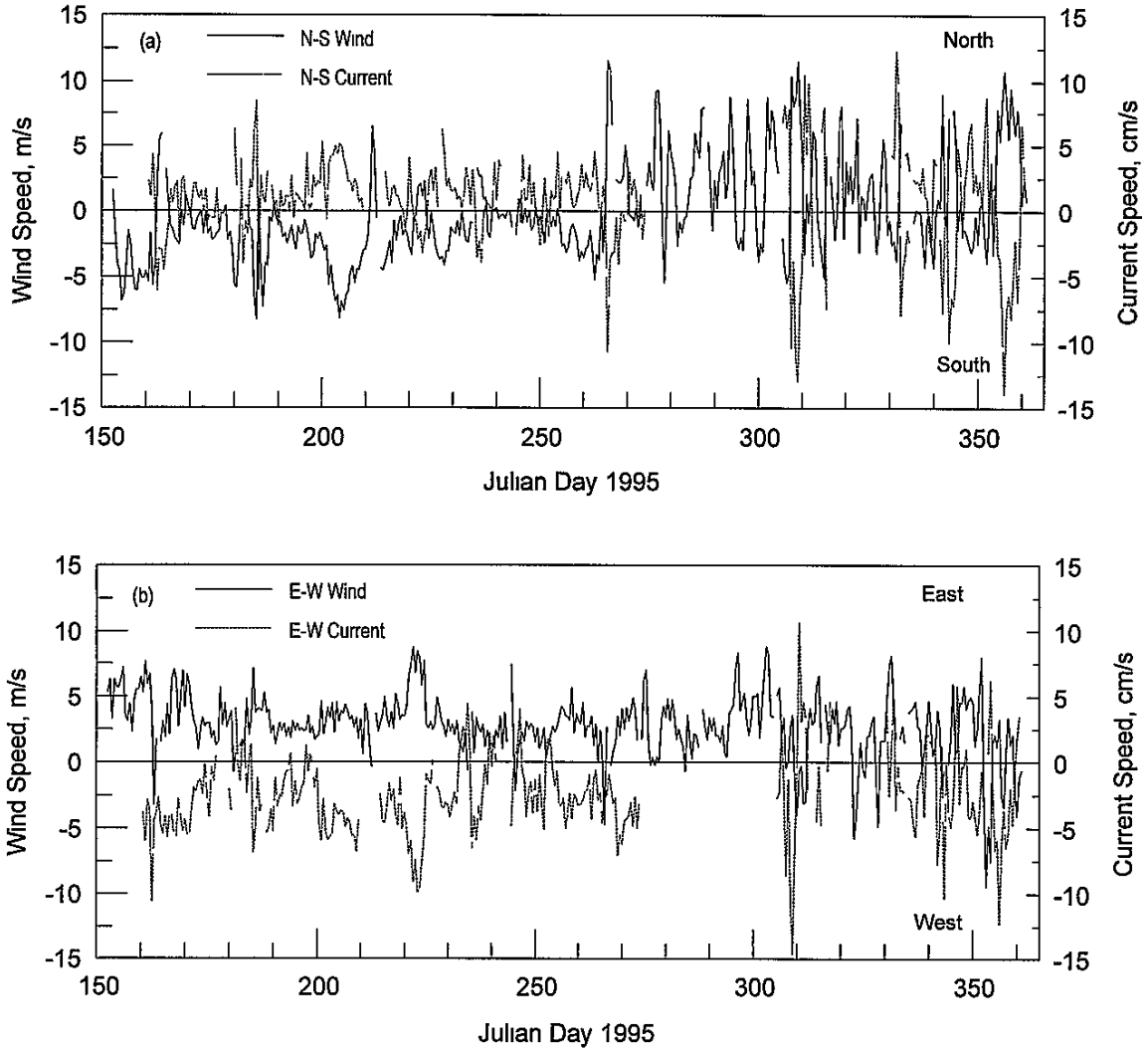

Figure 4.16. Decomposed wind and current components (with averaging and low-pass filter) from Naval Air Station and ULM1, respectively, for June, 1995, through December, 1995: (a) North-South components, (b) East-West components.

of the current flows almost exclusively to the north when the wind is from the south, and vice versa. The NS current speed tends to be approximately 0 8% of the NS wind speed. The E-W component of the current has an obscured response to the wind, without a strong preferential alignment associated with wind direction. However, direction of the current is concentrated toward the west as a response to the dominant easterly component of the wind.

The NS and EW components of the wind and current for Yarborough and ULM2, respectively, are shown in Figure 4 18 The response of the current to the wind is less evident at ULM2 as compared to ULM1 during the summer months; however, general trends can be discerned. Currents during the summer months are weak, generally less than 5 cm/s for each component, even during periods of higher wind speeds such as between JD 200 (July 19) and JD 210 (July 29) During the fall and winter months, the current magnitude increases in response to the wind. The difference in the summer and winter current response to wind as shown in Figure 4 18 may be due to the difference in time scales of dominant summer and winter winds Because the diurnal wind and current motion have been filtered out of the data shown in the figure and the diurnal wind is strong during the summer, its influence on the currents does not appear in the figure and is discussed below. Winter winds are characterized by frontal activity generally lasting longer than one day so that the response of the current to the winter winds is evident

The decomposed wind and current components for the month of July, 1995, at Yarborough and ULM2, respectively, are shown in Figure 4 19. The wind and current data shown have been averaged over a period of 4 hours, but have not been low-pass filtered to remove the diurnal variance in motion The NS and EW components of the current follow the fluctuations in the diurnal wind. The resultant motion is a daily SW and NE cycling of the current at ULM2. This cycling is the result of the onshore wind that blows during the day and pushes water toward the west, into Baffin Bay In the evening, as the wind relaxes, the water moves out of Baffin Bay During the period from JD 202 (July 21) through JD 209 (July 28), a strong southerly wind was superimposed over the diurnal wind such that the wind from the south was increased in strength while the easterly diurnal wind pattern did not change During this period, the NS component of the current did not change much from the period preceding the southerly front However, the diurnal fluctuation of the EW component of the current was nearly eliminated because the frontal movement induced a near-steady easterly component of the current.

Comparison of the response of the current at ULM2 to the wind fluctuation on the diurnal versus longer time scales reveals that the current follows closely the fluctuations on the diurnal time scale (during the summer) and less closely those fluctuations with longer time periods.

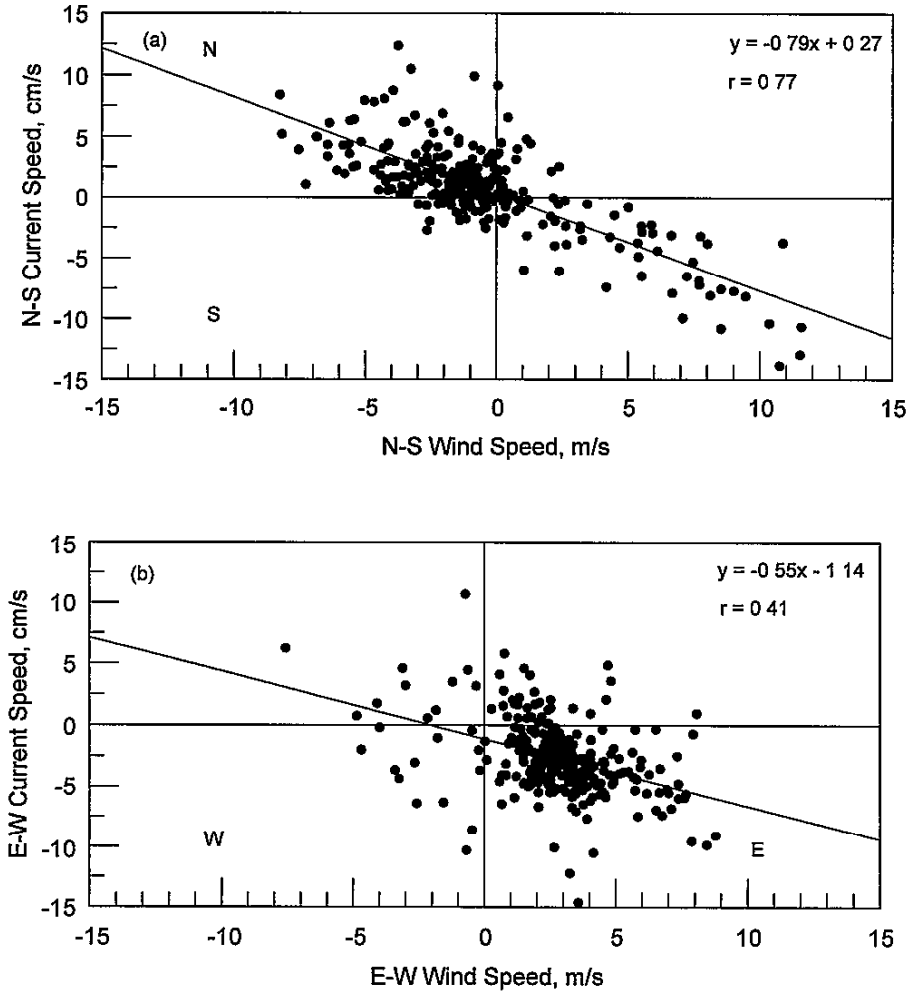

Figure 4 17 Wind speed components vs current speed components at Naval Air Station and ULM1: (a) N-S components, (b) E-W components

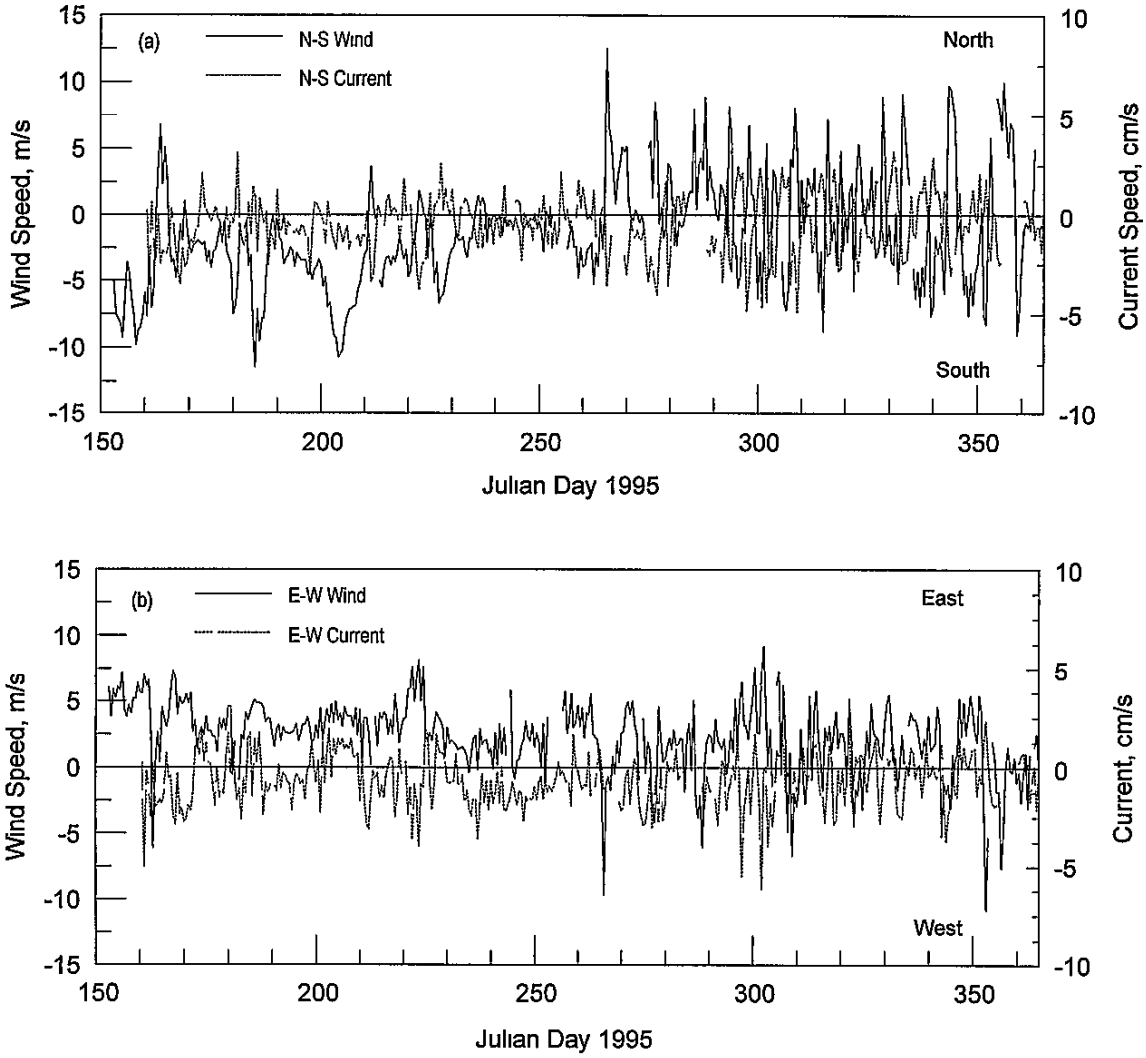

Figure 4.18. Decomposed wind and current components (with averaging and low-pass filter) from Yarborough and ULM2, respectively, for June, 1995, through December, 1995: (a) North-South components, (b) East-West components

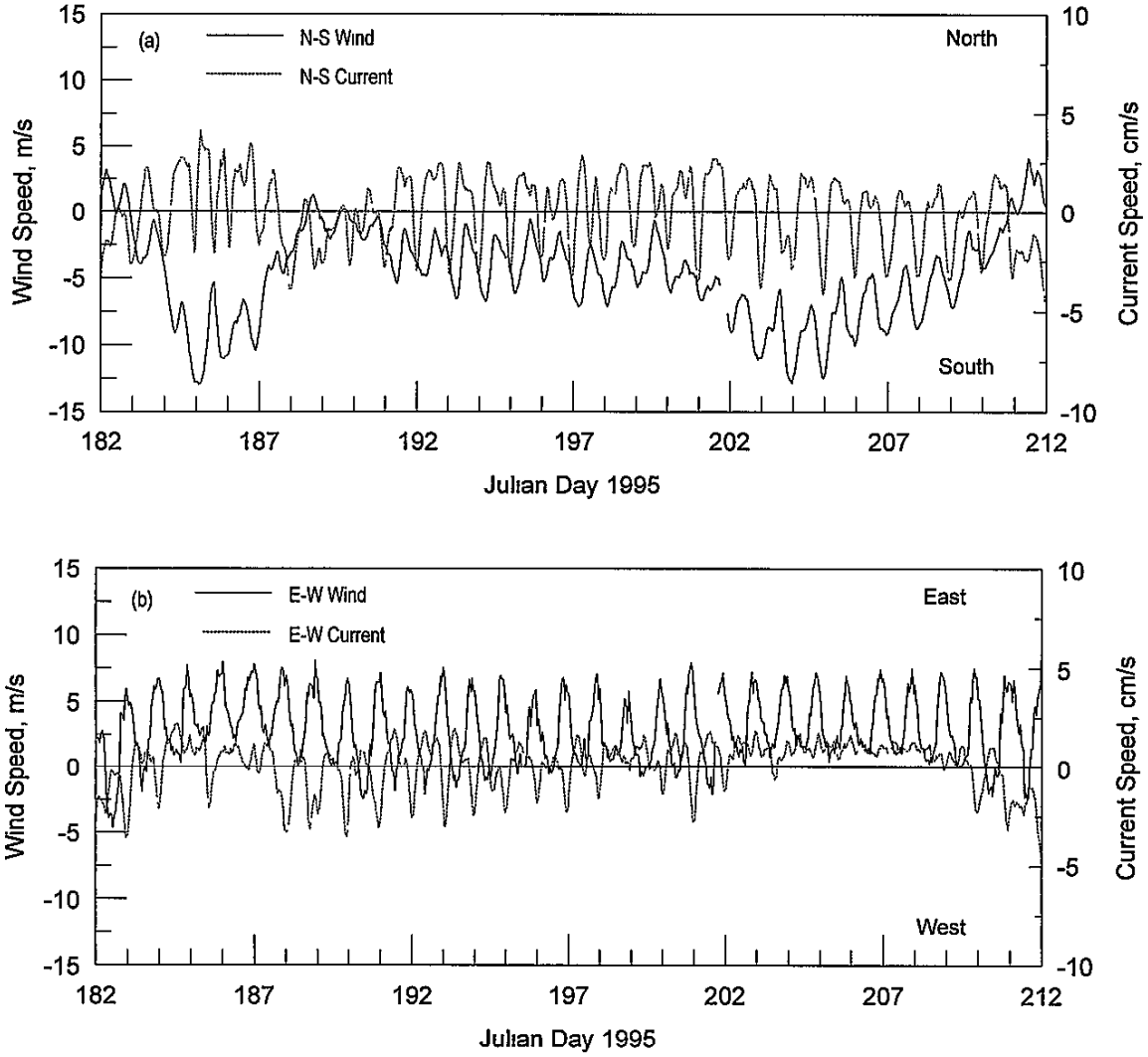

Figure 4.19. Decomposed wind and current components (without low-pass filtering) from Yarborough and ULM2, respectively, for July, 1995: (a) North-South components, (b) East-West components

The NS and EW wind and current components for Yarborough and ULM3 are shown in Figure 4.20. The response of the NS current component to NS wind forcing is readily apparent in the top panel. When the wind originates from the south, the current moves to the north and is persistent during the summer months following the summer wind. During the fall and winter, reversals in the NS wind component are generally followed by reversals in the NS current, although there are some periods when the current does not align with the wind, such as the two days preceding JD 300 (October 27).

The EW currents at ULM3 are of smaller magnitude than the NS components The reduced magnitude in the EW directions is due to two causes, 1) The EW wind component is smaller than the NS wind components and, therefore, will induce a smaller magnitude flow, and 2) The ULM is narrow in the cross-channel (EW) direction at the site of the ULM3 platform so that lateral water movement is restricted During the summer, even though the EW currents are small, their fluctuations follow that of the EW wind fluctuations but generally in the opposite direction, i e , the EW current tends to move in the opposite direction of the wind. This opposing flow may be counterintuitive at first thought, but considering the relatively narrow portion of the lagoon and the southern boundary with only the Land Cut to allow for water exchange, the currents are responding to not only the wind but also to the nearly enclosed location and boundaries on three sides This configuration of the laguna combined with the wind forcing may induce a three-dimensional flow pattern such that surface water moves toward the east and the return flow at depth moves water westward This return flow is weak as the predominant direction of current motion at ULM3 is along the channel.

The decomposed wind and currents, without the diurnal variations removed, during July, 1995, for Yarborough and ULM3, respectively, are shown in Figure 4.21 The NS and EW current responds to the NS and EW diurnal fluctuations in the wind, respectively The NS diurnal fluctuations in the current are larger than the EW fluctuations due to the relatively narrow lagoon in the EW direction The EW component of the current flowed toward the east 71% of the time in July, 1995, even under the influence of easterly wind This flow pattern provides support for the possible existence of a weak gyre in the region of ULM3.

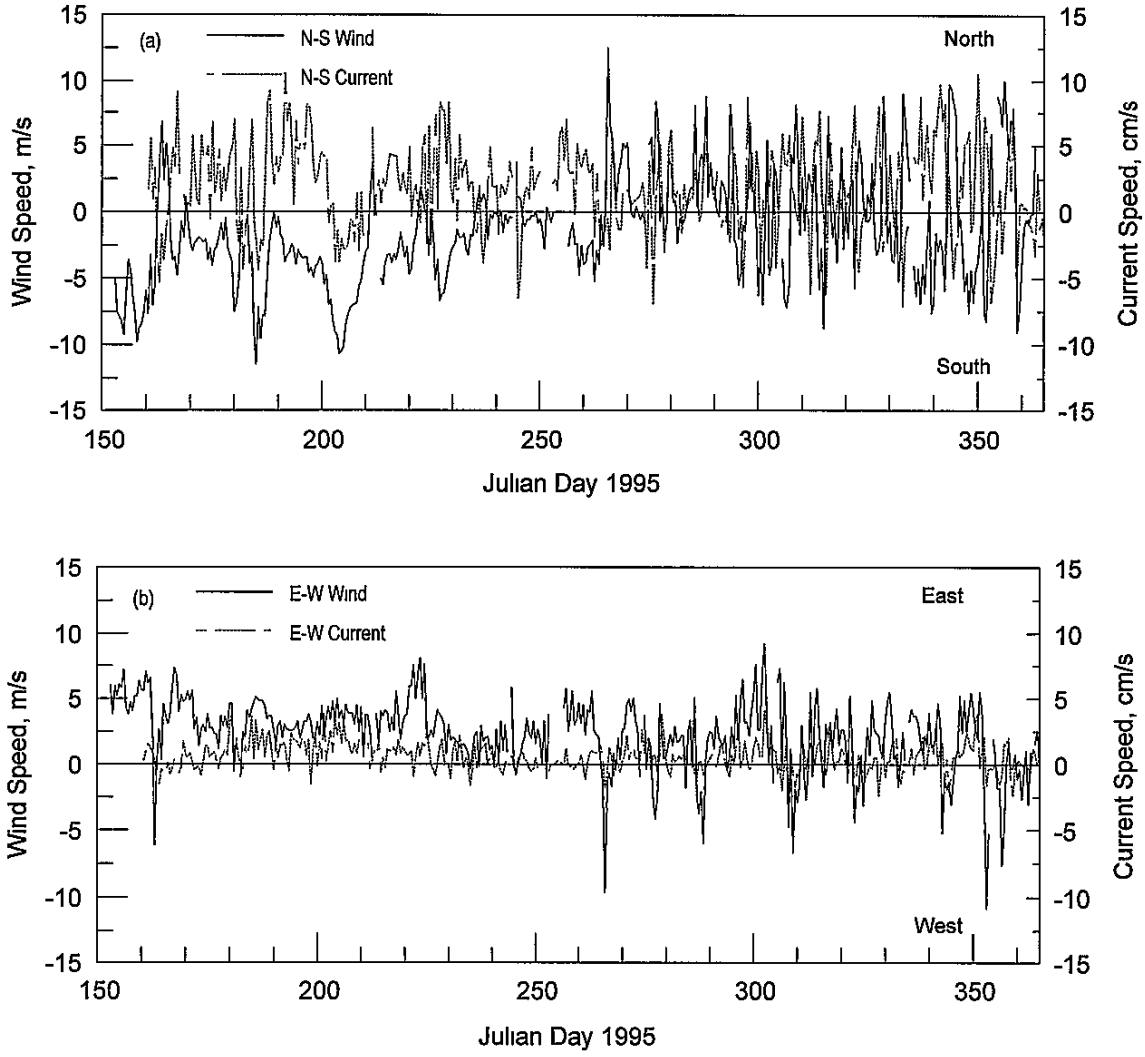

Figure 4.20. Decomposed wind and current components (with averaging and low-pass filter) from Yarborough and ULM3, respectively, for June, 1995 through December, 1995. (a) North-South components, (b) East-West components

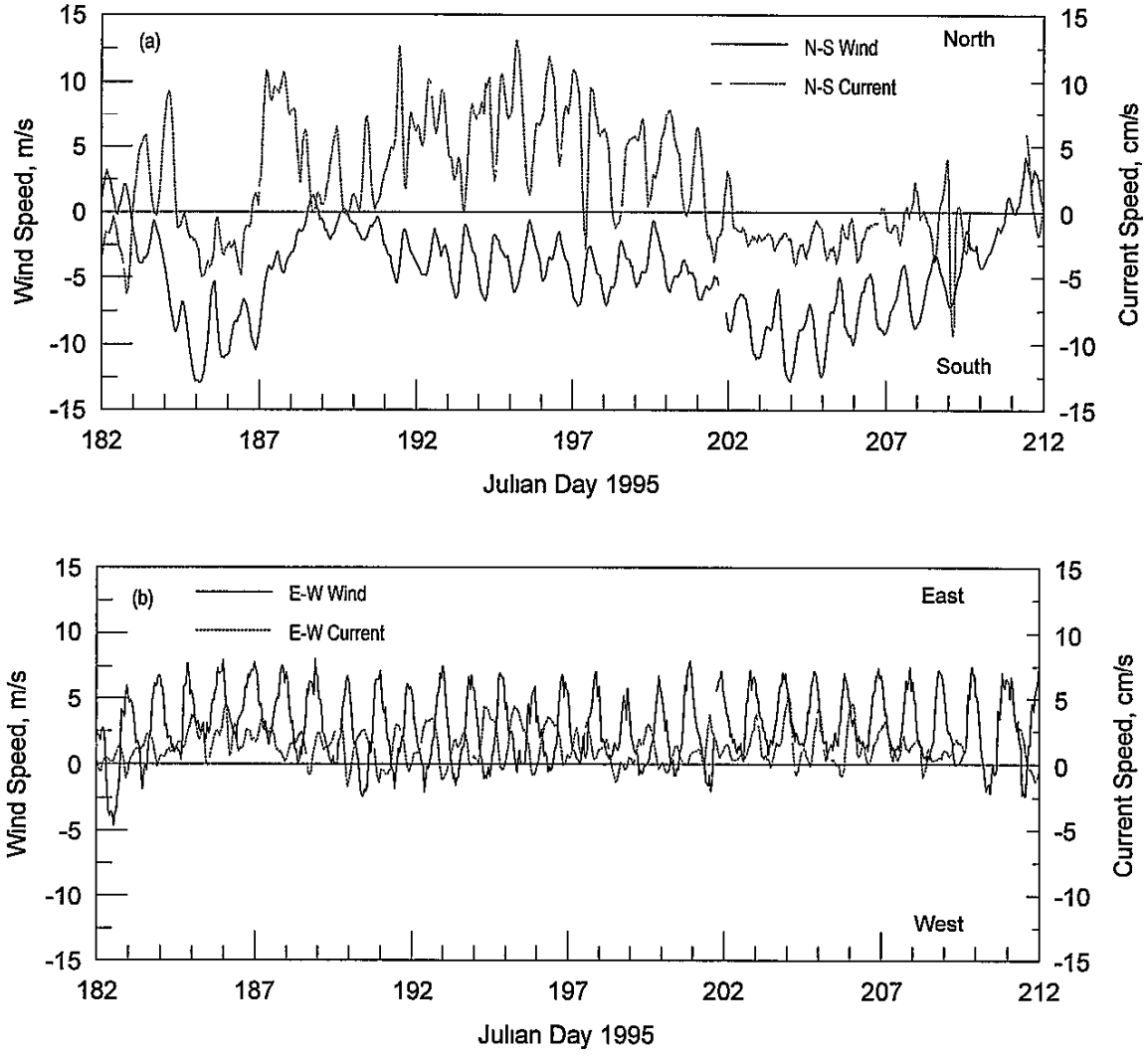

Figure 4.21. Decomposed wind and current components (without low-pass filtering) from Yarborough and ULM3, respectively, for July, 1995: (a) North-South components, (b) East-West components.

5. SEDIMENT RESUSPENSION AND TRANSPORT[5]

Sediment resuspension and transport processes at the study area are discussed in this chapter, together with the sediment particle size. Total suspended solids data collected during this study are discussed in the context of the dynamic physical processes

5.1 Sediment Resuspension and Transport Processes

The resuspension of sediment depends on several variables including sediment type, grain-size distribution, wave climate, water depth, and magnitude and period(s) of the flow Resuspension of sediment into the water column occurs once the flow velocity exceeds a critical threshold, and forces holding the particle in place (including gravity and chemical bonding) are overcome Once a particle is in suspension, it can be transported by the current to another location The distance transported depends on the strength of the current and its spatial and temporal variation, as well as on the fall velocity of the suspended particle The fall velocity of a particle (the velocity at which a particle falls through the water column) is dependent on the grain size, specific gravity, shape, and the dynamic viscosity of the fluid, as well as the amount of turbulence and possible density and flow structure of the fluid

The flow that provides the force for lifting grains from the bottom is a combination of the tidal and wind-generated currents and the surface wave orbital velocity. Because the waves are developed and driven by local wind, sediment resuspension will depend on the strength, duration, and direction of the wind, as well as the length of the water body over which the wind blows (the fetch). Regions of the study area that are not greatly fetch limited, such as the locations of ULM1 and ULM2, can experience high waves (1.5 m high waves have been visually observed) that can potentially induce erosional stresses on the bottom The location of ULM3 is fetch limited and experiences smaller wind-generated waves.

In a study investigating the response of suspended sediment to wind forcing in Corpus Christi Bay, the suspended sediment concentration was found to be correlated to the direction of maximum fetch (Shideler 1984) During north winds, greater turbidities were found to occur in the southern region of Corpus Christi Bay When winds were directed onshore, less turbid water

[5] Adele Militello and Nicholas C Kraus, Conrad Blucher Institute for Surveying and Science, Texas A&M University-Corpus Christi

flowed into Corpus Christi Bay from the ULM and Aransas Pass and other regions of higher turbidity occurred in Nueces Bay and the northwestern portion of Corpus Christi Bay

Water depth also plays a role in sediment suspension, especially with regard to wind-generated waves A wave of given height and period located in deeper water will produce less stress on the bottom than the same wave in shallower water Thus, during periods of seasonal low water, waves may induce erosion at a greater rate than during periods of higher water Very shallow regions exist within the study area that are highly susceptible to erosion by waves, especially under low-water conditions. These shallow areas include dredged material placement sites along the GIWW in both Corpus Christi Bay and the ULM.

Storms can cause substantial movement of sediment in a short period of time Hurricanes have caused breaching of the barrier island and subsequent deposition of large amounts of sediment into the bays and lagoons of Texas (McGowan and Scott 1975) The most intense hurricanes that have struck the south Texas coast were Carla (1961), Beulah (1967), Celia (1970), and Allen (1980) (National Hurricane Center 1996) Breaching of Corpus Christi Pass occurred in 1961 during the passage of Hurricane Carla and again by Hurricane Beulah in 1967. After breaching in 1967, a flood tidal delta formed as the pass closed (Davis, *et al* 1973). Hurricanes Celia and Allen struck the south Texas coast in 1970 and 1980, respectively Within the study area, Packery Channel, Newport Pass, and Corpus Christi Pass are classified as active hurricane washover (areas that are breached during storms) channels (White, *et al* 1978)

Vessel-induced motions can resuspend sediment through generation of intense currents by water displacement, in the case of barges and ships, and by wakes Monitoring of sediment resuspension in Old Tampa Bay revealed that large-vessel (barges and ships) motion substantially increased the TSS concentration to a peak value approximately 30 times greater than the ambient TSS concentration (Levesque and Schoellhamer 1995). The time-series of TSS concentration closely followed that of the vessel-motion such that the peak TSS concentration occurred just after the peak current velocity and drawdown. TSS concentration levels decreased over time as the vessel motion attenuated Trawling can also induce sediment resuspension by nets that are dragged along the bay or lagoon bottom (Levesque and Schoellhamer 1995)

5.2 Sediment Description

The general pattern of sediments in the ULM is formed of three regions of sediment types running roughly parallel to the axis of the lagoon The sediment types are characterized by, 1) material similar to that of the mainland (sand, gravel, and beach rock) on the western flank of the lagoon, 2) fine material (clayey sand, sandy clay) with some shell in the deeper portions of the lagoon, and 3) sand near Padre Island (Dickenson, *et al* 1972) Shepard and Rusnak (1957) describe the majority of material in the deeper portions of the ULM as shelly sand Sand is present throughout the sediments of the lagoon bottom, and its dominance is largely the result of transport from Padre Island under the predominant southeast winds and washover during severe storms (Fisk 1959) Baffin Bay is composed mostly of clay-sized material in its central, deeper regions, but material similar to the deeper parts of ULM is found in the remaining deeper portions (Shepard and Rusnak 1957)

The flats that separate the ULM from the LLM are largely the result of eolian and wind-tidal processes (Miller 1975). Formation of the flats resulted from strong and persistent winds, predominantly from the southeast, and a low-energy lagoonal environment where deposition of sand and finer-sized material was favored over erosion The surface composition of the flats varies spatially, but the predominant deposits consist of, 1) firm clays with sand, 2) firm clays, 3) loose sand, and 4) firm sands with interbedded gray clays (Fisk 1959). The course of the GIWW runs through areas with bottoms composed predominantly of firm clays with sand and firm sands with interbedded gray clays

5.3 Analysis of Sediment Resuspension

The physical processes pertaining to sediment resuspension at each of the three monitoring stations were assessed to determine the conditions under which sediment particles are placed into the water column and then transported. The analysis was undertaken through comparison of TSS, wind, and currents An integrated approach that considers the wind-current, wind-TSS, and current-TSS relationships was taken to encompass the range of processes and responses for sediment resuspension and transport within the study site The influence of waves is discussed qualitatively because wave data were not available, but general wave conditions such as well-developed waves at ULM1 under strong northerly winds, are known Analysis of other parameters that can influence sediment resuspension, such as bottom type and grain size distribution, are not included in this overview discussion.

TSS and wind speed at ULM1, ULM2, and ULM3 are shown in Figures 5.1, 5 2, and 5 3, respectively, for the duration of the monitoring project. The wind-speed data were averaged over a 4-hr period then low-pass filtered as described in Chapter 4 The dredging interval marked in the upper panel indicates when dredging took place within 5,000 ft of the platforms. The time axis has its origin at 00 00 GMT on January 1, 1995. Negative values indicate time in 1994 such that a value of -60 indicates November 2, 1994, and a value of -30 indicates December 2, 1994 In Figure 5.1, two peaks of TSS with concentrations near 150 μg/mL occurs during and immediately after the dredging interval. Because the first peak occurs during dredging and the winds are relatively mild (< 8 m/s), the increase in TSS is most likely due to dredging activities. Within 1 day, the suspended solids settled out of the water column, and the TSS returned to the pre-dredging background level The second peak occurs during a period of SE wind with speed reaching 13 m/s indicating that the strong wind conditions caused an increase in suspended solids. The TSS recovers rapidly and return to pre-frontal levels within 1 day High concentrations of TSS correspond to dredging at stations ULM2 and ULM3 (Figures 5.2 and 5 3) These peaks return to background levels rapidly.

There is seasonal variability in the TSS and the wind speed, as is apparent in Figures 5.1, 5 2, and 5 3 The baseline (non-peak values) TSS levels are higher during the winter and spring months than during the summer months but were generally less than 50 μg/mL. These baseline concentrations are in the same range as those found by Dunton, *et al.* (1994) at two sites in the ULM north of Baffin Bay. Winter winds having a northerly component will tend to cause greater wave heights at ULM1 because of the long fetch across Corpus Christi Bay Winds originating out of the southeast, typical during the summer, have limited fetch at the position of the ULM1 platform Of the three stations, ULM2 tends to have the highest mean TSS concentration and variance during the winter possibly due to its relatively unsheltered location As described previously, lower waters occur in the winter and spring which, combined with the stronger NE winds, would promote greater sediment resuspension than in the summer. TSS concentration at ULM3 is the lowest overall showing no peaks above 200 μg/mL except during dredging The location of the ULM3 platform is relatively sheltered, with limited fetch on the east, south, and west sides so that generation of well-formed waves is infrequent

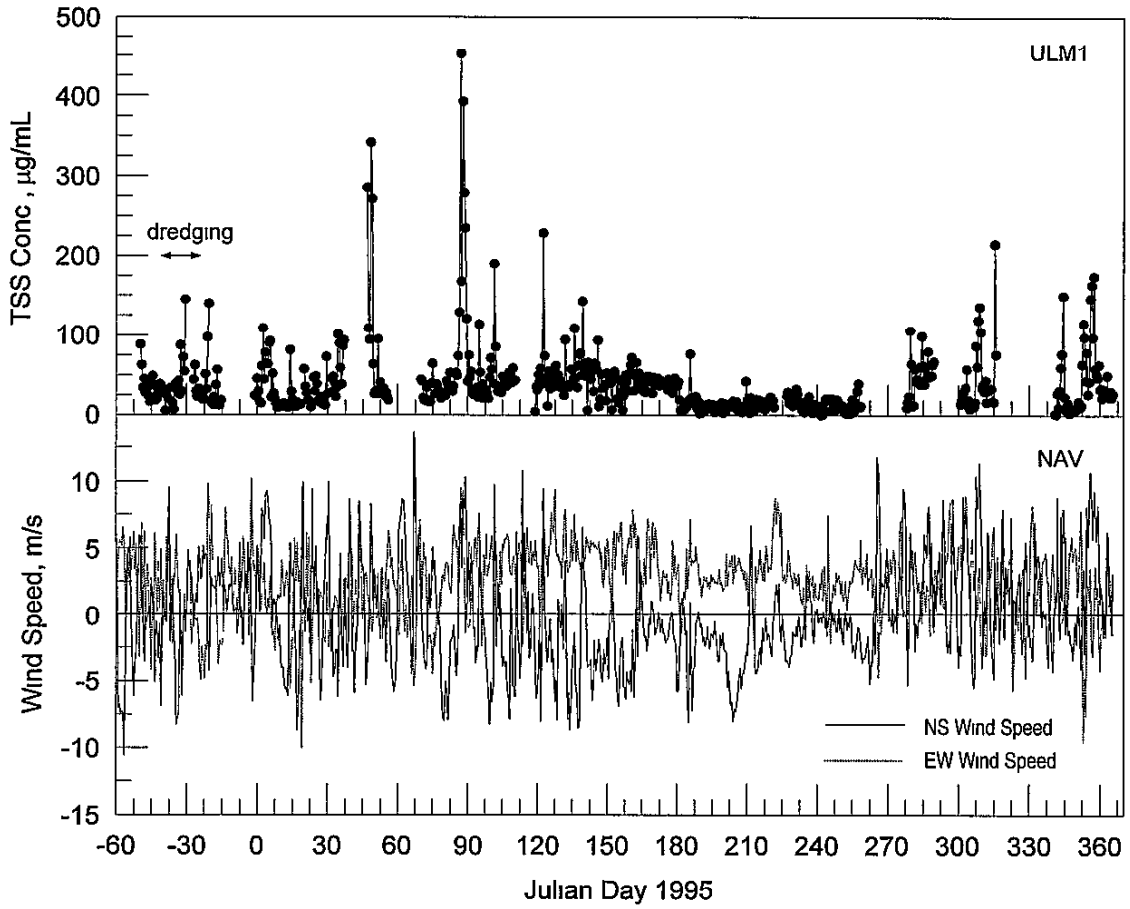

Figure 5.1 Total suspended solids concentration and wind speed components over the monitoring period at ULM1 and Naval Air Station, respectively

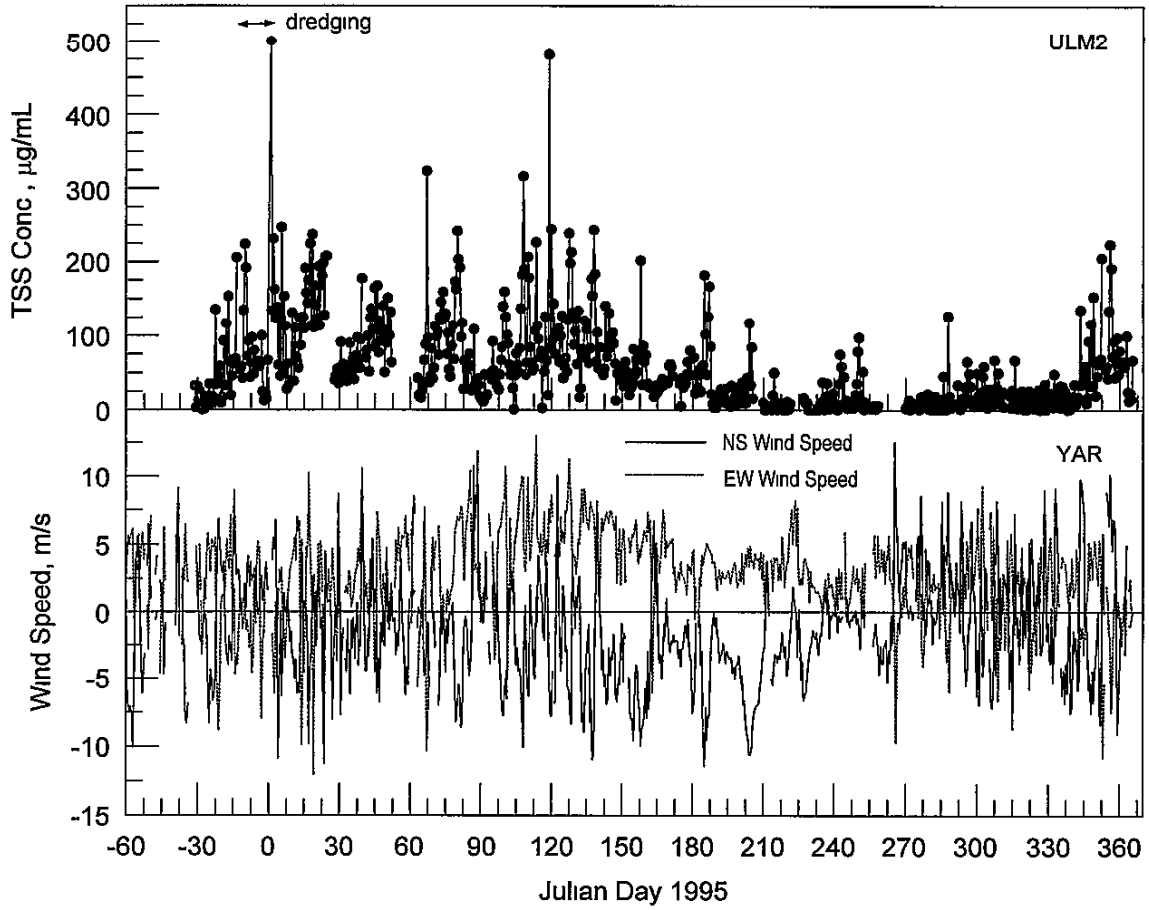

Figure 5.2 Total suspended solids concentration and wind speed over the monitoring period at ULM2 and Yarborough, respectively.

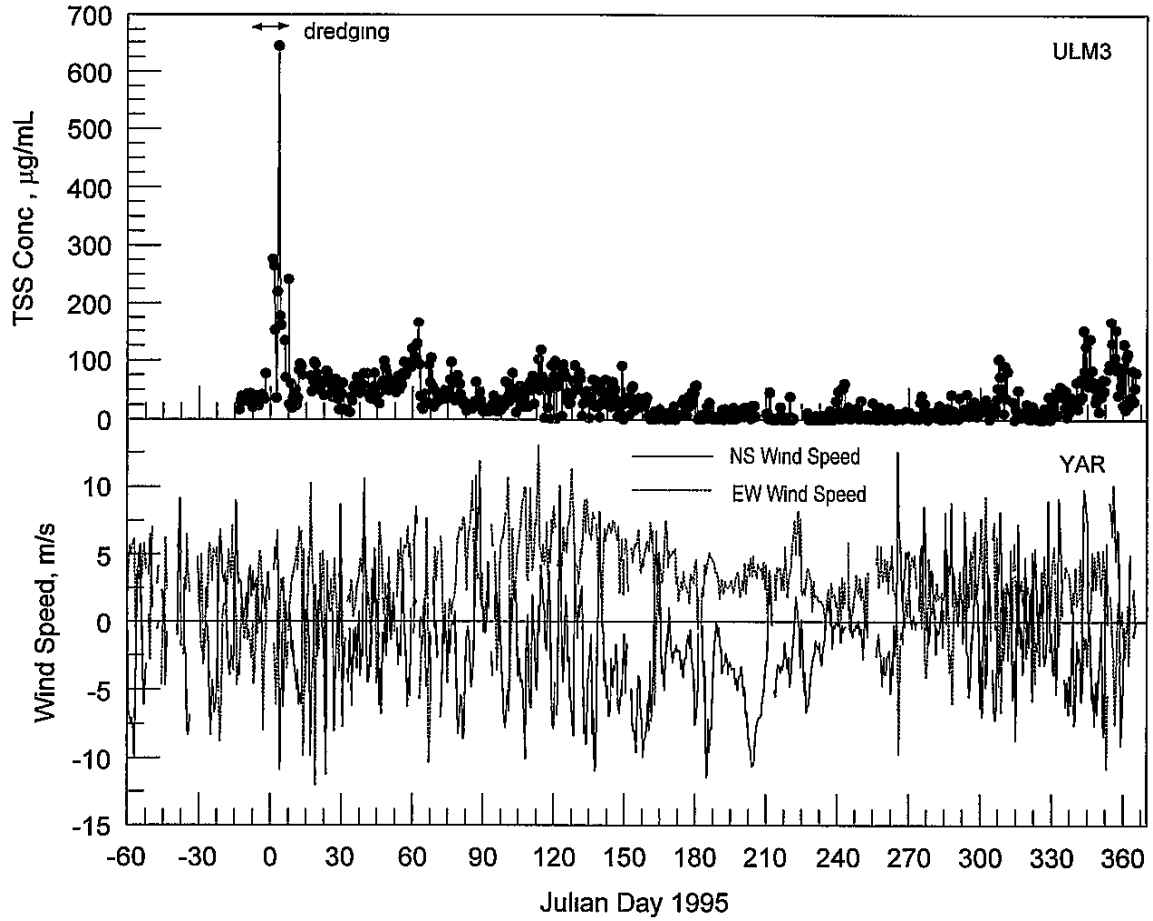

Figure 5 3 Total suspended solids concentration and wind speed over the monitoring period at ULM3 and Yarborough, respectively

A plot of TSS versus the NS and EW components of the wind at ULM1 and Naval Air Station, respectively, is shown in Figure 5.4 Concentrations of TSS above 150 µg/mL occur almost exclusively under conditions of northeast winds Comparison of the wind conditions under which the highest TSS concentrations occurred (Figure 5 4) and the time series of TSS concentrations at ULM1 (Figure 5.1) reveals that the maximum TSS concentrations occur during the fall, winter, and spring when northerly fronts pass through the area Frontal winds from the north can persist for days and are known to generate large waves in the southern region of Corpus Christi Bay These high-energy conditions create motions within the water column that are sufficiently strong to initiate sediment into the water column. Winds originating from any direction appear to be capable of producing sediment concentrations less than 50 µg/mL, but there is clustering of the data points for winds from the south and east. Plots similar to

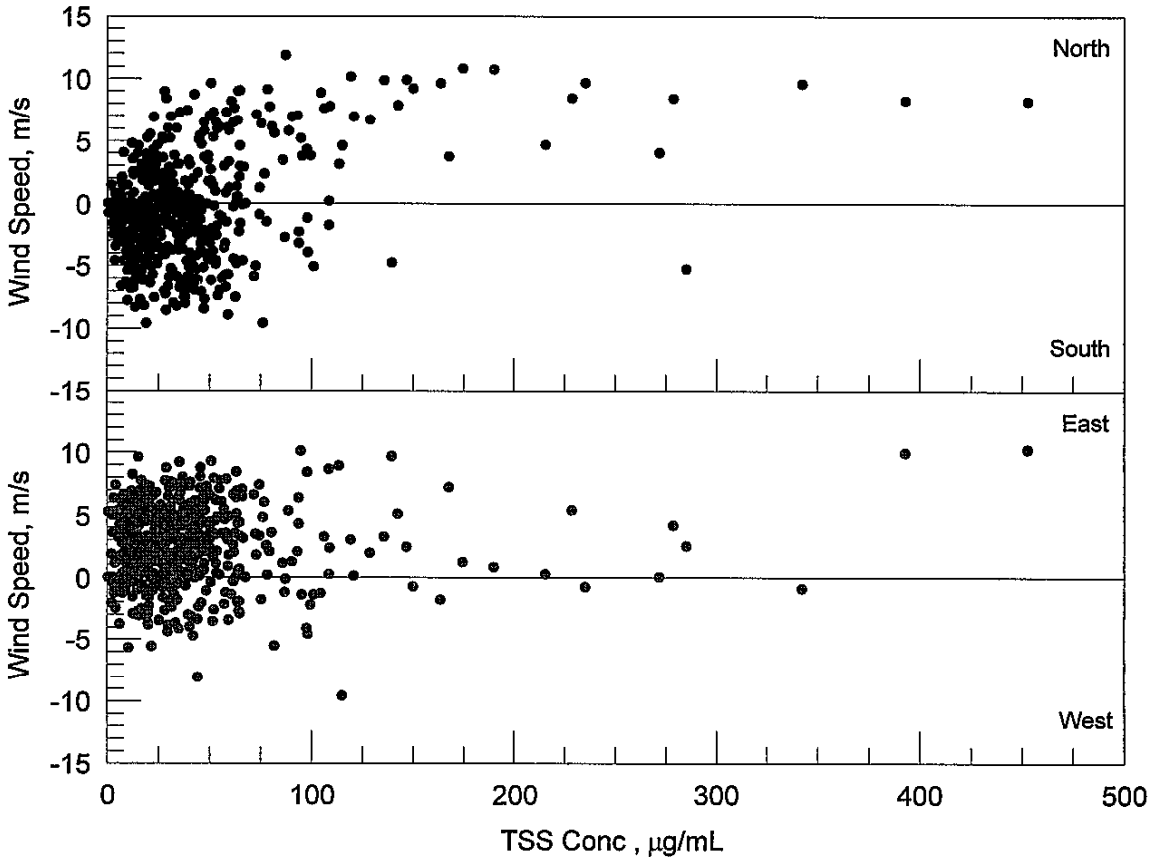

Figure 5.4. TSS concentration vs. NS and EW wind speed components at ULM1 and Naval Air Station, respectively

Figure 5 4 were generated for TSS and wind components at ULM2 and ULM3, but no preferred association with wind speed or direction could be determined so that the plots are not included within this report

Time-series plots of TSS and components of the current from June, 1995, through December, 1995, are shown in Figures 5.5, 5.6, and 5 7 for stations ULM1, ULM2, and ULM3, respectively. For low TSS concentrations, the current at each station does not appear to be correlated to current speed. At ULM1, when the current components exceed approximately 10 cm/s, the TSS concentrations appear to covary with the current At ULM2 and ULM3, there appears to be no direct correlation between TSS concentration and speed of the orthogonal current components Figure 5 8 shows the TSS concentration vs the current speed for the NS and EW components of the current at ULM1 For TSS concentrations exceeding approximately 50 μg/mL, the currents flow almost exclusively to the south and west

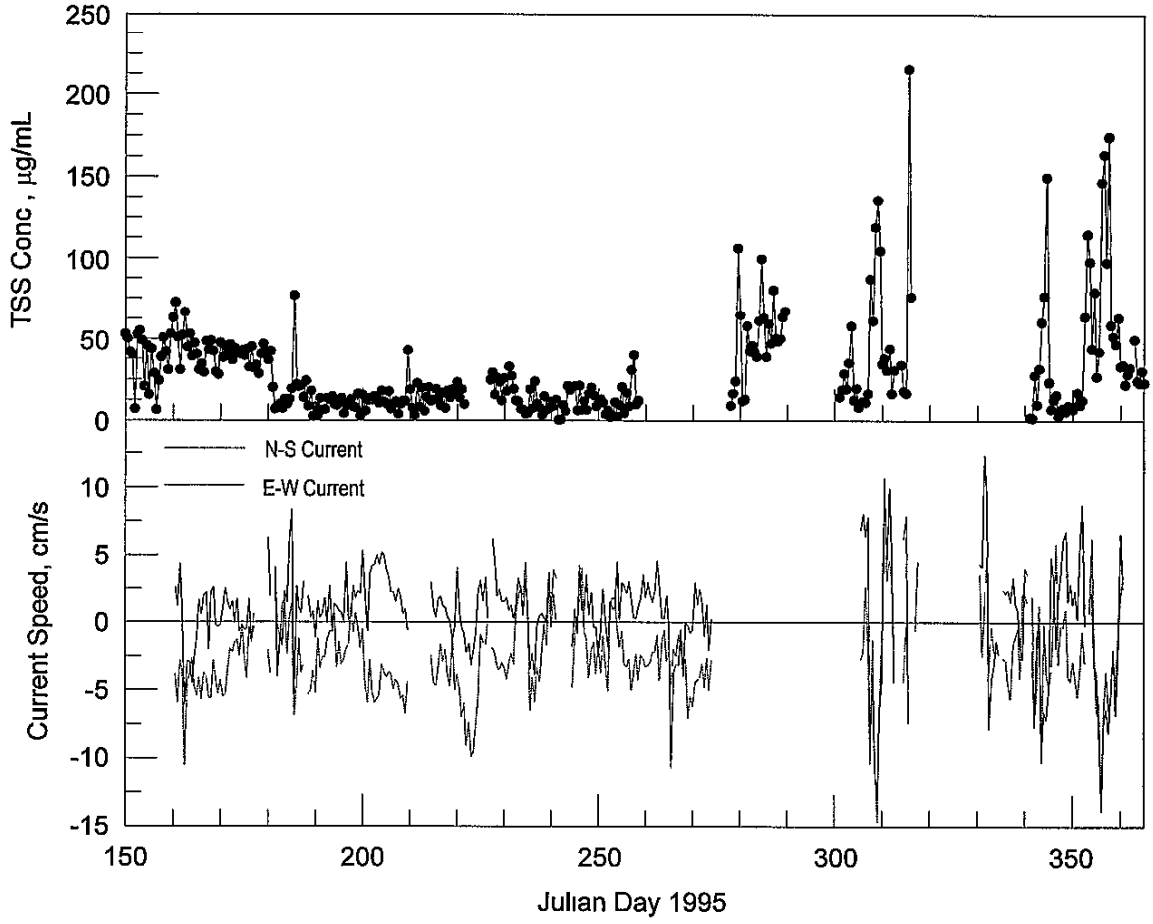

Figure 5.5. Total suspended solids concentration and current components at ULM1 from June, 1995, through December, 1995.

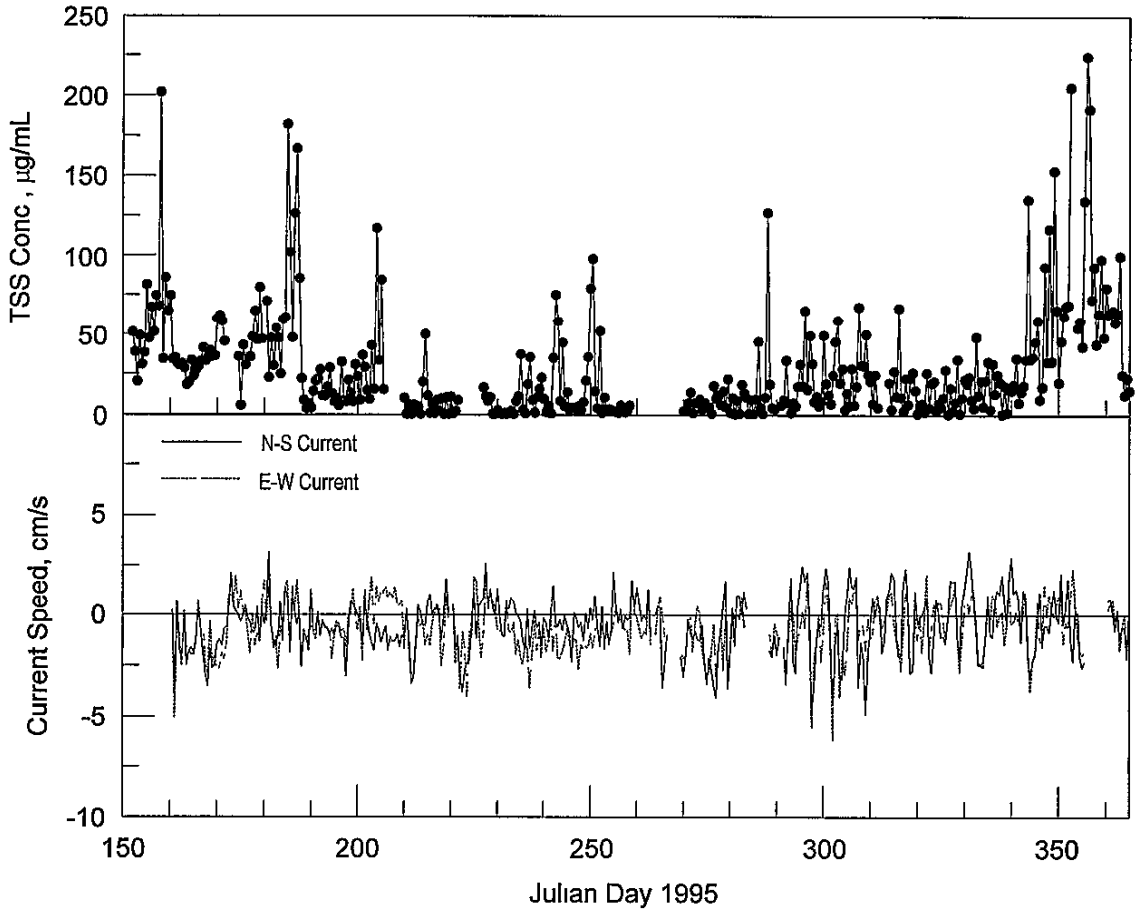

Figure 5 6. Total suspended solids concentration and current components at ULM2 from June, 1995, through December, 1995

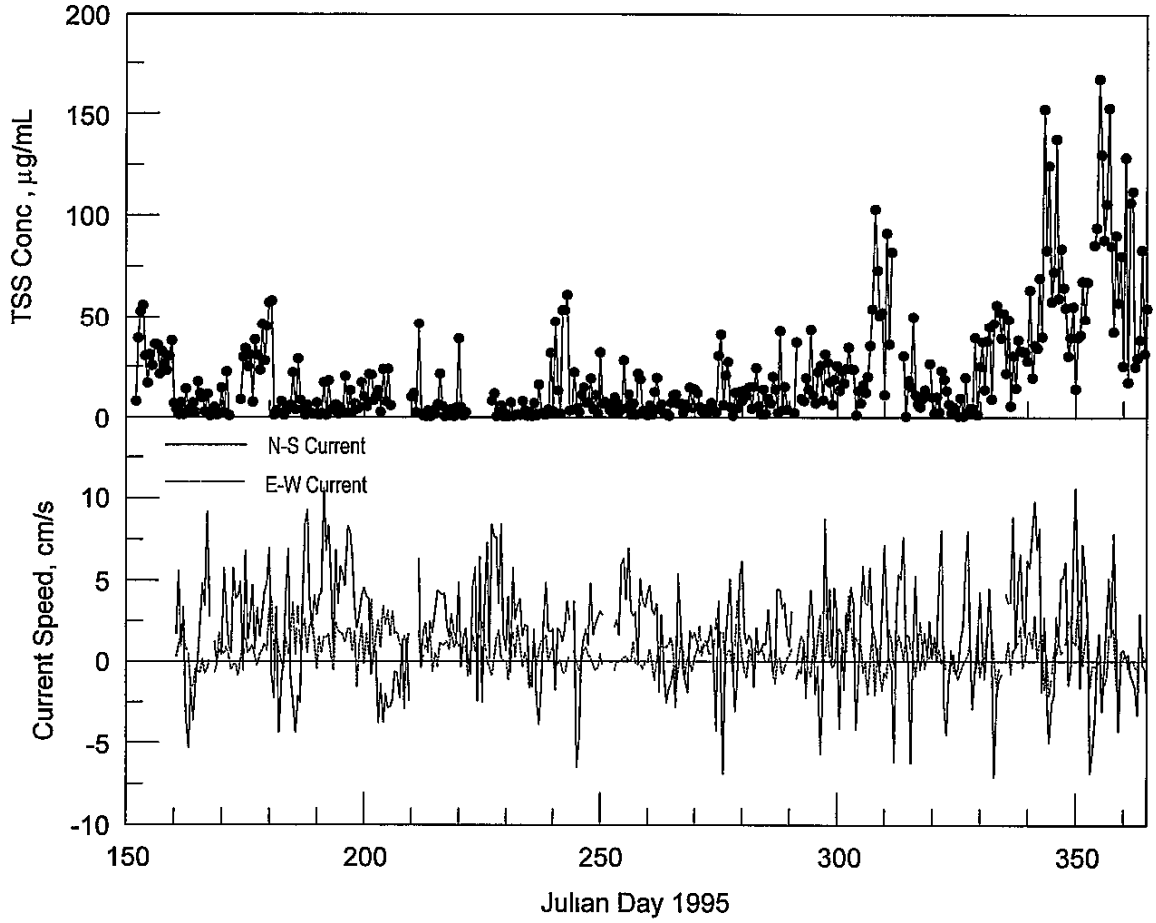

Figure 5 7. Total suspended solids concentration and current components at ULM3 from June, 1995, through December, 1995

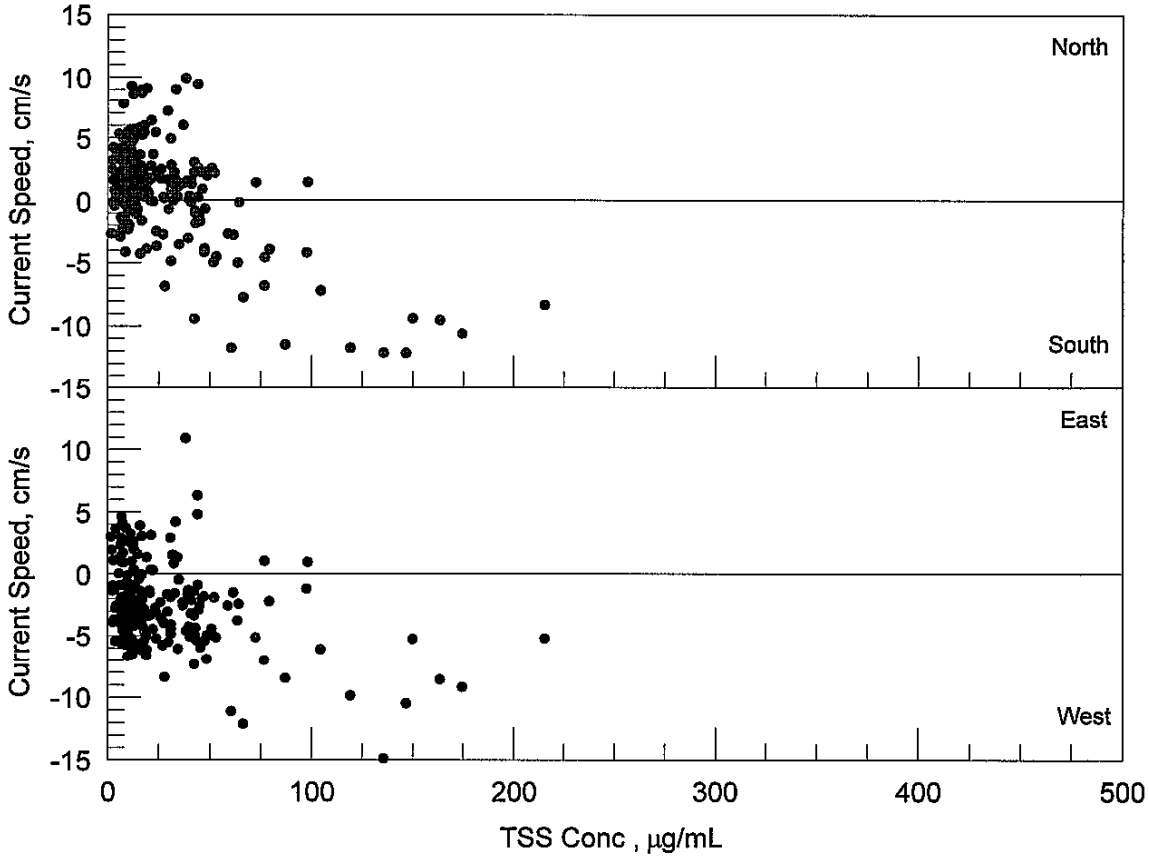

Figure 5.8. TSS concentration vs NS and EW current components at ULM1

Particle size determination from water samples revealed that the median diameter of most samples fell in the mud class size The diameter size separating the sand and mud classes of grains is 62 µm (Friedman and Sanders 1978) Figure 5 9 shows the median grain sizes for ULM1, ULM2, and ULM3 during 1995. At ULM1, the typical median particle size ranges from about 10 to 50 µm, corresponding to the medium to coarse silt size classes (silt and clay comprise the mud size class). Median particle sizes fell into about the same range at ULM2; however, particles in the 60 to 90 µm (very fine sand) range were found to frequently occur during the winter. The median particle size typically fell into a band between 10 and 60 µm (medium to very coarse silt) at ULM3, with higher values, corresponding to very fine sand occurring in the winter. For all three stations, the variability in median particle size was greater during the late winter and spring than during the summer months The stronger wave-induced orbital velocities of the higher waves of winter appear to be capable of suspending particles with larger diameters

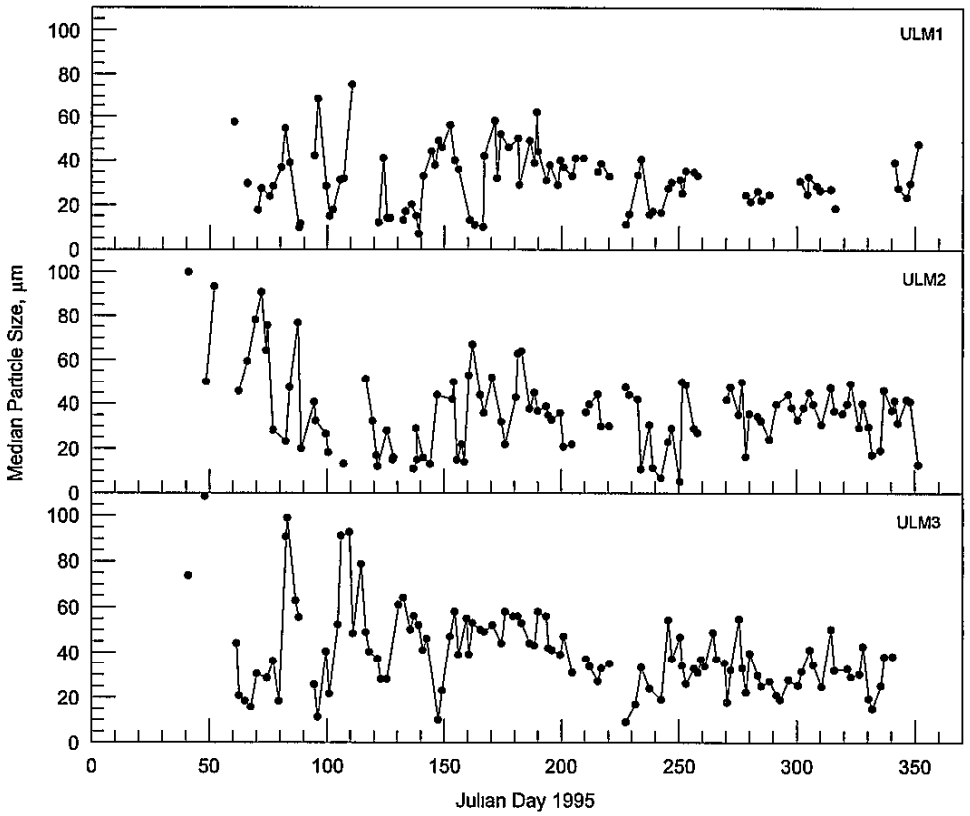

Figure 5 9 Median particle diameter during 1995 for ULM1, ULM2, and ULM3

5.4 Analysis of Sediment Transport

Baseline TSS concentrations at ULM1 lie in the range of approximately 0 to 50 µg/mL and do not occur under strongly preferential wind or current conditions Because these baseline concentrations persist throughout the year, but being slightly lower in the summer as compared to winter, they may represent a source of sediment that can be associated with deposition in any lower-energy region of Corpus Christi Bay

The TSS concentrations at ULM2 showed no preferential response to wind or currents. Because the mouth of Baffin Bay is known to have a high-energy wave climate, waves can be a source of sediment resuspension throughout the year However, because currents at the station do not show a strong directional preference, the material can be deposited in any lower-energy area and inferences cannot be made with the existing data set of deposition areas It is suspected that a significant amount of the sediment that is deposited in the high-shoaling reach of the

GIWW near and the mouth of Baffin Bay is derived from the mud flats lying south of the ULM. Discussion of this potential source of material is presented in the following paragraphs

The TSS concentrations at ULM3 showed no preferential response to wind or currents, but the area is a high-shoaling rate region of the study site Because the region around ULM3 is well-sheltered in three directions, the wave climate is mild so that waves are most likely not a significant source of sediment resuspension A hypothesis is presented here to explain the high rate of deposition There are two potential sources of sediment for the southern section of the ULM; 1) Wind-blown sand, and 2) Particles flowing into the GIWW from the mud flats south of the Land Cut during periods when the flats become inundated.

During periods of southeast to south winds, water can be piled up (setup) on the northern end of the LLM and similarly be set down on the southern end of the ULM This setup on the south end of the Land Cut coupled with setdown on the north end can cause a gradient in hydraulic head along the channel that induces flow to the north The setup-setdown driving enhances the direct wind-induced current A conceptual model for this hypothesis is shown in Figure 5 10. This northward flowing water can carry sediments washed into it from the mud flats, and these sediments can be deposited in the southern reaches of the ULM Because most (90 to 100%) of the material dredged from the GIWW in the region of ULM3 was categorized as mud (as reported in the 1994-1995 dredging records), this potential source of fine-grained particles is probable. Additionally, the wave climate in the ULM south of the mouth of Baffin Bay is mild so that wave action may not be a significant source of sediment resuspension into the water column.

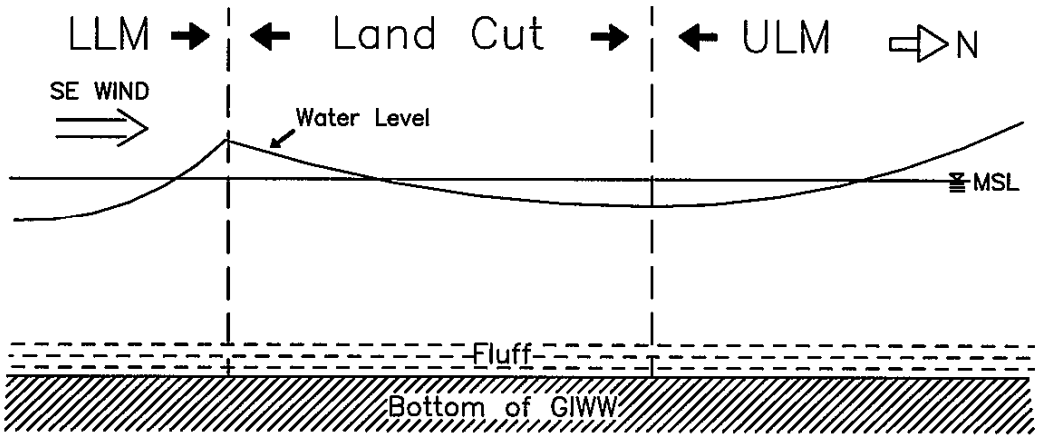

Figure 5.10. Conceptual model of wind-induced hydraulic head from the northern LLM to the southern ULM

6. LIGHT ATTENUATION[6]

6.1 Introduction

Although many factors influence seagrass growth (e.g., temperature, salinity, nutrients) underwater light availability is the single most important factor governing the growth and distribution of seagrasses (Kenworthy and Haunert 1991) Worldwide, there has been a greater than 50% decline in seagrass areal coverage over the last couple of decades, presumably as a result of decreased water clarity and quality (see Dennison *et al* 1993 for review). The loss of seagrass habitat is closely correlated with reductions in underwater light either as a result of natural or anthropogenic factors.

Seagrasses are the cornerstone of health and productivity in South Texas estuaries The Laguna Madre stretches approximately 115 miles from Corpus Christi Bay to the Brazos Santiago pass at Port Isabel (Collier and Hedgpeth 1950). Researchers estimate that 80% of all seagrasses along the Texas coast occur within the Laguna (Quammen and Onuf 1993). Finfish landings in the Laguna are consistently the highest in Texas and are highly correlated with the extensive seagrass beds (Texas Department of Natural Resources 1979). Until recently, productivity in the upper Laguna Madre (ULM) was dominated by the seagrass *Halodule wrightii* Aschers ; however, since the onset of the brown tide algal bloom in 1990 productivity has been dominated by phytoplankton The brown tide has reduced underwater light levels at the seagrass canopy by more than 50% (Dunton 1994) resulting in the loss of seagrass biomass Although the full extent of seagrass losses is not yet known since the bloom is ongoing, preliminary estimates suggest seagrasses below about 1.4 m depth are in jeopardy (Onuf 1994).

Light with wavelengths between 400 and 700 nm is referred to as photosynthetically active radiation (PAR) and is the energy source driving photosynthesis in all plants. The basic unit of light for any given wavelength is a photon. The amount of photosynthesis that a plant can carry out is directly proportional to the number of photons received by the photosynthetic apparatus. For submerged plants, the light environment is the result of the collective interaction of light and water, involving the processes of reflection, absorption and scattering (Kirk 1994) The reflection of light is primarily important only at the surface, where photons interact directly with

[6] James E Kaldy and Kenneth H Dunton, University of Texas Marine Science Institute, Port Aransas, Texas

the air/water interface Once in the water column, the ultimate fate of light is to be either scattered or absorbed Scattering and absorption are caused by the interaction of photons with water and with the dissolved or particulate materials in the water. Different materials, e.g. water, gelbstoff (dissolved long chain organic compounds), suspended solids and phytoplankton, will scatter or absorb photons in a characteristic manner. Thus, the specific underwater light environment observed is the result of light interacting with a variety of materials in the water column (Kirk 1994).

Scattering effectively increases the path length that a given photon travels and increases the probability that the photon will be absorbed (Kirk 1994) Particles >2 m are the primary agents of light scattering within the water column, although their size is large in relation to the wavelengths of light (Kirk 1994) Extreme light absorption and scattering in the water column can limit the amount of energy available to drive photosynthesis. Thus, as a result of scattering and absorption the underwater light environment is diffuse (i e , not unidirectional) and extremely variable both temporally and spatially

The terminology associated with quantifying the underwater light environment can be complex. Strictly speaking, irradiance is defined as the radiant flux incident on a receiving surface from all directions per unit surface area and is measured in units of Watts m^{-2} (LI-COR Inc , 1979) Often irradiance is used synonymously with photon flux, which refers to the quantity of photons reaching a surface from all directions per unit surface area per unit time (mol photons m^{-2} s^{-1}). There is no official International System of Units (ISU) unit of photon flux. A mole of photons is defined as Avogadro's number of photons (6 022 x 10^{23} photons) However, since the mole is an ISU unit, all of the prefixes associated also apply, e g mol photons m^{-2} s^{-1} Photon flux units are particularly useful since photosynthesis is a quantum process, which depends on the number of photons of PAR reaching the photosynthetic apparatus

Traditionally, oceanographers have defined the photic zone as the depth to which 1% of surface irradiance (SI) penetrates (Kirk 1994) This definition works well for phytoplankton which consist of individual cells in the open ocean *Halodule wrightii* (shoalgrass), the dominant seagrass in ULM, maintains 60 to 80% of the total biomass in below-ground tissues (roots and rhizomes) of the plant (Dunton 1994). These underground tissues are dependent upon the above-ground fraction to supply both energy (fixed carbon) and oxygen for respiration As a result of the large energy demands imposed by both the leaf and below-ground tissues seagrasses require substantially higher light levels than phytoplankton A recent literature survey concluded that worldwide, seagrasses require ca 11% SI for growth and survival (Duarte 1991) The State of Florida recently set water clarity guidelines at 10% SI in an attempt to prevent further loss of

seagrass-habitat (Kenworthy and Haunert 1991) However, recent research coupling plant physiological measurements with long-term continuous *in situ* light measurements have shown that the annual minimum light requirements for *Halodule wrightii* are 18% SI (Dunton 1994) and that *Thalassia testudinum* requires > 14% SI (Lee and Dunton1996). Based on these and other findings the general consensus of seagrass biologists in the United States is that seagrasses require between 18 and 25% SI on an annual basis (Kenworthy and Haunert 1991).

The primary objective of this study was the long-term characterization of the underwater light environment in a seagrass bed (Blucher Remote) and at three fixed platform locations. Corpus Christi Bay (CCB, ULM1), the mouth of Baffin Bay (ULM2) and just north of the land-cut (ULM3) These data will provide estimates of the duration of turbidity as a result of dredged material placement and the influence of wind-driven dredged material resuspension.

The following were the specific objectives of the light data acquisition team

1. To continuously measure *in situ* levels of underwater PAR at a seagrass bed near the Blucher platform for the contracted duration of the upper Laguna Madre project

2 To evaluate surface and underwater PAR data collected by Blucher staff at ULM1, ULM2 and ULM3 in the upper Laguna Madre

3 To assess changes in water transparency and the underwater light field at the remote site and the platforms in the upper Laguna

4. To determine the duration of dredging impacts on the underwater light environment along the Gulf Intracoastal Waterway (GIWW) in upper Laguna.

6.2 Materials and Methods

6 2 1 Fixed Platforms

Measurements of PAR were collected continuously using a LI-193SA spherical (4B) quantum-sensor (underwater) and LI-190SA cosine corrected (2B) quantum sensor (surface) providing input to a datalogger designed, built and maintained by Blucher staff The underwater sensor was mounted on the south-east corner at about 1 m below mean sea level (MSL). The terrestrial sensor was mounted above the platform and sensor locations were chosen to avoid shading by the platform structure. Instantaneous PAR was measured at 6 minute intervals and

data were retrieved via radio telemetry and archived at the Blucher Institute Archived data were then integrated to obtain hourly values and made available for analysis. Data processing procedures and calculations are described in the following section

6 2 2 Remote Station Description

Equipment designed to continuously measure PAR was deployed in an *H wrightii* bed near ULM3. The datalogger was located near GIWW channel marker #47 at approximately 27° 10' 47 5" N and 97° 25' 45 5" W (Trimble non-differential GPS coordinates), which is about 1 5 km south of ULM3 Underwater light values were collected continuously between 7 November 1994 and 10 January 1996.

Measurements of PAR were collected continuously using a LI-193SA spherical (4B) quantum-sensor (underwater) providing input to a LI-1000 datalogger (LI-COR Inc , Lincoln, Nebraska, USA) The datalogger was contained in a weighted clear polycarbonate underwater housing (Ikelite, model 5910) and wired to the sensor via a waterproof bulkhead connector (Crouse-Hinds, Series 41 Penetrator). The underwater sensor was mounted on a 3 cm diameter PVC pole about 25 cm above the seabed to minimize fouling by drift algae and seagrass blades Average sensor depth was 80 cm based on data collected during monthly maintenance visits (n = 15). Instantaneous PAR was measured at 1 minute intervals and integrated hourly Light sensors are calibrated or checked for accuracy annually and are accurate to ± 5% (traceable to National Bureau of Standards); stability is ± 2% over any 1-year period and data is recorded with a precision of ± 0.01 μmol photons m^{-2} s^{-1}

The dataloggers were checked at monthly intervals and preliminary data inspection was carried out in the field. When anomalous data were found, the problem was isolated and corrected using standard trouble-shooting procedures Typically, this involved replacing a cable or sensor When less than 50% of the total memory remained, the datalogger was removed from the field and replaced with another unit. On each datalogger maintenance trip, the sensor was cleaned and the polyethylene bag over the sensor was replaced The bag minimizes direct biofouling of the sensor globe, greatly increasing the time between recalibration Previous analysis indicates that the clear polyethylene bag has a negligible effect on light measurements On most occasions fouling of the bag was minimal

Data quality was assured by comparing trends in the data collected at the remote site to analogous data sets collected in the region (near channel marker 151, Dunton unpub. data) Problems in a data set are usually readily apparent (e g large positive or negative night time values).

Data were downloaded from the datalogger, printed, proofed for anomalies, corrected if necessary and added to the database In addition, light attenuation coefficients were calculated using the Bouger-Lambert Law:

$$k = \frac{\ln (I_o / I_z)}{z}$$

where I_O is incident (surface) irradiance, I_Z is irradiance at depth z (average sensor depth in meters) and k is the attenuation coefficient (m^{-1}) Attenuation coefficients (k values) quantify the amount of light absorbed in the water column, providing an index of water transparency Underwater and terrestrial light measurements from a given station were used to calculate k values, with the exception of the Blucher Remote station, where terrestrial data from ULM3 was used to calculate k values Sensor depth at the Blucher Remote station was measured monthly and the average used to calculate k values. At all platforms the sensor depth was about 1 m below mean sea level (MSL). The continuous long-term nature of the data set minimizes the relatively small tidal signal in the Laguna Madre

6 2 3 Statistical Comparisons

Statistical analyses were carried out using PC SAS (SAS Institute 1990) on a 486 PC For each site, a one-way ANOVA was used to examine differences in the attenuation coefficient during various phases of the project (pre-dredging vs during-dredging vs 1-year post-dredging). If statistically significant differences ($P < 0\ 05$) were found, then a Tukey's multiple comparisons test was used to determine where the differences occurred The implicit assumption of this statistical model, is that climatic conditions were identical for the pre-dredging and 1-year post dredging time period. In some cases, incomplete data sets prevented rigorous analysis of hypotheses, making interpretation difficult

Pre-dredging was defined as the time period between initiation of data collection and the time when the dredge was close to the site The during-dredging period was defined as the 14 day period when the dredge was closest to the site The 1 year post-dredging period was defined as the same dates as pre-dredging during the following year (1995) The post-dredging data used

for ULM3 were collected 11 months after dredging had occurred (November, 1995), since the 1-year data (December, 1995) were not available for analysis

6.3 Results

6 3 1 ULM1

Surface irradiance at ULM1 varied between 2 6 and 57 6 mol m^{-2} d^{-1} (Figure 6 1) and there appears to be a slight seasonal trend. Underwater light was variable with values ranging between 0 and 52 mol m^{-2} d^{-1} (Figure 6 1) Average summer underwater values (June through August, 1995) were 19 mol m^{-2} d^{-1}, which was about 80% higher than the average winter values (3.4 mol m^{-2} d^{-1}; November, 1994, through February, 1995)

The amount of light reaching the 1 m depth at ULM1 ranged between 2.5 and 85 % Surface Irradiance (SI), while *k* values ranged between 0 2 and 3 7 m^{-1} (Figure 6.2). Statistical analysis indicated that there were no significant differences (P = 0.15) in *k* values with respect to the different activity periods (Table 6.1); however, the incomplete nature of the data set prevents adequate interpretation

Table 6.1. ULM 1. Summary of mean (± SE) attenuation coefficients, underwater PAR and percent surface irradiance. Sample date represents the time period examined as defined in the methods, while n refers to the actual number of data points available. Mean *k* values were not significantly different.

Dredging Phase	Sample Date	Sample Size, n	Mean k value, m^{-1}	Mean UW PAR, (mol m^2/day)	Mean Percent SI
pre-dredging	Nov 2 to Nov 20, 1994	5	1 4 (0 5)	9 (3)	35 (9)
during-dredging	Nov 25 to Dec 8, 1994	12	2 4 (0 2)	2 (0 5)	11 (2)
post-dredging	Nov 2 to Nov 24, 1995	8	1 7 (0 5)	9 (3)	29 (8)

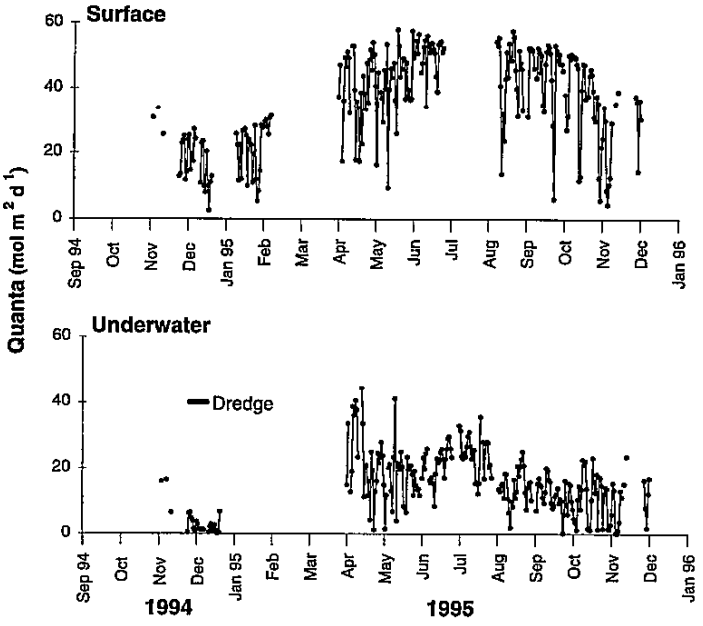

Figure 6 1 Continuous measurements of surface and underwater irradiance at ULM1 in upper Laguna Madre from November, 1994 to December 1995.

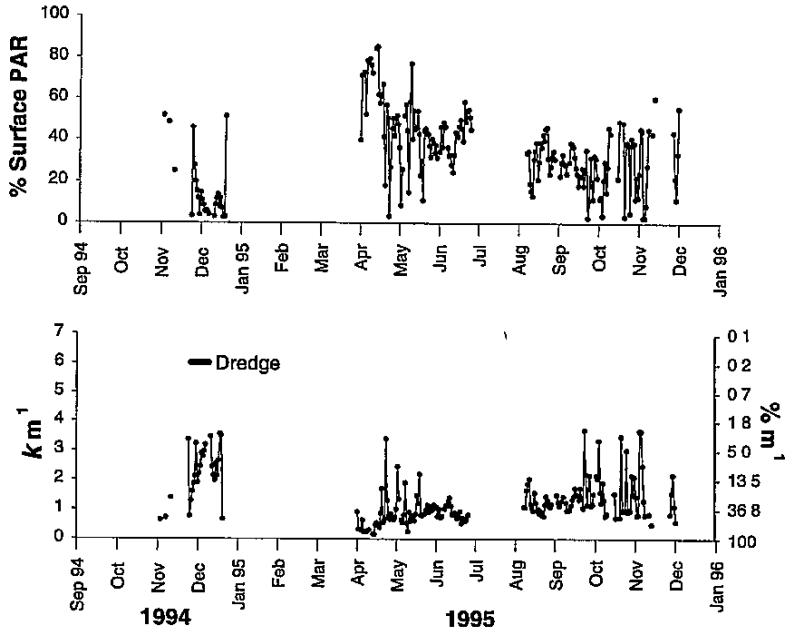

Figure 6 2. Percent surface PAR and attenuation coefficients (k values) at ULM1 in upper Laguna Madre from November, 1994 to December, 1995

6 3 2 ULM2

Surface irradiance at ULM2 ranged between 7 and 58 mol m^{-2} d^{-1} (Figure 6 3) A seasonal trend is evident with winter values averaging 22 mol m^{-2} d^{-1} and summer values averaging 48 mol m^{-2} d^{-1} (Figure 6.3). Daily underwater irradiance ranged between 0 and 21 mol m^{-2} d^{-1} Average underwater light varied during the different phases of the project, ranging between 1.1 and 4.6 mol m^{-2} d^{-1} (Table 6 2) Average summer underwater values (June through August, 1995) were 11 mol m^{-2} d^{-1}, which is about 73% higher than the average winter values (3 mol m^{-2} d^{-1}; November, 1994, through February, 1995).

The amount of light reaching sensor depth at ULM2 varied between 3 and 53 % SI (Figure 6 4), while during the different phases of the project average underwater light varied between 5 and 22% SI (Table 6 2) Attenuation coefficients (*k* values) during the year varied between 0.6 and 3.9 m^{-1} (Figure 6.4) Analysis indicates that there were statistically significant ($P < 0\ 05$) differences in *k* values between dredging phases (Table 6 2) Post-dredging *k* values were significantly lower than either pre-dredge or during-dredging *k* values, but there was no difference between pre- and during-dredging *k* values However, the limited sample size available for the post-dredging phase may have biased the analysis

Table 6.2. ULM 2. Summary of mean (± SE) attenuation coefficients, underwater PAR and percent surface irradiance. Sample date represents the time period examined as defined in the methods, while n refers to the actual number of data points available. Statistical analysis was only performed on *k* values, different letters denote statistically significant differences ($P < 0.05$).

Dredging Phase	Sample Date	Sample Size, n	Mean k value, m^{-1}	Mean UW PAR, (mol m^2/day)	Mean Percent SI
pre-dredging	Nov 18 to Dec 19, 1994	30	3 0 (0 1)[a]	1 2 (0 1)	5 (0 3)
during-dredging	Dec 20, 1994 to Jan 5, 1995	16	2 8 (0 2)[a]	1 1 (0 2)	8 (2)
post-dredging	Nov 18 to Nov 30, 1995	13	1 8 (0 2)[b]	4 6 (0 7)	22 (3)

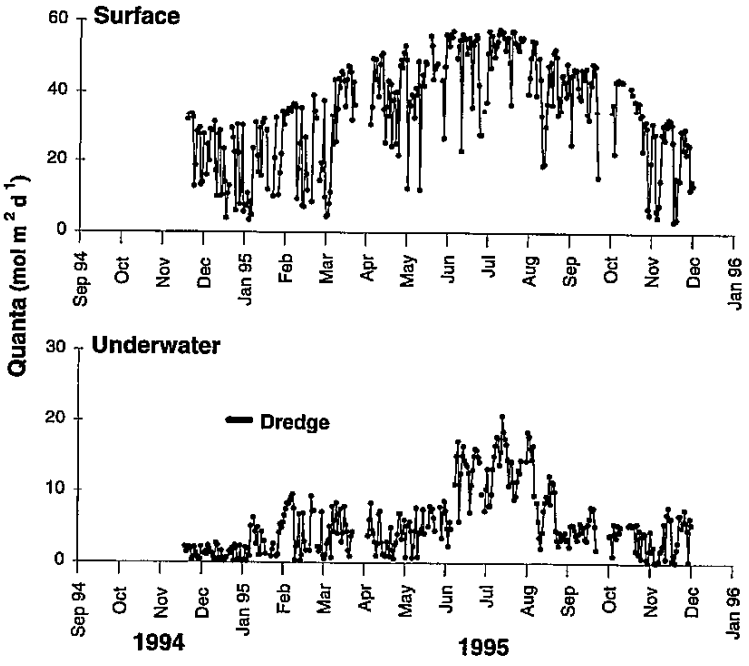

Figure 6 3 Continuous measurements of surface and underwater irradiance at ULM2 in upper Laguna Madre from November, 1994 to December, 1995

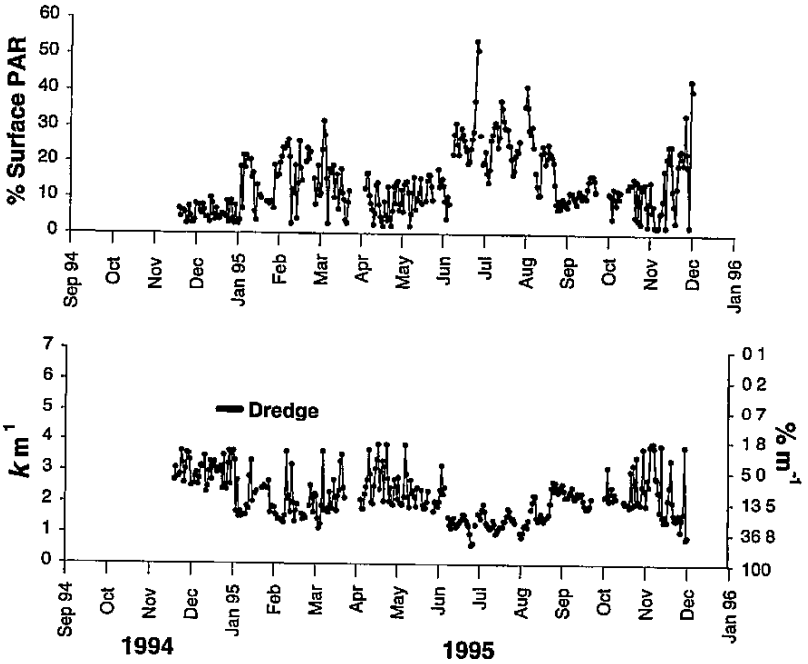

Figure 6.4 Percent surface PAR and attenuation coefficients (k values) at ULM2 in upper Laguna Madre from November, 1994 to December, 1995.

6 3 3 ULM3

Daily surface irradiance varied between 3.6 and 60 mol m^{-2} d^{-1} (Figure 6 5) A seasonal pattern is also evident with average winter values of 22 mol m^{-2} d^{-1} and average summer values of 51 mol m^{-2} d^{-1} (Figure 6.5). Over the entire study period, underwater irradiance was variable and ranged between ca 0 and 17 mol m^{-2} d^{-1} (Figure 6.5), while during the different dredging phases values were about 1 mol m^{-2} d^{-1} (Table 6 3) Average summer underwater irradiance was 7 mol m^{-2} d^{-1}, (June to August, 1995) which was almost 80% higher than the average winter value of 1.5 mol m^{-2} d^{-1} (November, 1994, to February, 1995).

Based on the available data, 9% SI reached the sensor depth on an annual basis, with values ranging between 1 and 30% SI (Figure 6 6). During the dredging phases values ranged between 5 and 6% SI (Table 6-3), while attenuation coefficients (*k* values) varied between 1.2 and 3 8 m^{-1}, with an annual average of 2 6 m^{-1} Analysis indicates there were no statistically significant differences (P = 0 13) between dredging phases (Table 6 3).

Table 6.3. ULM 3. Summary of mean (± SE) attenuation coefficients, underwater PAR and percent surface irradiance. Sample date represents the time period examined as defined in the methods, while n refers to the actual number of data points available. Mean k values were not significantly different.

Dredging Phase	Sample Date	Sample Size, n	Mean k value, m^{-1}	Mean UW PAR, (mol m^2/day)	Mean Percent SI
pre-dredging	Dec 21, 1994 to Jan 14, 1995	24	3 2 (0 1)	1 0 (0 2)	5 (0 5)
during-dredging	Jan 15 to Jan 29, 1995	14	3 0 (0 1)	1 1 (0 1)	5 (0 3)
post-dredging	Nov 1 to Nov 30, 1995	28	2 9 (0 1)	1 6 (0 2)	6 (0 5)

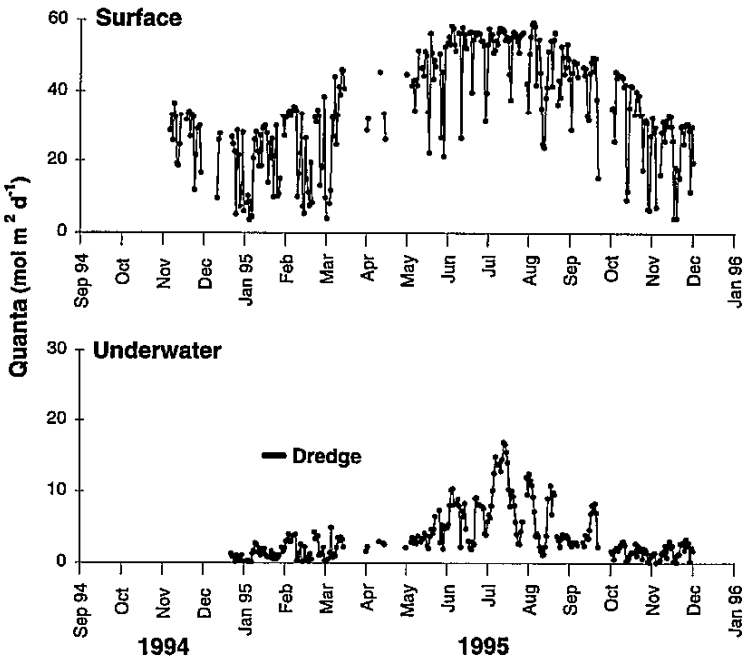

Figure 6 5 Continuous measurements of surface and underwater irradiance at ULM3 in upper Laguna Madre from November, 1994 to December, 1995.

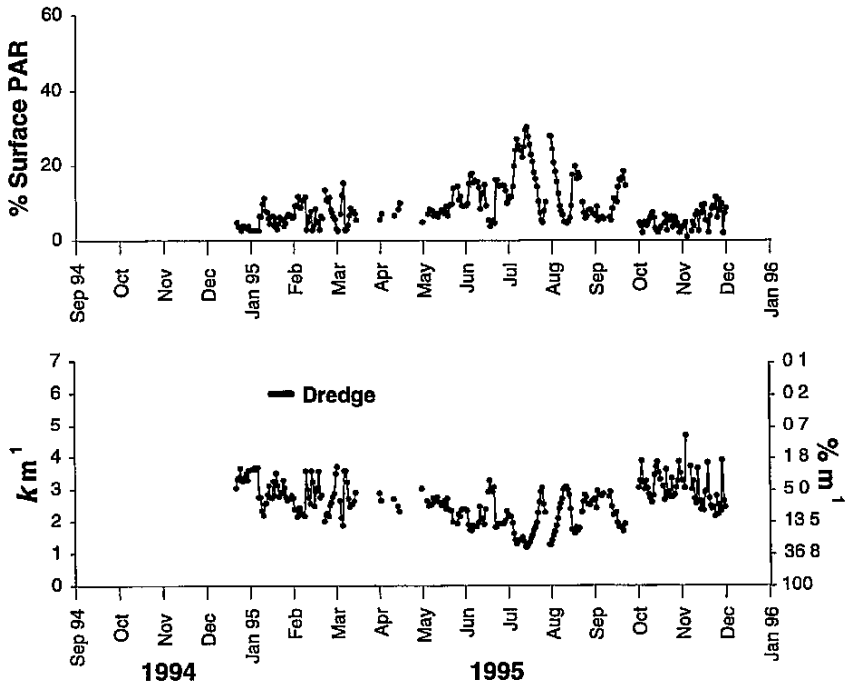

Figure 6 6. Percent surface PAR and attenuation coefficients (k values) at ULM3 in upper Laguna Madre from November, 1994 to December, 1995.

6 3 4 Remote

Surface irradiance from ULM3 was used for the calculation of percent SI and *k* values at the remote station, since it was the closest available data (see previous section for details) Underwater light values were collected continuously between November 7, 1994 and January 10, 1996 when data collection was terminated. The January 1995 data gap in the underwater light was caused by battery failure (see quarterly reports for details) and as a result new procedures were implemented to prevent future problems The gap during August 1995 was a result of the sensor being buried by a 1 m thick layer of drift algae and detritus (Kaldy, pers obs). Overall, underwater irradiance ranged between 0 and 26 mol m^{-2} d^{-1} (Figure 6.7) Average underwater summer values were 12 1 mol m^{-2} d^{-1}, which were about 80% higher than the average winter values of 2.3 mol m^{-2} d^{-1}.

Since percent SI and *k* values were calculated from surface and underwater data, the incomplete data set resulted from the combined missing values. The amount of underwater light reaching the seagrass bed ranged between 0 2 and 43% SI (Figure 6 8), while during the different dredging phases, values were about 9% SI (Table 6 4) During the *Halodule wrightii* growing season, May through August, about 17% SI reached the seagrass bed. Attenuation coefficients (*k* values) varied between 1 and 8 m^{-1}, during the *H wrightii* growing period average *k* values were 2 4 m^{-1} (Figure 6.8) Analysis indicates that there were no statistically significant (P = 0 77) differences in *k* values between the different phases of dredging (Table 6 4)

Table 6.4. Remote Station. Summary of mean (± SE) attenuation coefficients, underwater PAR and percent surface irradiance. Sample date represents the time period examined as defined in the methods, while n refers to the actual number of data points available. Mean k values were not significantly different.

Dredging Phase	Sample Date	Sample Size, n	Mean k value, m^{-1}	Mean UW PAR, (mol m^2/day)	Mean Percent SI
pre-dredging	Nov 8 to Nov 28, 1994	18	3 5 (0 3)	2 7 (0 5)	9 (1)
during-dredging	Jan 15 to Jan 29, 1995	5	3 0 (0 2)	1 9 (0 4)	10 (2)
post-dredging	Nov 8 to Nov 28, 1995	21	3 4 (0 3)	2 4 (0 3)	10 (1)

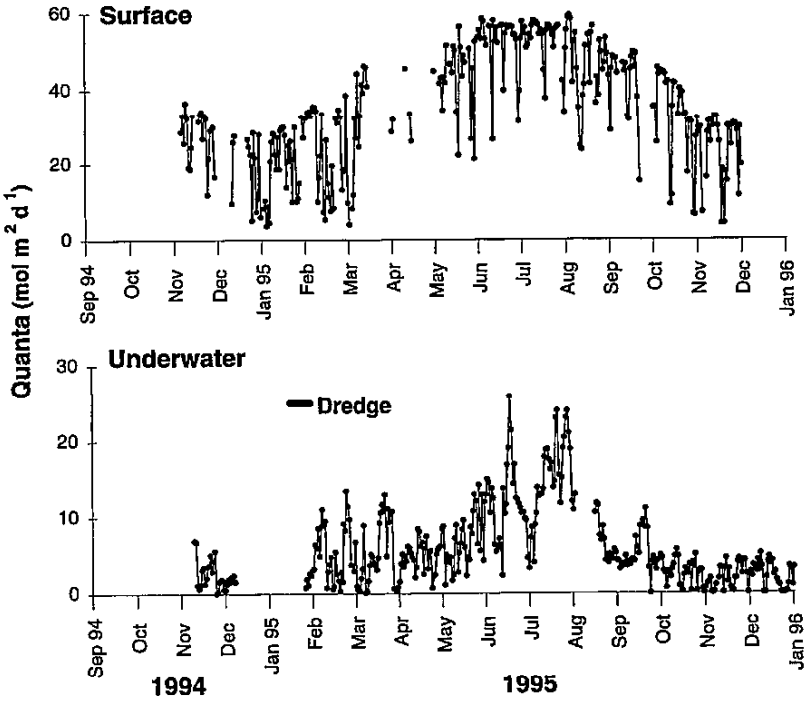

Figure 6 7 Continuous measurements of surface (ULM3) and underwater irradiance at Blucher remote in upper Laguna Madre from November, 1994 to December, 1995

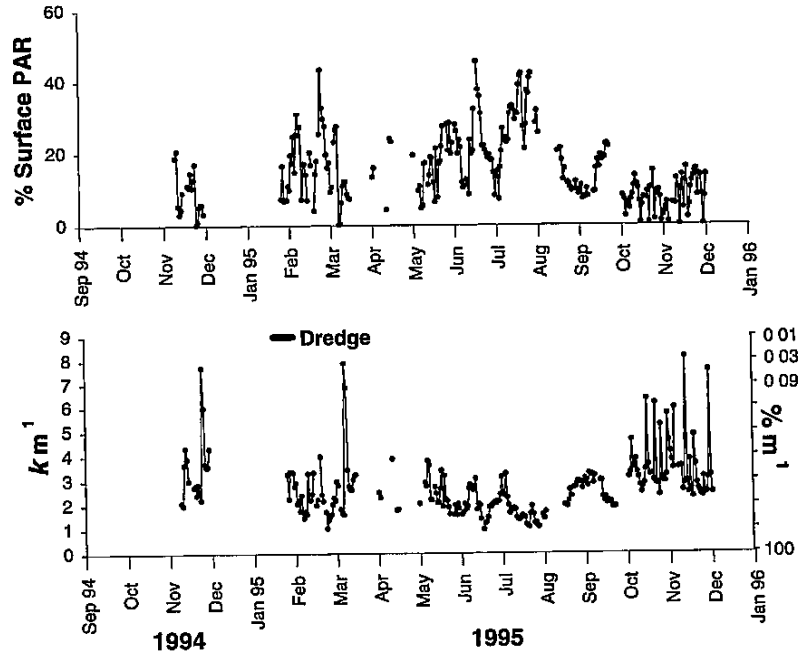

Figure 6 8 Percent surface PAR and attenuation coefficients (k values) at Blucher remote in upper Laguna Madre from November, 1994 to December, 1995

6.4. Discussion

Surface irradiance was variable on both daily and seasonal scales. Daily variability was probably a result of variable atmospheric conditions such as fog and cloud cover Seasonal changes in surface irradiance are probably a result of changing planetary declination as the earth rotates around the sun Also, seasonal patterns may be related to the passage of fronts which are more common during the winter than during the summer. In general, the data collected at the platforms compares well with literature values for this area Dunton (1994) found that average winter irradiance in south Texas is 30 mol m^{-2} d^{-1}, while average summer irradiance is about 58 mol m^{-2} d^{-1}.

One of the most interesting aspects of the underwater data was the relatively weak relationship of underwater light to surface irradiance (Figures 6 1, 6 3, 6 5, and 6.7). Although summer underwater irradiance tended to be higher than winter, the data were highly variable, making the seasonal signal weak These data suggest that the underwater light environment was controlled by the materials suspended in the water column Using a five-year continuous data set, Dunton (1994) documented uncoupling of terrestrial and submarine light in the upper Laguna Madre (ULM), which was attributed to scattering and absorption by materials in the water column During a six month study in several South Texas estuaries, including two sites in ULM, total suspended solids (TSS; including phytoplankton and sediments) accounted for 75 to 100% of the light attenuation within the water column (Dunton *et al* in press). Onuf (1994) showed that underwater light levels in lower Laguna Madre was significantly reduced by sediment resuspension for 18 months after dredging activity had ceased. Kaldy and Dunton (1996) found significantly reduced underwater light for about 250 days after dredging Thus, it appears that dredging impacted are variable and site specific

Estuarine and coastal waters are generally characterized by attenuation coefficients (k values) ranging between 0 2 and 3 0 with extremes of >10 m^{-1} (Kirk 1994), while k values in Texas estuaries generally range between 0 5 and 2 5 m^{-1} (Dunton *et al.* in press). During this study, attenuation coefficients as large as 8 m^{-1} were observed The lowest k values consistently occurred during June, July, and August, when wind velocities were lowest Extreme k values are generally the result of large scale disturbances caused by either natural or anthropogenic forces (Zimmerman *et al* 1991 and references therein) During the course of this study there were three large scale disturbances, the maintenance dredging of the GIWW, the ongoing brown tide, and short-term wind events associated with passing fronts Dredging activities have been shown to decrease the amount of underwater light available to plants by the initial suspension and subsequent wind-driven resuspension of dredged material in the water column (Dennison *et al*

1993, Onuf 1994, Pulich and White 1991) However, the presence of brown tide as a confounding factor makes determination of dredging impacts difficult. Brown tide is a phytoplankton bloom of a chrysophyte alga (Stockwell *et al* 1993) Recent work suggests that this is a new genus and species, tentatively named *Aueroumbra lagunensis* (H DeYoe, pers comm.) Dunton *et al* (in press) concluded that as a result of the brown tide there was a significant relationship between chlorophyll *a* values and light attenuation in the ULM (r^2 = 0 65) Chlorophyll *a* values in brown tide areas tend to be between 20 and 70 g Chl *a* L^{-1} (Stockwell *et al.* 1993), however, record high values up to 200 g Chl. *a* L^{-1} were recorded during this study period (Dunton, unpubl. data) In the ULM, brown tide has caused more than a 50% decrease in underwater light levels and as a result threatens seagrass populations in the deeper areas of Laguna (Dunton 1994) Brown and Kraus (1996) showed strong correlations between wind speed, total suspended solids and light attenuation, indicating that short-term wind events can dramatically influence underwater light

One objective of this study was to quantify the duration of dredging activities impact upon the underwater light environment Previous studies in the Laguna Madre have shown that dredging activities can have an impact on underwater light for 8 to 18 months (Kaldy and Dunton 1996, Onuf 1994) However, with the exception of ULM2, there were no significant differences ($P > 0$ 05) between the dredging phases in the upper Laguna (Tables 6 1 through 6 4) In this study, brown tide was a confounding factor that may have masked any dredging signal In addition, the limited sample size may prevent detection of differences Although the time period encompassed by the analysis was typically on the order of 2 to 4 weeks, the actual sample size was often much smaller (Tables 6 1 through 6 4) as a result of data gaps These gaps are especially noticeable in the plots of percent SI and *k* values, since a gap in either the surface or underwater data prevents calculation of these parameters for that time period Comparing means that have large differences in sample size can be misleading Definitive quantification of the temporal extent of dredging activity impacts on underwater light will require a long-term data set that is not confounded by brown tide, including a year of baseline data collected prior to dredging activities and extending at least 24 months thereafter

The underwater irradiance data collected as part of this project shows a gradient of decreasing water clarity from ULM1 to ULM3 (Table 6.5). Values at ULM 1 are almost 3-fold higher than the light requirements of *Halodule*, while those at ULM3 are almost 2-fold lower than *Halodule* minimum light requirements (annual % SI) However, it should be pointed out that ULM1 is within Corpus Christi Bay proper, where brown tide occurs sporadically Also, the underwater values presented for the platforms (Tables 6 1, 6 2, 6 3, and 6 5) are calculated for light at sensor depth and not at the bottom The fixed platforms were located in 1 5 to 2 m of water, which was below the lower limit of seagrasses in the

ULM, especially since the onset of the brown tide Underwater irradiance at the sediment surface calculated using k values from the platforms, indicate that the light environment would be insufficient to support seagrass growth and survival The lack of seagrasses in the vicinity of the Blucher platforms supports this hypothesis

The datalogger equipment at the remote site was deployed in an existing seagrass bed near the GIWW Underwater irradiance during the growing season was about 17% SI, while the annual average was about 15% SI (Table 6 5) These values are slightly lower than the literature values of 18% SI for the minimum light requirements of *H wrightii* (Dunton 1994, Onuf 1996) This discrepancy is probably related to gaps in the data set and probably represents an underestimate of underwater light availablity It appears that these light levels are adequate for the long term maintenance of *H wrightii*, however, any further reductions in underwater irradiance would probably threaten the survival of beds at these depths

Table 6.5. Comparison of seagrass minimum light requirements with underwater light values measured at sensor depth from the fixed platforms.

Seagrass	% SI	Underwater Light Mol photons m^2/yr
Halodule wrightii	18[a]	2200[a]
Thalassia testudinum	> 14[b]	> 1600[b]
Syringodium filiforme	> 15[c d]	> 1600[c d]
ULM1	43	5723[e]
ULM2	16	2100[e]
ULM3	11	1670[e]
Remote	15	2397

[a] Dunton 1994
[b] Lee 1995
[c] Dennison 1991
[d] Kenworthy et al 1991
[e] Values represent light levels at 1 m below MSL

6.5 Conclusions

In general, there appears to be a north-south turbidity gradient with clearer water in Corpus Christi Bay and more turbid water near the land cut (Fix-3) This gradient is probably directly related to the presence of brown tide The significant light reduction associated with anthropogenic activities in previous studies in Laguna Madre (Kaldy and Dunton 1996, Onuf 1994) and world wide (Dennison *et al.* 1993) suggests that the lack of a significant differences in underwater light; noted in this study are probably a result of confounding factors (i e , brown tide) and a limited data set Brown tide was a confounding factor that probably inhibited the detection of dredging impacts by masking the signal of suspended sediments on light attenuation coefficients (k values) Also, a more continuous record of underwater and terrestrial irradiance is required to detect dredging impacts, since data gaps result in variable sample size which limits the statistical sensitivity to differences among dredging phases.

7. CONCLUSIONS AND RECOMMENDATIONS[7]

The monitoring conducted for this study provided an extensive and high-quality data set for supporting environmental and engineering studies associated with dredging operations along the GIWW in the ULM. The measurements serve as a foundation for understanding circulation and processes associated with resuspension and transport of sediment in the vicinity of the GIWW Major observations relating to the movement of sediment are summarized in the following

1. Wind dominates the motion over the study area on the daily and frontal (approximately 5 days) time scales Wind-generated currents, on the time scale of days, flow across the GIWW in the southern end of Corpus Christi Bay near the intersection of the bay with the ULM This cross-current is produced by the predominantly southeast wind that persists throughout the summer and the frequent north fronts that occur during the winter months At the mouth of Baffin Bay, the diurnal wind is responsible for the flow into and out of Baffin Bay South of the mouth of Baffin Bay, the laguna is narrow and sheltered to the south, so that the current flows mainly north or south, even in response to the easterly component of the wind.

2. Sediment resuspension at the northern end of the study site and at the mouth of Baffin Bay is inferred to be caused predominantly by waves In the southern end of Corpus Christi Bay, winds moving across the bay from the north generate of large waves These waves produce erosional stresses on the bottom and initiate sediment into the water column The mouth of Baffin Bay is unsheltered in most directions and experiences high-energy wind waves that resuspend sediment South of Baffin Bay, the laguna is well sheltered and not expected to experience large waves very often

3. A clockwise gyre may exist in Corpus Christi Bay under persistent southeast wind, causing flow toward the northwest in southern Corpus Christi Bay The cross-channel current that occurs in the southern Corpus Christi Bay will transport sediment into the GIWW, where it can be deposited.

4. A hypothesis formulated in this study provides a possible explanation for the high shoaling rate in the southern ULM, a region of relatively low wave energy Southeasterly winds

[7] Adele Militello and Nicholas C Kraus, Conrad Blucher Institute for Surveying and Science, Texas A&M University-Corpus Christi

induce setup at the northern end of the LLM and set down at the southern end of the ULM such that a gradient in hydraulic head is produced over the length of the Land Cut inducing flow to the north The head enhances the current directly induced by the wind, increasing the flow and transport of sediment into the southern end of the ULM The mud flats through which the Land Cut traverses are regularly innundated by wind-induced water-level fluctuations. The water coming off the flats may be a source of fine-grained particles that flow into the GIWW, move northward, and are subsequently deposited in the more quiescent water of the GIWW north of the Land Cut

5. Maintenance dredging has been required at periodic intervals in the GIWW from the southern end of Corpus Christi Bay to the northern end of the Land Cut Areas requiring most frequent dredging are the northern 10,000 ft of the study area and the region extending from the mouth of Baffin Bay to the Land Cut Greater volumes of sediment have been dredged from the GIWW after intense hurricanes have struck the south Texas coast.

6 Sediment deposition over the monitoring period occurred at a higher rate in the southern end of Corpus Christi Bay (approx 2 ft/yr) as compared to the southern ULM (approx. 1 ft/yr) Sediment suspension is favored under the low waters and high waves of winter in Corpus Christi Bay (and in Baffin Bay)

Recommendations for reducing deposition of material into the GIWW

On the southern end of Corpus Christi Bay, placement of dredged material on the west side of the GIWW may reduce the amount of sediment deposited into the channel. Because the greatest suspended sediment concentrations were found to occur under NE winds and SW currents, material located in placement sites on the eastern side of the GIWW may be eroded and transported across the GIWW and possibly deposited in the channel.

To reduce material deposition in the southern portion of the ULM, the amount of material entering the GIWW from the south must be reduced Because this material is transported by wind as well as by water, multiple and innovative strategies must be considered To reduce the transport of sediment from Padre Island, it is recommended that sand fences be emplaced on the west side of the Island to block transport into the laguna In addition, vegetation of the dunes would enhance stability of the sediment

Reduction of maintenance dredging frequency in the southern reach of the ULM could also be achieved by overdredging allowing for a greater volume of material to be deposited into the channel before dredging would be required[8]

Reduction of deposition of fine-grained material transported from the flats south of the study site could be achieved by diking along the GIWW in the Land Cut, where possible Diking would prevent water-borne transport of fine particles into the GIWW from the mud flats when the flats become inundated

In shallow water, sediment resuspension is known to be caused by wind-generated waves, usually dominating suspension produced by tidal current. The monitoring performed for the period covered by this report did not include measurement of waves, so that no quantification of wave parameters in relation to sediment resuspension could be performed. However, wave growth is related to impressed winds on the water surface We strongly recommend that long-term (1 year or more) measurements of waves be collected in addition to the measurements so that the influence of waves on resuspension of sediments can be evaluated.

[8] Recommendation provided by Mr Johnny French, U S Fish and Wildlife Service, Corpus Christi, Texas

REFERENCES

Behrens, E W , 1966 Surface Salinities for Baffin Bay and Laguna Madre, Texas, April 1964-March 1966 *Publications of the Institute of Marine Science, University of Texas*, **11,** 168-173.

Brown, C A. and N C. Kraus (eds.) 1997. Environmental monitoring of dredging and processes in the Lower Laguna Madre Final Report to the US Army Corps of Engineers. 118 p

Collier, A. and Hedgpeth, J W., 1950. An Introduction to the Hydrography of Tidal Waters of Texas. *Publications of the Institute of Marine Science, University of Texas*, **1**(2), 120-194.

Davis, R. A , Fingleton, W. G , Allen, G. R , Crealese, C. D , Johanns, W. M , O'Sullivan, J A , Reive, C. L , Scheetz, S J , and Stranaly, G. L , 1973 Corpus Christi Pass A Hurricane Modified Tidal Inlet on Mustang Island, Texas. *Contributions in Marine Science,* **17,** 123-131

Dennison, W. C., Orth, R. J , Moore, K. A , Stevenson, J. C , Carter, V , Kollar, S., Bergstrom, P. W , and Batuik, R A., 1993. Assessing water quality with submersed aquatic vegetation. *BioScience,* **43,** 89-94.

Dennison, W C., 1991 Photosynthetic and growth responses of tropical and temperate seagrasses in relation to secchi depth, light attenuation and daily light period In. Kenworthy, W J. and D E Haunert (eds) The light requirements of seagrasses proceedings of a workshop to examine the capability of water quality criteria, standards and monitoring programs to protect seagrasses NOAA Technical Memorandum NMFS-SEFC-287. 181 p

Dickenson, K A , Berryhill, H L., and Holmes, C W , 1972 Criteria for Recognizing Ancient Barrier Coastlines In Rigby, K and Hamblin, W K (eds), *Recognition of Ancient Sedimentary Environments,* SEPM, Tulsa, Oklahoma, 192-214

Diener, R , 1975 *Cooperative Gulf of Mexico Estuarine Inventory and Study, Texas Area Description* NOAA Technical Report, NMFS CIRC-393, Seattle Washington

Duarte, C M , 1991 Seagrass depth limits *Aquatic Botany,* **40,** 363-377

Dunton, K. H , 1994 Seasonal Growth and Biomass of the Subtropical Seagrass *Halodule wrightii* in Relation to Continuous Measurements of Underwater Irradiance *Marine Biology*, **120,** 479-489.

Dunton, K H , Kaldy, J E , and Lee, K -S , 1994. Attenuation of Light in Two Subtropical Estuaries in Texas Final Report, University of Texas at Austin Marine Science Institute, Port Aransas, Texas.

Dunton, K H., Kaldy, J E., and Lee, K -S (in press) Light attenuation and water column characteristics over seagrass beds in two subtropical estuaries in Texas *Contributions in Marine Science*

Fisk, H N , 1959 Padre Island and the Laguna Madre Flats, Coastal South Texas. Second Coastal Geography Conference. In: Russell, R H. (ed), *Second Coastal Geography Conference,* Lousiana State University, Baton Rouge, Lousiana, 103-151

Friedman, G M. and Sanders, J E , 1978. *Principles of Sedimentology* John Wiley & Sons, New York

Kaldy, J. E. and Dunton, K. H , 1996 Light attenuation processes in the lower Laguna Madre of Texas In: C A Brown and N C. Kraus (eds,), Environmental monitoring of dredging and processes in the lower Laguna Madre Final Report to the US Army Corps of Engineers 118 p.

Kenworthy, W. J , Fonseca, M S , and Dipiero, S. J., 1991 Defining the ecological light compensation point for seagrasses *Halodule wrightii* and *Syringodium filiforme* from long-term submarine light regime monitoring in the southern Indian River In Kenworthy, W J. and D E. Haunert (eds), The light requirements of seagrasses: proceedings of a workshop to examine the capability of water quality criteria, standards and monitoring programs to protect seagrasses NOAA Technical Memorandum NMFS-SEFC-287 181 p

Kenworthy, W.J and D E. Haunert (eds), 1991 The light requirements of seagrasses proceedings of a workshop to examine the capability of water quality criteria, standards and monitoring programs to protect seagrasses NOAA Technical Memorandum NMFS-SEFC-287. 181 p

Kirk, J T. O., 1994. *Light and Photosynthesis in Aquatic Ecosystems* Cambridge University Press, Cambridge

Kraus, N C., Lorhmann, A , and Cabrera, R , 1994 New Acoustic Meter for Measuring 3D Laboratory Flows *Journal of Hydraulic Engineering*, **120**(3), 406-412.

Lee, K -S , 1995. Abundance, production and carbon dynamics of the seagrass *Thalassia testudinum* in Corpus Christi Bay, Texas. Masters Thesis University of Texas at Austin, Austin, Texas 77 p

Lee, K -S. and K H. Dunton, 1996. Production and carbon reserve dynamics of the seagrass *Thalassia testudinum* in Corpus Christi Bay, Texas Mar Ecol Prog Sers **143**: 201-210

Levesque, V. A , and Schoellhamer, D H , 1995 Summary of Sediment Resuspension Monitoring Activities, Old Tampa Bay and Hillsborough Bay, Florida, 1988-91 U S Geological Survey, Water-Resources Investigations Report 94-4081

LI-COR, Inc , 1979 Radiation measurement LI-COR, Inc. Lincoln, Nebraska

National Hurricane Center, 1996 The Most Intense United States Hurricanes of This Century. \\www nhc noaa gov

McGowan, J. H. and Scott, A. J , 1975 Hurricanes as Geologic Agents on the Texas Coast. In Cronin, L E. (ed), *Estuarine Research, Volume II, Geology and Engineering,* Academic Press, New York, 23-46

Miller, J A , 1975 Facies Characteristics of Laguna Madre Wind-Tidal Flats In Ginsberg, R N (ed), *Tidal Deposits A Casebook of Recent Examples and Fossil Counterparts*, Springer-Verlag, New York, 67-73

Onuf, C. P , 1994 Seagrasses, Dredging and Light in Laguna Madre, Texas, U S A. *Estuarine, Coastal and Shelf Science,* **39,** 75-91.

Onuf, C.P., 1996. Seagrass responses to long-term light reduction by brown tide in upper Laguna Madre, Texas distribution and biomass patterns Mar. Ecol Prog. Sers. **138** 219-231

Pulich, W M. and White, W. A , 1991 Decline of submerged vegetation in the Galveston Bay System: chronology and relationships to physical processes. *Journal of Coastal Ressearch,* **7,** 1125-1138.

Quammen, M. L. And Onuf, C P , 1993. Laguna Madre. Seagrass Changes Continue Decades After Salinity Reduction *Estuaries,* **16**(2), 302-310.

SAS Institute, 1990 *SAS Procedures Guide, Version 6, Third edition* SAS Inc , Cary, North Carolina. 705 pp.

Shepard, F P. and Rusnak, G A , 1957 Texas Bay Sediments *Publications of the Institute of Marine Science, University of Texas,* **IV**(2), 5-13

Shideler, G L , 1984 Suspended Sediment Responses in a Wind-Dominated Estuary of the Texas Gulf Coast. *Journal of Sedimentary Petrology,* **54**(3), 731-745

Smith, N. P , 1977 Meteorological and Tidal Exchanges Between Corpus Christi Bay, Texas, and the Northwestern Gulf of Mexico *Estuarine and Coastal Marine Science,* **5,** 511-520

Smith, N P , 1978 Intracoastal Tides of the Upper Laguna Madre, Texas *The Texas Journal of Science*, **XXX**(1), 84-95

Smith, N P., 1988. The Laguna Madre of Texas: Hydrography of a Hypersaline Lagoon In. Kjerfve, B (ed), *Hydrodynamics of Estuaries, Volume II, Estuarine Case Studies*, CRC Press, Inc , Boca Raton, Florida, 31-40

Smith, N P., 1989 An Investigation of the Heat Energy Budget of a Coastal Bay *Contributions in Marine Science*, **31**, 1-16

Stockwell, D. A., Buskey, E J., and Whitledge, T , E , 1993 Studies on conditions conducive to the development and maintenance of a persistent "brown tide" in Laguna Madre, Texas *In* T J. Smayda and Y Simizu (eds) *Toxic Phytoplankton Blooms in the Sea* Elsevier, Amsterdam, 693-698.

Texas Department of Water Resources, 1979 The influence of freshwater inflows upon the major bays and estuaries of the Texas Gulf Coast executive summary Texas Department of Water Resources, Austin, Texas, 40-43.

U.S. Army Corps of Engineers, 1968. Report on Hurricane Beulah, 8-21 September 1967 U S Army Engineer District, Corps of Engineers, Galveston, Texas.

U.S. Army Corps of Engineers, 1971. Report on Hurricane Celia, 30 July - 5 August 1970 U S. Army Engineer District, Corps of Engineers, Galveston, Texas.

U.S Army Corps of Engineers, 1981 Report on Hurricane Allen, 3-10 August 1980. U.S. Army Engineer District, Corps of Engineers, Galveston, Texas.

White, W A , Morton, R A., Kerr, R. S , Kuenzi, W. D , and Brogden, W. B., 1978 Land and Water Resources, Historical Changes, and Dune Criticality Mustang and North Padre Islands, Texas. Report of Investigations No 92, Bureau of Economic Geology, University of Texas at Austin, Texas

Zetler, B D , 1980 Tides at Port Mansfield, Laguna Madre, Texas *Marine Geodesy*, **4,** 3, 237-247

Zimmerman, R. C., J. L. Reguzzoni, S. Wyllie-Echeverria, M Josselyn and R S Alberte, 1991 Assessment of environmental suitability for growth of Zostera marina L (eelgrass) in San Francisco Bay *Aquatic Botany,* **39,** 353-366.

Appendix A. Dredging Dates, Locations, and Volumes for the 1994-1995 Dredging Cycle

Table A.1. Dates, locations, and volume of material dredged per unit length during the 1994 -1995 dredging cycle.

Date	Starting Station	Ending Station	Vol/length, m^3/m
November 19, 1994	0 + 000	1 + 600	56
November 20, 1994	1 + 600	2 + 500	64
November 21, 1994	2 + 500	3 + 800	64
November 22, 1994	3 + 800	4 + 800	64
November 23, 1994	4 + 800	----	
November 24, 1994	4 + 800	5 + 500	64
November 25, 1994	5 + 500	6 + 600	56
November 26, 1994	6 + 600	7 + 300	56
November 27, 1994	7 + 300	7 + 450	56
November 28, 1994	7 + 450	7 + 550	56
November 29, 1994	7 + 550	8 + 000	56
November 30, 1994	8 + 000	8 + 150	49
December 1, 1994	8 + 150	8 + 700	49
December 2, 1994	8 + 700	9 + 200	49
December 3, 1994	9 + 200	9 + 750	49
December 4, 1994	9 + 750	10 + 000	38
December 5, 1994	10 + 000		0
December 6, 1994		10 + 000	0
December 7, 1994	99 + 400	98 + 750	57
December 8, 1994	98 + 750	98 + 000	
December 8, 1994	99 + 400	99 + 950	39
December 9, 1994	99 + 950	101 + 500	51
December 10, 1994	101 + 500	102 + 300	51
December 11, 1994	102 + 300	103 + 000	44
December 12, 1994	142 + 000	141 + 700	51
December 13, 1994	141 + 700	141 + 000	
December 13, 1994	142 + 000	142 + 800	62
December 14, 1994	142 + 800	143 + 950	74
December 15, 1994	143 + 950	145 + 200	74
December 16, 1994	145 + 200	146 + 400	61
December 17, 1994	146 + 400	147 + 600	67
December 18, 1994	147 + 600	148 + 800	56
December 19, 1994	148 + 800	149 + 000	54

December 19, 1994	164 + 700	164 + 500	54
December 20, 1994	164 + 500	163 + 200	54
December 21, 1994	163 + 200	161 + 900	48
December 22, 1994	161 + 900	160 + 400	36
December 23, 1994	160 + 400	160 + 000	
December 23, 1994	164 + 700	164 + 900	46
December 26, 1994	164 + 900	165 + 900	56
December 27, 1994	165 + 900	167 + 500	41
December 28, 1994	167 + 500	169 + 200	41
December 29, 1994	169 + 200	170 + 000	41
December 29, 1994	174 + 000	173 + 500	46
December 30, 1994	173 + 500	171 + 500	46
December 31, 1994	171 + 500	170 + 000	46
January 1, 1995	174 + 000	176 + 000	46
January 2, 1995	176 + 000	177 + 700	46
January 3, 1995	177 + 700	179 + 000	36
January 4, 1995	183 + 500	185 + 000	61
January 5, 1995	183 + 500	181 + 900	61
January 6, 1995	181 + 900	180 + 400	50
January 7, 1995	180 + 400	179 + 200	61
January 8, 1995	179 + 200	179 + 000	50
January 8, 1995	186 + 800	185 + 600	53
January 9, 1995	185 + 600	185 + 000	
January 9, 1995	186 + 800	187 + 800	38
January 10, 1995	187 + 800	189 + 700	26
January 11, 1995	189 + 700	191 + 450	41
January 12, 1995	191 + 450	192 + 000	
January 12, 1995	194 + 000	193 + 150	36
January 13, 1995	193 + 150	192 + 000	
January 13, 1995	194 + 000	194 + 550	36
January 14, 1995	194 + 550	196 + 300	33
January 15, 1995	196 + 300	196 + 500	45
January 15, 1995	201 + 000	199 + 750	46
January 16, 1995	199 + 750	198 + 100	46
January 17, 1995	198 + 100	196 + 500	46
January 18, 1995	201 + 000	202 + 000	41
January 19, 1995	202 + 000	203 + 800	42
January 20, 1995	203 + 800	205 + 000	41
January 22, 1995	211 + 900	211 + 050	51
January 23, 1995	211 + 050	209 + 700	56
January 24, 1995	209 + 700	208 + 600	181
January 25, 1995	208 + 600	207 + 650	77

January 26, 1995	207 + 650	206 + 900	84
January 27, 1995	206 + 900	206 + 050	84
January 28, 1995	206 + 050	205 + 100	77
January 29, 1995	205 + 100	205 + 000	
January 29, 1995	211 + 900	212 + 100	41
January 30, 1995	212 + 100		0
February 17, 1995	212 + 100	214 + 200	25
February 18, 1995	214 + 200	215 + 800	25
February 19, 1995	215 + 800	217 + 000	25

Appendix B. Julian Day Calendar

Mon/ Day	Jan	Feb	Mar	Apr	May	Jun	Jul	Aug	Sep	Oct	Nov	Dec
1	1	32	*60*	*91*	*121*	*152*	*182*	*213*	*244*	*274*	*305*	*335*
2	2	33	*61*	*92*	*122*	*153*	*183*	*214*	*245*	*275*	*306*	*336*
3	3	34	*62*	*93*	*123*	*154*	*184*	*215*	*246*	*276*	*307*	*337*
4	4	35	*63*	*94*	*124*	*155*	*185*	*216*	*247*	*277*	*308*	*338*
5	5	36	*64*	*95*	*125*	*156*	*186*	*217*	*248*	*278*	*309*	*339*
6	6	37	*65*	*96*	*126*	*157*	*187*	*218*	*249*	*279*	*310*	*340*
7	7	38	*66*	*97*	*127*	*158*	*188*	*219*	*250*	*280*	*311*	*341*
8	8	39	*67*	*98*	*128*	*159*	*189*	*220*	*251*	*281*	*312*	*342*
9	9	40	*68*	*99*	*129*	*160*	*190*	*221*	*252*	*282*	*313*	*343*
10	10	41	*69*	*100*	*130*	*161*	*191*	*222*	*253*	*283*	*314*	*344*
11	11	42	*70*	*101*	*131*	*162*	*192*	*223*	*254*	*284*	*315*	*345*
12	12	43	*71*	*102*	*132*	*163*	*193*	*224*	*255*	*285*	*316*	*346*
13	13	44	*72*	*103*	*133*	*164*	*194*	*225*	*256*	*286*	*317*	*347*
14	14	45	*73*	*104*	*134*	*165*	*195*	*226*	*257*	*287*	*318*	*348*
15	15	46	*74*	*105*	*135*	*166*	*196*	*227*	*258*	*288*	*319*	*349*
16	16	47	*75*	*106*	*136*	*167*	*197*	*228*	*259*	*289*	*320*	*350*
17	17	48	*76*	*107*	*137*	*168*	*198*	*229*	*260*	*290*	*321*	*351*
18	18	49	*77*	*108*	*138*	*169*	*199*	*230*	*261*	*291*	*322*	*352*
19	19	50	*78*	*109*	*139*	*170*	*200*	*231*	*262*	*292*	*323*	*353*
20	20	51	*79*	*110*	*140*	*171*	*201*	*232*	*263*	*293*	*324*	*354*
21	21	52	*80*	*111*	*141*	*172*	*202*	*233*	*264*	*294*	*325*	*355*
22	22	53	*81*	*112*	*142*	*173*	*203*	*234*	*265*	*295*	*326*	*356*
23	23	54	*82*	*113*	*143*	*174*	*204*	*235*	*266*	*296*	*327*	*357*
24	24	55	*83*	*114*	*144*	*175*	*205*	*236*	*267*	*297*	*328*	*358*
25	25	56	*84*	*115*	*145*	*176*	*206*	*237*	*268*	*298*	*329*	*359*
26	26	57	*85*	*116*	*146*	*177*	*207*	*238*	*269*	*299*	*330*	*360*
27	27	58	*86*	*117*	*147*	*178*	*208*	*239*	*270*	*300*	*331*	*361*
28	28	59	*87*	*118*	*148*	*179*	*209*	*240*	*271*	*301*	*332*	*362*
29	29		*88*	*119*	*149*	*180*	*210*	*241*	*272*	*302*	*333*	*363*
30	30		*89*	*120*	*150*	*181*	*211*	*242*	*273*	*303*	*334*	*364*
31	31		*90*		*151*		*212*	*243*		*304*		*365*

Add 1 to italicized values during a leap year